UNIVERSITÉ
CÔTE D'AZUR

informatiques / *mathématiques*
Inria

Thèse de doctorat

Présentée en vue de l'obtention du

grade de docteur en Science

mention Informatique

de

UNIVERSITÉ CÔTE D'AZUR

par

Hlib Mykhailenko

Distributed edge partitioning

Dirigée par Fabrice Huet et Philippe Nain

Résumé

Pour traiter un graphe de manière répartie, le partitionnement est une étape préliminaire importante car elle influence de manière significative le temps final d'exécutions. Dans cette thèse nous étudions le problème du partitionnement réparti de graphe. Des travaux récents ont montré qu'une approche basée sur le partitionnement des sommets plutôt que des arêtes offre de meilleures performances pour les graphes de type power-laws qui sont courant dans les données réelles. Dans un premier temps nous avons étudié les différentes métriques utilisées pour évaluer la qualité d'un partitionnement. Ensuite nous avons analysé et comparé plusieurs logiciels d'analyse de grands graphes (Hadoop, Giraph, Giraph++, Distributed GrahpLab et PowerGraph), les comparant à une solution très populaire actuellement, Spark et son API de traitement de graphe appelée GraphX. Nous présentons les algorithmes de partitionnement les plus récents et introduisons une classification. En étudiant les différentes publications, nous arrivons à la conclusion qu'il n'est pas possible de comparer la performance relative de tout ces algorithmes. Nous avons donc décidé de les implémenter afin de les comparer expérimentalement. Les résultats obtenus montrent qu'un partitionneur de type Hybrid-Cut offre les meilleures performances. Dans un deuxième temps, nous étudions comment il est possible de prédire la qualité d'un partitionnement avant d'effectivement traiter le graphe. Pour cela, nous avons effectué de nombreuses expérimentations avec GraphX et effectué une analyse statistique précise des résultats en utilisation un modèle de régression linéaire. Nos expérimentations montrent que les métriques de communication sont de bons indicateurs de la performance. Enfin, nous proposons un environnement de partitionnement réparti basé sur du recuit simulé qui peut être utilisé pour optimiser une large parte des métriques de partitionnement. Nous fournissons des conditions suffisantes pour assurer la convergence vers l'optimum et discutons des métriques pouvant être effectivement optimisées de manière répartie. Nous avons implémenté cet algorithme dans GraphX et comparé ses performances avec JA-BE-JA-VC. Nous montrons que notre stratégie amène à des améliorations significatives.

iv

Abstract

In distributed graph computation, graph partitioning is an important preliminary step because the computation time can significantly depend on how the graph has been split among the different executors. In this thesis we explore the graph partitioning problem. Recently, edge partitioning approach has been advocated as a better approach to process graphs with a power-law degree distribution, which are very common in real-world datasets. That is why we focus on edge partitioning approach. We start by an overview of existing metrics, to evaluate the quality of the graph partitioning. We briefly study existing graph processing systems: Hadoop, Giraph, Giraph++, Distributed GrahpLab, and PowerGraph with their key features. Next, we compare them to Spark, a popular big-data processing framework with its graph processing APIs — GraphX. We provide an overview of existing edge partitioning algorithms and introduce partitioner classification. We conclude that, based only on published work, it is not possible to draw a clear conclusion about the relative performances of these partitioners. For this reason, we have experimentally compared all the edge partitioners currently available for GraphX. Results suggest that Hybrid-Cut partitioner provides the best performance with respect to the execution time of the graph processing algorithm. We then study how it is possible to evaluate the quality of a partition before running a computation. To this purpose, we carry experiments with GraphX and we perform an accurate statistical analysis using a linear regression model. Our experimental results show that communication metrics like vertex-cut and communication cost are effective predictors in most of the cases. Finally, we propose a framework for distributed edge partitioning based on distributed simulated annealing which can be used to optimize a large family of partitioning metrics. We provide sufficient conditions for convergence to the optimum and discuss which metrics can be efficiently optimized in a distributed way. We implemented our framework with GraphX and performed a comparison with JA-BE-JA-VC, a state-of-the-art partitioner that inspired our approach. We show that our approach can provide significant improvements.

Table of Contents

List of Figures

List of Algorithms

List of Tables

Chapter 1

Introduction

Contents

1.1 Motivation and Objectives

The size of read-world graphs obligates to process them in a distributed way. That is why, graph partitioning is the indispensable preliminary step performed before graph processing. In addition to the fact that graph partitioning is an NP hard problem, there is clearly, lack of research dedicated to graph partitioning, e.g., it is not clear how to evaluate the quality of a graph partition, how different partitioners compare to each other, and what is the final effect of partitioning on the computational time. Moreover, there is always a trade-off between simple and complex partitioners: complex partitioners may require a partitioning time too long to nullify the execution time savings.

In this work we tried to tackle these issues. In particular our objectives were: to find a correct way to compare partitioners (especially, before running actual graph processing algorithms), to identify an objective function the partitioner should optimize, and to design a partitioner which can optimize this function.

1.2   Contributions

We present below the main contributions of this thesis.

We have considered all the edge partitioners in the literature and provided new classification for them. From the literature it was not possible to compare all partitioners. That is why we compared them by ourselves on GraphX. Results suggest that `Hybrid-Cut` partitioner provides the best performance.

To evaluate the quality of a partition before running the computation we have performed a correct statistical analysis using a linear regression model which showed us that communication metrics are more effective predictors than balance metrics.

In order to optimize a given objective function (e.g., a communication metric) we have developed and implemented a new graph partitioner framework based on simulated annealing and new distributed asynchronous Gibbs sampling techniques.

The contributions presented in this thesis are included in the following publications:

– H. Mykhailenko, F. Huet and G. Neglia, "Comparison of Edge Partitioners for Graph Processing" 2016 International Conference on Computational Science and Computational Intelligence (CSCI): December 15-17, 2016, Las Vegas. This paper provides an overview of existing edge partitioning algorithms.

– H. Mykhailenko, G. Neglia and F. Huet, "Which metrics for vertex-cut partitioning?," 2016 11th International Conference for Internet Technology and Secured Transactions (ICITST), Barcelona, 2016, pp. 74-79. This paper focuses on edge partitioning and investigates how it is possible to evaluate the quality of a partition before running the computation.

– H. Mykhailenko, G. Neglia and F. Huet, "Simulated Annealing for Edge Partitioning" DCPerf 2017: Big Data and Cloud Performance Workshop at INFOCOM 2017, Atlanta. This paper proposes a framework for distributed edge partitioning based on simulated annealing.

1.3 Outline

In Chapter 2 we provide background overview, we define the graph partitioning problem, the notations we used in this thesis, the existing partitioning metrics, and the existing graph processing frameworks.

Next, in Chapter 3 we overview existing edge partitioning algorithms and introduce a classification of the partitioners.

After, Chapter 4 shows that a linear model can explain significant part of the dependency between partitioning metrics and execution time of graph processing algorithms. We suggest that communication metrics are the most important ones.

Chapter 5 presents a new distributed approach for graph partitioning based on simulated annealing and asynchronous Gibbs sampling techniques. We have implemented our approach in GraphX

Finally, we conclude and discuss the perspectives in Chapter 6.

Chapter 2

Context

Contents

In this chapter we introduce the graph partitioning problem and the notation we used. We describe existing metrics which evaluate the quality of a partition. We explain what is GraphX, and why we have selected it to perform experiments on graphs. We make a brief overview of other existing graph processing systems (such as Apache Hadoop, Apache Giraph, etc) and show their key features. Finally, we describe the computational resources we used in our experiments.

2.1   Problem definition

Analyzing large graphs is a space intensive operation which usually cannot be performed on a single machine. There are two reasons why a graph has to be distributed: memory and computation issues. Memory issue occurs when the whole graph should be loaded in RAM. For example, a graph with one billion of edges would require at least $8|E|$ bytes of space to store information about the edges, where E is the set of edges, and this does not include computational overhead — in practice, graph processing would require several times more space. Even if a machine has enough RAM to store and process a graph, it can take an unacceptably long time if a graph is not-partitioned, but is instead processed using a single computational thread.

In order to overcome memory and computational issues, we need to partition a graph into several components. Then, a partitioned graph can be processed in parallel on multiple cores independently of whether they are on the same machine or not. Naturally, the size of each component is smaller than the original graph, which leads to smaller memory requirements.

There has been a lot of work dedicated to designing programming models and building distributed middleware graph processing systems to perform such a computation on a set of machines. A partitioned graph is distributed over a set of machines. Each machine then processes only one subset of the graph — a component — although it needs to periodically share intermediate-computation results with the other machines.

Naturally, to find an optimal partition, graph partitioning problems arise.

Graph partitioning splits a graph into several sub-graphs so that achieve better computational time of a graph processing algorithm under two conflicting aspects. The first aspect — balance — says that the size of each component should be almost the same. It comes from the fact that graphs are processed by clusters of machines and if one machine has too big component then it will slow down the whole execution. The second aspect — communication — says that partitioning should reduce how much components overlap with each other. As a trivial example, if a graph has different disconnected components and each executor gets assigned one of them, executors can in many cases work almost independently.

Graph partitioning is different from graph clustering and community detection problems. The number of clusters is not given in clustering problems whether in graph partitioning the number of components is given and it is multiple to some specific computational resource such as number of the threads available. Comparing to community detection, graph partitioning has an additional constraint which is balance, i.e., size of all the partitions should be relatively the same.

Partitioning algorithms (partitioners) take as an input a graph, and split it into N components. In particular, we are interested in partitioners that can be executed in a distributed way. A distributed partitioner is an algorithm which is composed of several instances, where each instance performs partitioning using the same algorithm but on a different components of graph. Each instance represents a copy of algorithm with the unique component of the graph and some resources assigned to it, such as computational threads and RAM. Instances of the distributed partitioner may or may not communicate among themselves. In what follows, we assume the number of instances of a distributed partitioner equals N, the number of components of the graph.

While partitioning can significantly affect the total execution time of graph processing algorithms executed on a partitioned graph, finding a relatively good partition is intrinsically an NP hard problem, whose state space is $N^{|E|}$, i.e., we can place each of $|E|$ edges in N components.

Moreover, before finding an appropriate partitioning, tuning the cluster and the different application parameters can be itself a hard problem [1].

In practice, existing partitioners rely on heuristics to find good enough trade-offs between balance and communication properties. It is always possible to sacri-

fice balance in favor of communication and vice versa, e.g., we can achieve perfect balance by partitioning edges or vertices in a round robin fashion or we can keep the whole graph in a single component and get the worst balance with the best communication property.

Two approaches were developed to tackle graph partitioning problem: vertex and edge partitioning (see Figure 2.1). A classic way to distribute a graph is the *vertex partitioning* approach (also called edge-cut partitioning) where vertices are assigned to different components. An edge is *cut*, if its vertices belong to two different components. *Vertex* partioners try then to minimize the number of edges cut. More recently, *edge partitioning* (so-called vertex-cut partitioning) has been proposed and advocated [2] as a better approach to process graphs with a power-law degree distribution [3] (power-law graphs are common in real-world datasets [4, 5]). In this case, edges are mapped to components and vertices are cut if their edges happen to be assigned to different components. The improvement can be qualitatively explained with the presence, in a power-law graph, of hubs, i.e., nodes with degree much larger than the average. In a vertex partitioning, attributing a hub to a given partition easily leads to i) computation unbalance, if its neighbors are also assigned to the same component, or ii) to a large number of edges cut and then strong communication requirements. An edge partitioning partitioner may instead achieve a better trade-off, by cutting only a limited number of hubs. Analytical support to these findings is presented in [6]. For this reason many new graph computation frameworks, like GraphX [7] and PowerGraph [2], rely on edge partitioning.

2.2   Notations

Let us denote the input directed graph as $\mathcal{G} = (V, E)$, where V is a set of vertices and E is a set of edges. Edge partitioning process splits a set of edges into N disjoint subsets, $E_1, E_2, \ldots, E_N$. We call $E_1, E_2, \ldots, E_N$ a partition of $\mathcal{G}$ and E_i an edge-component (or simply component in what follows). We say that a vertex v belongs to component E_i if at least one of its edges belongs to E_i.

Note that an edge can only belong to one component, but a vertex is at least in one component and at most in N. Let $V(E_i)$ denote the set of vertices that belong
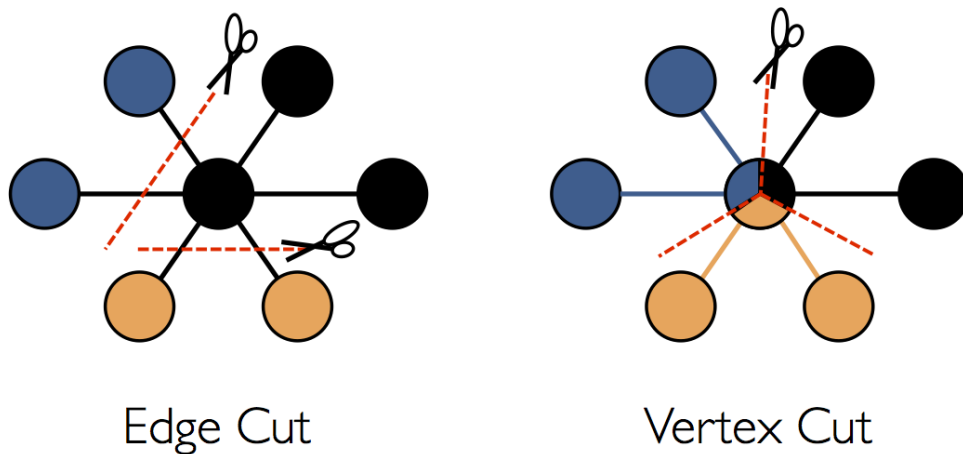
Figure 2.1 – Edge Cut (vertex partitioning) and Verex Cut (edge partitioning) [8]

to component E_i. Let $src(e)$ and $dst(e)$ denote the source and destination vertices of an edge e respectively. $E(V(E_i)) \triangleq \{e \in E_i : src(e) \in V(E_i) \lor dst(e) \in V(E_i)\}$ denotes the set of edge which are attached to vertices attached to the set of edge E_i. The vertices that appear in more than one component are called frontier vertices. Each frontier vertex has then been cut at least once. $F(E_i)$ denotes the set of frontier vertices that are inside component E_i, and $\bar{F}(E_i) \triangleq V(E_i) \backslash F(E_i)$ denotes the set of vertices in component E_i that were not cut.

2.3 Partition quality

Different partitioners provide different partitions, however it is not obvious which partition is better. Partition quality can be evaluated in two ways. One way is to evaluate the effect of the partition on the algorithm we want to execute on the graph, e.g., in terms of the total execution time or total communication overhead. While this analysis provides the definitive answer, it is clear that we would like to choose the best partition before running an algorithm. The second way uses metrics which can be computed directly from the partition without the need to run the target algorithm. We call the first set of metrics execution metrics and the second one partition metrics.

2.3.1   Execution metrics

A partition is better than another if it reduces the execution time of the specific algorithm we want to run on the graph. In some cases the partitioning time itself may not be negligible and then we want to take it into account while comparing the total execution times.

Partitioning time: it is time spent to partition a graph using a particular computing resources. This metric shows how fast a partitioner works and not the final effect on the partitioned graph.

Execution time: this metric measures the execution time of a graph processing algorithm (such as `Connected Components`, `PageRank`, `Single Source Shortest Path`, etc.) on a partitioned graph using some specific computing resources.

Some other metrics may be used as proxies for these quantities.

Network communication: it measures in bytes of traffic or in number of logical messages, how much information has been exchanged during the partitioning or the execution of graph processing algorithms.

Rounds: this metric indicates the number of rounds (iterations) performed by the partitioner. It can only be applied to iterative partitioners. This metric is useful to compare the impact of a modification of a partitioner and to evaluate its convergence speed. This metric can provide an indication of the total partitioning time.

2.3.2   Partition metrics

Partition metrics can be split into two groups. In the first group there are the metrics that quantify *balance*, i.e., how homogeneous the partitions' sizes are. The underlying idea is that if one component is much larger that the others, the computational load on the corresponding machine is higher and then this machine can slow down the whole execution. The metrics in the second group quantify *communication*, i.e., how much overlap there is among the different components, i.e., how many vertices appear in multiple components. This overlap is a reasonable proxy for the amount of inter-machine communication that will be required to merge the results of the local computations. The first two metrics below are *balance metrics*, all the other ones are *communication metrics*.

Balance (denoted as BAL): it is the ratio of the maximum number of edges in a component to the average number of edges across all the components:

$$\text{BAL} = \frac{\max\limits_{i=1,...N} |E_i|}{|E|/N}.$$

Standard deviation of partition size (denoted as STD): it is the normalized standard deviation of the number of edges in each component:

$$\text{STD} = \sqrt{\frac{1}{N} \sum_{i=1}^{N} \left(\frac{|E_i|}{|E|/N} - 1 \right)^2}$$

Replication factor (denoted as RF): it is the ratio of the number of vertices in all the components to the number of vertices in the original graph. It measures the overhead, in terms of vertices, induced by the partitioning. The overhead appears due to the fact that some vertices get cut by graph partitioning algorithm.

$$\text{RF} = \sum_{i=1}^{N} |V(E_i)| \frac{1}{|V|}$$

Communication cost (denoted as CC): it is defined as the total number of frontier vertices and measures communication overhead due to the fact that framework will synchronize states of vertices that were cut:

$$\text{CC} = \sum_{i=1}^{N} |F(E_i)|$$

Vertex-cut (denoted as VC): this metric measures how many times vertices were cut. For example, if a vertex is cut in 5 pieces, then its contribution to this metric is 4.

$$\text{VC} = \sum_{i=1}^{N} F(E_i) + \sum_{i=1}^{N} \bar{F}(E_i) - |V|$$

Normalized vertex-cut: it is a ratio of the *vertex-cut* metric of the partitioned graph to the expected *vertex-cut* of a randomly partitioned graph.

Expansion: it was originally introduced in [9, 10] in the context of vertex

partitioning. In [11] *expansion* was adapted to edge partitioning approach. It measures the largest portion of frontier vertices across all the components.

$$\text{Expansion} = \max_{i=1,\dots N} \frac{|F(E_i)|}{|V(E_i)|}$$

Modularity: as *expansion*, *modularity* was proposed in [9, 10] and later adapted to edge partitioning approach in [11] as follows[1]:

$$\text{Modularity} = \sum_{i=1}^{N} \left(\frac{|V(E_i)|}{|V|} - \left(\sum_{j \neq i} \frac{|F(E_i) \cap F(E_j)|}{|V|} \right)^2 \right)$$

The *modularity* measures density of the components — how many vertices are inside component comparing to those that are between components. The higher it is, the better is partitioning.

It should be noticed that RF, CC, and VC metrics are linear combinations of each others:

$$\begin{aligned}
\text{RF} &= \sum_{i=1}^{N} |V(E_i)| \frac{1}{|V|} \\
&= \sum_{i=1}^{N} (|\bar{F}(E_i)| + |F(E_i)|) \frac{1}{|V|} \\
&= 1 - \frac{\text{VC}}{|V|} + \frac{\text{CC}}{|V|}
\end{aligned}$$

In the next chapter we evaluate if these metrics are indeed good proxies for the final execution time of different algorithms.

2.4   Pregel model

We will briefly overview the Pregel model [12] which is illustrated in Figure 2.2. Pregel introduces a computational model where a graph processing algorithm is executed in an iterative way. Each iteration is called a *superstep*. Vertices can be

---

[1]Both expansion and modularity could also be defined normalized to the number of edges rather than to the number of vertices.
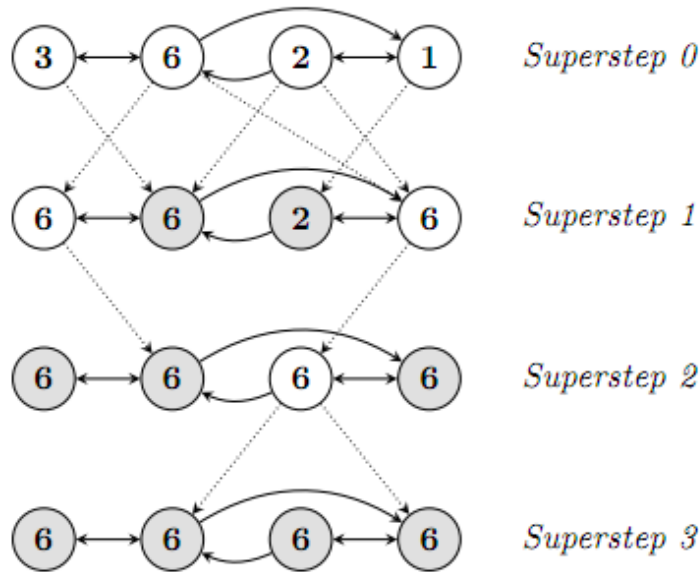
Figure 2.2 – Pregel model [12]

either active or inactive. At *superstep* 0 all vertices are active. Each active vertex computes some function during a superstep and then becomes inactive. Each vertex has the possibility to send a message through outgoing edges to neighbor vertices and this message will be available only in the next superstep. All vertices that received some messages become active until they explicitly decides to turn to inactive. After all messages are received, a new *superstep* can start: all vertices that received messages will perform some local computations. All messages sent to a vertex are aggregated into a single message using some commutative function.

The Pregel API consists of three basic functions, which developer should implement: *sendMessage*, *mergeMessage* and *applyMessage*. *sendMessage* takes an edge and produces messages to none, one, or both of the adjacent vertices. All messages dedicated to one vertex are merged in a single message by *mergeMessage*. Finally, *applyMessage* uses a merged message and a vertex value to produce a new vertex value which will replace the previous one.

2.5   Apache Spark

Apache Spark [13] is a large-scale distributed framework for general purpose data processing. It relies on the concept of Resilient Distributed Dataset [14] (see Section 2.5.1) and Bulk Synchronous Parallel (see Section 2.5.2) model. Spark basic functionality (Spark Core) covers: scheduling, distributing, and monitoring jobs, memory management, cache management, fault recovery, and communication with data source.

Spark itself is implemented on a JVM [15] program, using the Scala [16] programming language.

Spark can use three cluster managers: *Standalone* (a native part of Spark), *Apache Mesos*, [17] and *Hadoop YARN* [18]. All these cluster managers consist of one *master* program and several *worker* programs. Several Spark applications can be executed by one cluster manager simultaneously. A Spark application launched, using one of the scripts provided by Spark, on the *driver* machine, is called a *driver* program (see Figure 2.3). The *driver* program connects to a *master* program, which allocates resources on *worker* machines and instantiates one *executor* program on each *worker* machine. Each *executor* may operate several components using several cores. *Driver*, *master*, and *worker* programs are implemented as Akka actors [19].

Fault tolerance in Spark is implemented in the following manner. In case a task failed during execution but the executor is still work, then this task is rescheduled on the same executor. Spark limits (by the property *spark.task.maxFailures*) how many times a task can be rescheduled before finally giving up on the whole job. In case the cluster manager loses a worker (basically the machine stops responding) then the cluster manager reschedules tasks previously assigned to the working machine. It is easy to reschedule a failed task thanks to the fact that all RDDs (see next section) are computed as ancestor of other RDDs, according to the principle of RDD lineage [20].
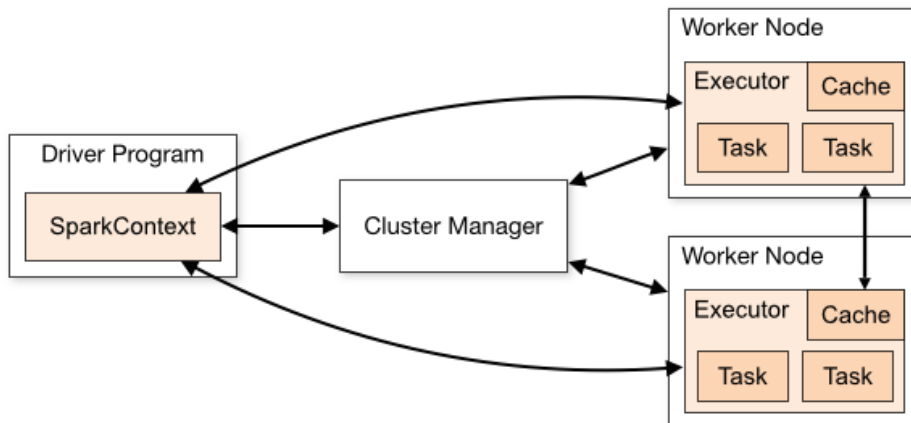
Figure 2.3 – Spark standalone cluster architecture [21]

2.5.1 Resilient Distributed Dataset

A Resilient Distributed Dataset (RDD) is an immutable, distributed, lazy-evaluated collection with predefined set of operations. An RDD can be created from either raw data or another RDD (called parent RDD). An RDD is partitioned collection, and its components are distributed among the machines of the computational cluster. Remember that both an RDD and a partitioned graph are distributed data structures, which are partitioned into components. Note that the number of components N can be different from the number N_m of machines, i.e multiple components can be assigned to one machine . The set of operations which can be applied to an RDD came from the functional programming paradigm. The advantage is that the developer should only correctly utilize RDD operations but should not take care of synchronization and information distribution over the cluster, which come out-of-the-box. This advantage comes at the price of a more restricted set of operations available.

One of the main ideas behind RDD is to reduce slow[2] interaction with hard-disk by keeping as much as possible in RAM memory. Usually, the whole sequence of RDDs is stored in RAM memory without saving it to the file system. Nevertheless, it can be impossible to avoid using hard-disk, despite of the fact that Spark uses

---

[2]Approximately, sequential access to a hard-disk is about 6 times slower and random access 100,000 slower, than access to RAM, according to [22].

memory serialization (to reduce memory occupation) and lazy-evaluation.

There are two kinds of operations that can be executed on RDDs: transformations and actions. All transformations are lazy evaluated operations which create a new RDD from an existing RDD. There are two types of transformations: *narrow* and *wide* (see Figure 2.4).

Narrow transformations preserve partitioning between parent and child RDD and do not require inter-node communication/synchronization. *Filter, map, flatMap* are the examples of *narrow* transformations (all of them are related to functions in functional programming). Let us consider the *filter* transformation: it is a higher-order function, which requires a function that takes an item of an RDD and returns a boolean value (basically it is a predicate). After we apply a *filter* transformation to an RDD $r1$, we get a new RDD $r2$, which contains only those items from $r1$, on which the predicate given to *filter* returned the *true* value.

A *wide* transformation requires inter-node communication (so-called *shuffles*). Examples of wide transformations are *groupByKey, reduceByKey, sortByKey, join* and so on. Let us consider the *groupByKey* transformation. It requires that items of the RDD (on which it will be applied) are represented as key-value pairs. For example, we have the following component:

$$component = [(k1, v1), (k2, v2), (k2, v3), (k1, v4), (k1, v5), (k3, v6), (k3, v7), \dots]$$

Initially, each component contains some part of the RDD, *groupByKey* first groups key-value pairs with similar ids in each component independently (this preparation require inter-node communication):

$$k1 \Rightarrow [v1, v4, v5]$$
$$k2 \Rightarrow [v2, v3]$$
$$k3 \Rightarrow [v6, v7]$$
$$\dots$$

Then each component sends all its groups to the dedicated components according to the key of the group. Each key is related to one component by using *Hash-*
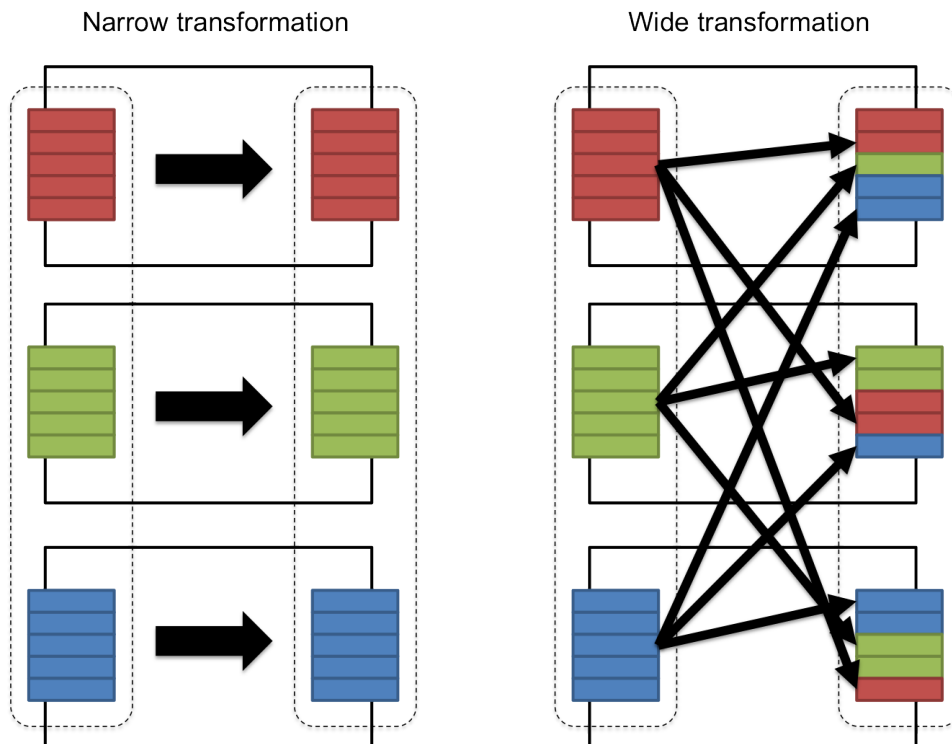
Figure 2.4 – Narrow and wide transformations [23]

Partitioner.[3] In this way, a *groupByKey* transformation can compute to which component each key belongs. After it has computed all $N - 1$ (remember that N is number of components) messages to others components (all groups dedicated to one component form single message), it can start to send them as following:

$$messageForComponent0 \Rightarrow [k3 \Rightarrow [v6, v7], k2 \Rightarrow [v2, v3]]$$
$$messageForComponent1 \Rightarrow [k1 \Rightarrow [v1, v4, v5]]$$

$$\ldots$$

After a component has received all messages dedicated to it, it can finally merge all the groups of key-values.

An action returns some value from an existing RDD, e.g., *first*, *collect*, *reduce* and so on. Only when an action is called on an RDD, it is actually evalu-

---

[3]It partitions based on key by using hash funciton.

ated. An invoked action submits a job to the DAGScheduler, the class responsible for scheduling in Spark. A submitted job represents a logical computation plan made from a sequence of RDD transformations with an action at the end. The DAGScheduler creates a physical computation plan which is represented as a directed acyclic graph (DAG) of stages (see Figure 2.5). There are two types of stages: ResultStage and ShuffleMapStage. The DAG is ended with a ResultStage. Each ShuffleMapStage stage consists of sequence of narrow transformations followed by a wide transformation. Each stage is split in N tasks.

In-memory caching in Spark follows Least Recently Used (LRU) policy [24]. Spark does not support automatic caching. Instead, the Spark user has to explicitly specify which RDD he/she would like to cache, and then the framework may cache it. If there is not enough space to cache, Spark applies LRU policy and removes some other RDDs from the cache. The user also can directly request to uncache an RDD.

To recap, Spark is based on several trending ideas:

– immutable collections (RDD), which simplify coding process;

– limited number of operations (transformations and actions) — users are restricted to use pure functions [25];

– use of RAM instead of disk, which accelerate computations.

2.5.2   Bulk Synchronous Parallel model

The Bulk Synchronous Parallel model(BSP) [27] is an abstract model, which is built on iterations. Each iteration consists of two parts: a local computation and a global information exchange. Each executor computes its own component of distributed data structure independently and after sends messages to other executors. A new iteration does not start until all components have received all messages dedicated to them (see Figure 2.6). This way, BSP implements a barrier synchronization mechanism [28, Chapter 17].

The total time of an iteration consist of three parts: the time to perform local computation by the slowest machine, the time to exchange messages, and, finally, the time to process barrier synchronization.
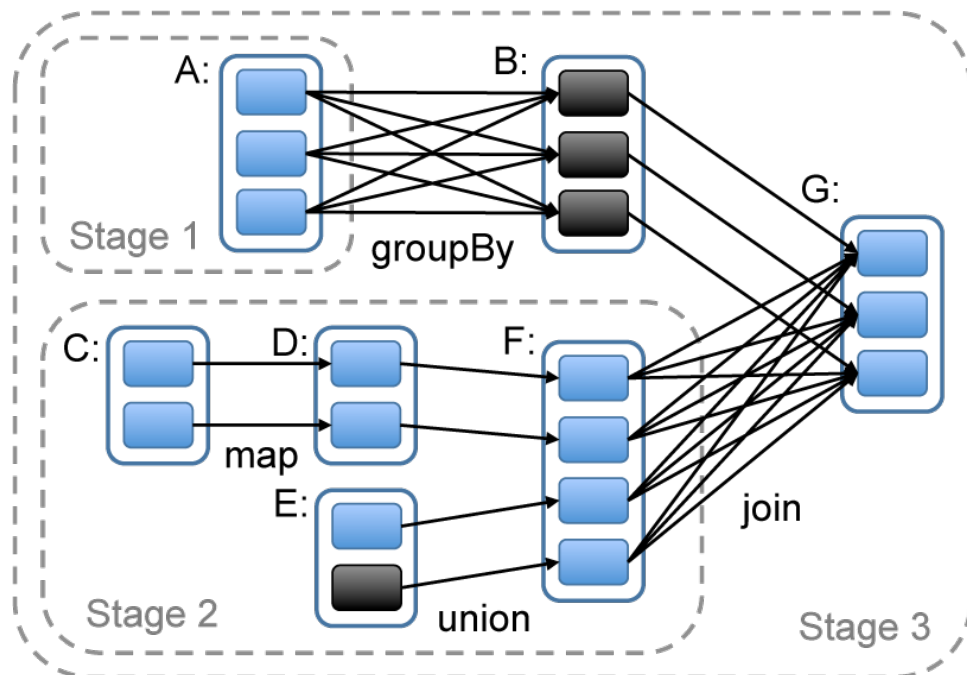
Figure 2.5 – Under The Hood: DAG Scheduler [26], where from **A**, **B**, **C**, **D**, **E**, **F** RDDs created **G** RDD.

In order to illustrate the application of BSP model in Spark, we consider the following sequence of transformations applied to RDD: *filter*, *map*, *reduceByKey*. The first two transformations are *narrow* one, thus they will be executed during a local computation step on each executor without synchronization (basically sequences of *narrow* transformations are squeezed in one transformation). Next the *reduceByKey* will be executed during a global information exchange.

2.5.3 GraphX

In this section we focus on the GraphX framework and the reasons why we selected it for our computations. In Section 2.6 we present the other graph processing frameworks which we considered while choosing the framework for our experiments.

GraphX [7] is an Apache Spark's API for graph data processing. GraphX programs are executed as Spark jobs. The framework relies on a vertex-cut partitioning approach and implements Pregel API as well.

A graph is stored in GraphX as two RDDs: a vertex RDD and an edge RDD.

Processors

Local
Computation

Communication

Barrier
Synchronisation
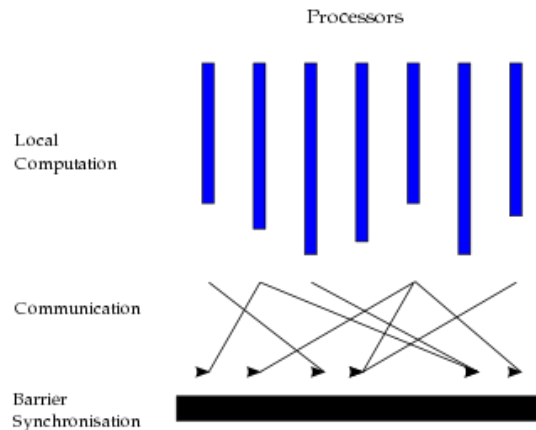
Figure 2.6 – Bulk synchronous parallel model [29]

A vertex RDD stores the ids of the vertices and their values. An edge RDD stores source and destination ids, and the values assigned to the edges. Each of these RDDs is split in N components, each assigned to a different executor.[4] A vertex RDD is always partitioned by a hash function based on the vertex ids, while the edge RDD is partitioned using a user-specified partitioner, i.e., usually graphs have much less vertices than edges, thus effect of partitioning of the vertex RDD is negligible. GraphX distributes the N components among the machines in a round robin fashion.

By default, GraphX considers all input graphs as directed ones, but an algorithm can work on its input as if it was an undirected graph. This is, for example, the case of the `Connected Components` algorithm built-in in GraphX. Other algorithms, like the GraphX implementation of `PageRank` [30], instead assume the input is directed. In this case, if one wants to process an undirected graph, he/she can pre-process the input and replace each undirected edge by two edges with opposite directions. An alternative approach is to modify the algorithm which is executed on a graph. For instance, the `PageRank` algorithm can be easily modified so that it sends messages in both directions of an edge.

---

[4]It is also possible to assign multiple partitions to the same executor, but we do not consider this possibility.

We have selected GraphX as a system on which we perform our experiments due to multiple reasons:

– GraphX is free to use;

– it supports edge partitioning;

– it is still under development and maintenance;

– it is built on top of Spark. Most of the effective solutions are based on Hadoop or Spark. As we discuss in the following section, we believe that Spark is more promising than Hadoop.

2.6 Other graph processing systems

In addition to GraphX, there are many frameworks for distributed graph processing, such as PowerGraph [2], Distributed GraphLab [31], Giraph [32], Giraph+ [33], etc.

According to the survey [34] parallel graph processing frameworks may be classified by programming model, by communication model, by execution model, by the platform on which their run.

There are few frameworks that support edge partitioning approach. We consider below those that are the most popular according to the number of citations.

2.6.1 Apache Hadoop

Apache Hadoop [35] is a distributed engine for general data processing and is probably one of the most popular ones. It is an open source implementation of the MapReduce framework [36]. Hadoop splits the original data-set into a number of chunks. A chunk is a sorted sequence of key-value pairs. Each chunk is independently processed in parallel by the *map* function. *Map* is a higher-order function [37], which requires, as an input, an argument function that takes a key-value pair and returns a sequence of key-values pairs: $< k1, v1 > \Rightarrow [< k2, v2 >]*$. The output of the *map* function is sorted and after, is processed by the *reduce* function. The *reduce* function requires as input argument function which takes

as input a sequence of values with the same key and returns a single value:
$< k2, [v2] > \Rightarrow < k2, v3 >$.

A distributed engine for data processing requires a distributed file system:
Hadoop uses the Hadoop Distributed File System (HDFS) [38]. An HDFS cluster
(see Figure 2.7) consists of a single master, called *Namenode* and several slaves,
called *Datanode*. *Namenode* is a global entry point of the HDFS cluster, and also
manages the global filesystem namespace. When a user stores a file in HDFS,
the *Namenode* splits it in several blocks, and distributes these blocks among the
Datanodes. In order to support fault tolerance, data blocks are replicated, by
default, three times. From the user point of view, HDFS provides usual hierarchical
file organization; it is possible to create/remove/rename files/directories.

As cluster manager Hadoop uses Yet Another Resource Negotiator (YARN) [18].
YARN provides such properties as scalability, reliability, fairness and locality. The
YARN system consists of a single master machine and multiple worker machines.
A *ResourceManager* (RM) daemon is installed on the master machine, and a
NodeManager (NM) is installed on slaves machine. The *ResourceManager* is the
central authority which controls resource usage and liveness of the nodes. Accepted
jobs (which were submitted to the RM through a public interface) are passed to
the scheduler. When there are enough resources, the scheduler starts the job by
instantiating an *ApplicationMaster* (AM). The AM is responsible for the job man-
aging, including changing dynamically resources consumption and error handling.
The AM starts by requesting resources from the RM. Resources provided by the
RM are called *containers*. A *Container* is a logical bundle of resources (e.g., "4GB
RAM, 2 CPU") which is related to a particular worker machine. One NM can
host several containers, each of these containers is related to a different AM, and
different user jobs/applications.

It is possible to process graphs using Hadoop, but, as it is the same for Spark,
this is not a very convenient way to process graphs. It is better to use some
superstructure on top of Hadoop or Spark (Giraph and GraphX respectively).

Spark provides much more higher-order functions than Hadoop which has only
map and *reduce*. Moreover, compared to Spark, Hadoop intensively uses the file
system (basically Spark creates RDDs in memory whether Hadoop saves all inter-
mediate results to the file system).
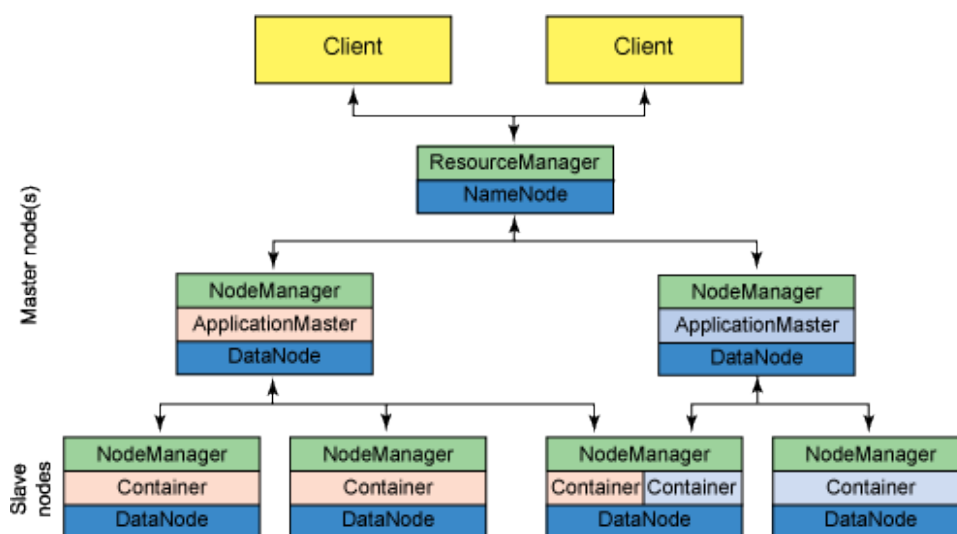
Figure 2.7 – YARN and HDFS nodes [35]

2.6.2 Giraph

Giraph [32] is an iterative graph processing framework, which is built on top of Hadoop, and an open-source implementation of Pregel [12]. Giraph also extends the Pregel model by providing shared aggregators, master computation, out-of-core computation, and more.

Master computations are optional centralized computations which take place before each *superstep*. They are implemented in the *MasterCompute* class. They can be used to change graph computation classes during run-time or to operate aggregators.

Aggregators are functions with associated values. The master node registers and initializes an aggregator with a commutative and associative function and initial value respectively in the *MasterCompute* class. A copy of the initial value is communicated to each worker. During each superstep each worker has read-only access to this value. Moreover, a worker can add a value to a given aggregator. At the end of the superstep, all values that were added to the aggregator are aggregated using the aggregator function into a single value. After, the *MasterCompute* can modify the aggregated value. There are two types of aggregators: persistent and nonpersistent. Nonpersistent aggregators reset their value to the initial value before aggregating values added from workers. Persistent aggregators do not reset

their values.

Giraph was designed to perform all computation in RAM. Unfortunately, it is not always possible, that is why Giraph can spill some data to hard disk. In order to reduce random swapping, user can use the out-of-core feature which allows explicit swapping. Developer can specify how many graph components or messages should be stored in-memory, while all rest will be spilled on disk using LRU policy [24].

Some application may intensively use messages which can exceed the memory limit. Usually, this issue can be easily solved by aggregating messages, but it can work only if messages are *aggregatable*, i.e., there should be an operation, which can merge two messages in one. This operation should be commutative and associative. Unfortunately, this is not always the case. For this reason, a *superstep splitting* technique was developed. It allows splitting a superstep into several iterations. During each iteration, each vertex sends messages only to some subset of its neighbors, so that, after all iterations of the superstep each vertex has sent messages to all its neighbors. Of course, there are some limitations:

– the function which updates vertex values after receiving fragments of all messages dedicated to this vertex should be aggregatable;

– the maximum amount of messages between two machines should fit in memory.

2.6.3   Giraph++

Giraph++ [33] is an extension of Giraph. This framework is based on a different conceptual model. It supports a graph-centric model instead of a vertex-centric, which means that instead of processing in parallel each set of vertices or edges, it processes some sub-graphs. The vertex-centric model is much easier to use. However, in Pregel (implemented in Giraph), a vertex has access only to the immediate neighbors and message from a vertex can only be sent to the direct neighbors. That is why, it takes a lot of supersteps to propagate some information from the source and destination vertices which appear in the same component.

In the graph-centric models the user operates on the whole component. There are two kinds of vertices: *internal* and *boundary* ones. An *internal* vertex appears

only in one component, a *boundary* one in multiple ones.

Giraph++ also performs a sequence of supersteps, and in each superstep, a user function is executed on each component. After this computation, the system synchronizes states of *boundary* vertices, because they connect components with each others.

2.6.4 Distributed GraphLab

The Distributed GraphLab [31] framework introduces a new asynchronous, dynamic, graph-parallel computation abstraction. It does not require iterative computation, but parallel asynchronous computations. Distributed GraphLab is based on three abstractions: the data graph, the update function, and the sync operation. The data graph is a directed graph which can store an arbitrary value associated with any vertex or edge. The update is a pure function which takes as input a vertex v and its scope S_v, and returns the new version of the scope and a set of vertices T. The scope of vertex v is the data associated with vertex v, and with adjacent edges and vertices. The update function has mutual exclusion access to the scope S_v. After the update function is computed, a new version of the scope replaces the older one and releases the lock. Eventually the set of vertices T will be processed in an update function (see Algorithm 1), that schedules future execution of itself on other vertices.

1: $T \leftarrow v_1, v_2, ...$ ▷ initial set of vertices
2: **while** $|T| > 0$ **do**
3:      $u \leftarrow removeVertex(T)$
4:      $(T', S_v) \leftarrow updateFunction(v, S_v)$
5:      $T \leftarrow T \cup T'$
6: **end while**

Algorithm 1 Execution model of Distributed GraphLab

Moreover, Distributed GraphLab supports serializable execution [28, Chapter 3]. In order to implement the chosen consistency level, Distributed GraphLab implements edge consistency and even vertex consistency. Edge consistency make sure that each update function has exclusive rights to read and write to its vertex
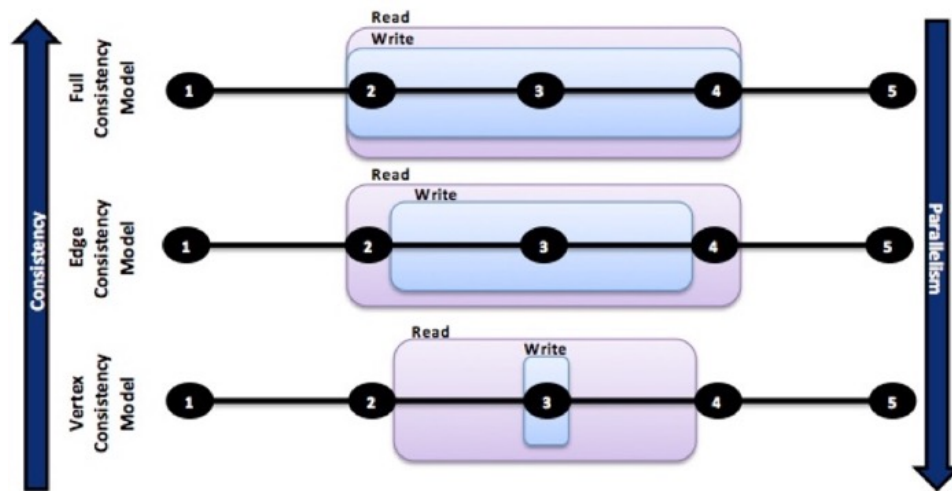
Figure 2.8 – Different consistency models [39] when algorithm tries to update value associated with vertex 3.

and adjacent edges, but read-only access to adjacent vertices. Vertex consistency provides exclusive read-write access to the vertex, and read-only to adjacent edges (see Figure 2.8).

2.6.5   PowerGraph

PowerGraph [2] relies on the GAS model (stands for *Gather*, *Apply* and *Scatter*). The GAS model is a mix of Pregel and Distributed GraphLab models. The GAS model took from Pregel commutative associative combiners. From Distributed GraphLab, the GAS model borrowed data graph and shared-memory view of computation. *Gather*, *Apply* and *Scatter* (GAS API) correspond to Pregel's *mergeMessage*, *applyMessage* and *sendMessage*.

Every Pregel or Distributed GraphLab program can be translated in a GAS model program. Moreover, this framework allows both synchronous (BSP), and asynchronous execution. It looks like asynchronous Pregel execution.

2.7 Computational clusters

In our experiments we used two computational clusters: *Nef cluster sophia* [40] and *Grid5000* [41].

Nef cluster sophia possesses multiple high performance servers, that are combined into a heterogeneous parallel architecture. It currently has 148 machines with more than 1000 cores. The cluster allows direct access to machines with an installed Linux (through *ssh* [42]) and to an already mounted distributed file system.

Grid5000 is a set of sites (each in a different French city), where each site has several clusters. Each cluster has a star network topology. Overall, *Grid5000* has more than 1000 machines with 8000 cores. *Grid5000* provides bare-metal deployment feature [43]. Thus working with Spark on *Grid5000* requires the following preliminary routine steps:

- prepare an image of the linux system with a pre-installed version of Spark

- book cluster resources using *OAR2* [44]

- deploy the prepared image on a cluster using *Kadeploy 3* [45]

- mount the distributed file system

- access cluster machines through *oarsh* [46]

- configure the master machine of the cluster

- launch the experiment

2.8 Conclusion

In this chapter we presented the graph partitioning problem along with metrics for partitioning quality. We have considered GraphX and other graph processing systems. We advocated selection GraphX as system on which we conduct experiments. Moreover, we mentioned computation clusters which are used in our experiments.

Chapter 3

Comparison of GraphX partitioners

Contents

We start our study of edge partitioning by an overview of existing partitioners, for which we provide a taxonomy. We survey published work, comparing these partitioners. Our study suggests that it is not possible to draw a clear conclusion

about their relative performance. For this reason, we performed an experimental
comparison of all the edge partitioners currently available for GraphX. Our results
suggest that `Hybrid-Cut` partitioner provides the best performance.

3.1   Introduction

The first contribution of this chapter is to provide an overview of all edge par-
titioners which, to the best of our knowledge, have been published in the past
years. Beside describing the specific algorithms proposed, we focus on existing
comparisons of their relative performance. It is not easy to draw conclusions
about which are the best partitioners, because research papers often consider a
limited subset of partitioners, different performance metrics and different compu-
tational frameworks. For this reason a second contribution in this chapter is an
evaluation of all the edge partitioners currently implemented for GraphX [7], one
of the most promising graph processing frameworks. Our current results suggest
that `Hybrid-Cut` [47] is probably the best choice, achieving significant reduction
of the execution time with limited time required to partition the graph. Due to
the fact that GraphX does not have a built-in function which provides values for
partitioning metrics, we have implemented a new GraphX functions to compute
them [48].

   This chapter is organized as follows. Section 3.2 presents all existing edge
partitioning algorithms and is followed by a discussion in Section 3.3 about what
can be concluded from the literature. Our experiments with GraphX partitioners
are described in Section 3.4. Finally, Section 3.5 presents our conclusions.

3.2   Classification of the partitioners

In this section we will first provide a classification of the partitioners. We al-
ready mentioned the main distinction between **vertex partitioning** and **edge
partitioning**, and the focus of this work is on the second one.

   We can classify partitioners by the amount of information they require; they
can be **online** or **offline** [49]. **Online** partitioners decide where to assign an edge

on the basis of local information (e.g., about its vertices, and their degrees). For this reason they can easily be distributed. On the contrary, in offline partitioners (like METIS [50]) the choice depends in general on the whole graph and multiple iterations may be needed to produce the final partitioning.

Some partitioner can refine the partitioning during the execution of a graph processing algorithm (e.g., those in Giraph [32]). For example, after several iterations of the `PageRank` algorithm, the graph can be re-partitioned, based on the current execution time of the algorithm itself.

Most of the non-iterative algorithms have a time complexity $\mathcal{O}(|E|)$, thus iterative algorithms have $\mathcal{O}(k|E|)$ time complexity, where k is the number of iterations of the partitioner.

In the rest of the section we introduce our own classification of partitioners, and we classify 16 partitioners according to our taxonomy. Table 3.1 provides a list of references where the following algorithms were first described or implemented.

3.2.1   Random assignment

The *random assignment* approach includes partitioners that randomly assign edges using a hash function based on some value of the edge or of its vertices. Sometimes, the input value of the hash function is not specified (e.g., [52]). Because of the law of large numbers, the random partitions will have similar sizes, thus these partitioners achieve good balance. The following partitioners adopt this approach.

RandomVertexCut

`RandomVertexCut` (denoted as RVC) partitioner randomly assigns edges to components to achieve good balance (with high probability) using a hash value computed for each source vertex id and destination vertex id pair. The hash space is partitioned in N sets with the same size. As a result, in a multigraph all edges with the same source and destination vertices are assigned to the same component. On the contrary, two edges among the same nodes but with opposite directions belong in general to different components.

Table 3.1 – Metrics used to evaluate partitioners grouped by papers (ET - execution time, PT - partitioning time, RF - replication factor, CC - communication cost, VC - vertex-cut)

Ref.	Partitioners	Execution metrics	Partitioning metrics
[2]	CanonicalRandomVertexCut	PT and ET (PowerGraph)	RF
	Greedy-Coordinated		
	Greedy-Oblivious		
[49]	RandomVertexCut	ET (GraphBuilder)	RF
	Greedy-Coordinated		
	Grid Greedy		
	Torus Greedy		
	Grid	-	
	Torus	-	
[51]	DFEP	ET and rounds (Hadoop and GraphX)	Balance, CC, STD
	DFEPC		
	JA-BE-JA	Rounds	
	Greedy-Coordinated	-	Balance and CC
	Greedy-Oblivious		
[52]	Random	-	VC, normalized VC, STD
	DFEP		
	DFEPC		
	JA-BE-JA		
	JA-BE-JA-VC		
[47]	Hybrid-Cut	ET(PowerLyra)	RF
	Ginger		
	Greedy-Coordinated		
	Greedy-Oblivious		
	Grid		
[53]	BiCut	ET and normalized network traffic (GraphLab)	RF
	Aweto		
	Grid		
[7]	RandomVertexCut	-	-
	CanonicalRandomVertexCut		
	EdgePartition1D		
	Grid		

CanonicalRandomVertexCut

`CanonicalRandomVertexCut` (denoted CRVC) works similar to RVC but first it orders two values of each edge: source vertex id and destination vertex id of this edge. Then, it applies the previous hash function and a modulo operation to obtain a hash value. Ordering values allows placing opposite directed edges that connect the same vertices into the same partition.

EdgePartition1D

`EdgePartition1D` is similar to `RandomVertexCut` but uses only the source vertex id of the edge in the hash function. Hence, all outgoing edges of the vertex will be placed in the same component. If the graph has nodes with very large out degree, this partitions will lead to poor balance.

Randomized Bipartite-cut (BiCut)

This partitioner is applicable only for bipartite-oriented graphs.[1] This partitioner relies on the idea that random assigning the vertices of one of the two independent sets of a bipartite graph may not introduce any replica. In particular, `BiCut` selects the largest set of independent vertices (vertices that are not connected by edges), and then splits it randomly into N subsets. Then, a component is created from all the edges connected to the corresponding subset (see Figure 3.1).

3.2.2 Segmenting the hash space

This approach complements random assignment with a segmentation of the hash space using some geometrical forms such as grids, torus, etc. It maintains the good balance of the previous partitioners, while trying to limit communication cost. For graph these partitioners can generate some upper bounds for the *replication factor* metric.

---

[1]Graph whose set of vertices can be split into two disjoint sets U and V, and every edge connects vertex from U and V
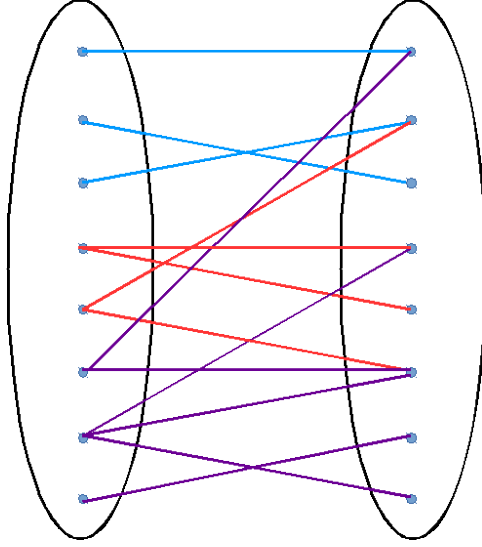
Figure 3.1 – Partition of bipaprtite graph into 3 components. First component has 3 blue edges. Second component has 4 red edges. Third component has 6 violet edges.

Grid-based Constrained Random Vertex-cuts (Grid)

It partitions edges in some *logical* grid G (see Figure 3.2) by using a simple hash function. G consists of M rows and columns, where $M \triangleq \lceil \sqrt{N} \rceil$ (N is number of components). For example the `EdgePartition2D` partitioner in [7] maps the source vertex to a column of G and the destination vertex to a row of G. The edge is then placed in the cell at the column-row intersection. All cells are assigned to components in a round robin fashion.

If $M = \sqrt{N}$ then one cell is assigned to one component, otherwise, if N is not a square number, then components will have either one or two cells. In the last case, we can roughly calculate *balance* metric (ratio between biggest component and average component size). Biggest component would have $2\frac{|E|}{M^2}$ edges, because two cells were assigned to it. Average number of edges in a component is still $\frac{|E|}{N}$. Hence, balance equals $\frac{2N}{M^2}$.

This partitioner guarantees that the RF is upper-bounded by $2\lceil \sqrt{n} \rceil - 1$, which is usually never reached.

A variant of this algorithm is proposed in [49], where two different column-row pairs are selected for the source and the destination and then the edge is randomly
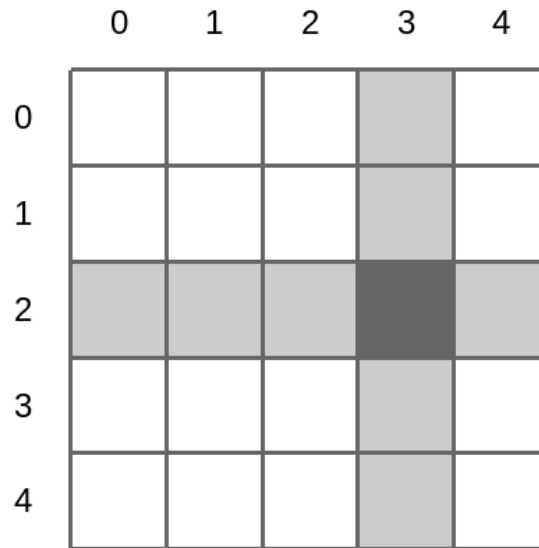
Figure 3.2 – Gird partitioning. Source vertex corresponds to row 2 and destination vertex corresponds to column 3.

assigned to one of the cell belonging to both pairs.

Torus-based Constrained Random Vertex-cuts (Torus)

It is similar to the `Grid` partitioner considered in [49] but relies on a *logical* 2D torus T (see Figure 3.3). Each vertex is mapped to one column and to $\frac{1}{2}R + 1$ cells of a given row of T, where R is the number of cells in a row. The rational behind $\frac{1}{2}R + 1$ is that, we do not want to use all the cells in the row to decrease an upper bound for *replication factor*. Thus, we use only half of cells in a row, plus one more — to be sure that two sets of cells (for source and for destination vertex) will overlap.

Then, as the previous partitioner, this consider the cells at the intersection of the two sets identified for the two vertices, and randomly selects one of them (again, cells are assigned to components in round robin fashion). In this way, the *replication factor* has an upper bound equal to $1.5\sqrt{N} + 1$.
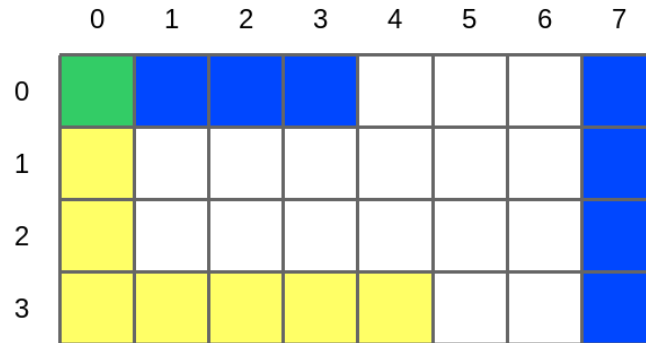
Figure 3.3 – Torus partitioner. Source vertex corresponds to row 3 and column 0, destination vertex corresponds to row 0 and column 7. These cells intersect in cell $(0, 0)$.

3.2.3   Greedy approach

During the edge assignment process, greedy partitioners assign each edge to a component in order to minimize the current communication metrics value. Basically, these partitioners first compute a subset of components where the edge can be placed. Then, they place the edge in a component that already contains edges with one of the same vertices.

Greedy Vertex-Cuts

To place the ith edge, this partitioner considers where the previous $i - 1$ edges have been assigned. Essentially, it tries to place an edge in a component which already contains the source and the destination vertices of this edge. If it is not possible, then it tries to allocate the edge to a component which contains at least one vertex of this edge. If no such a component can be found, the edge is assigned to the component that is currently the smallest one. The main difficulty here is to know where the previous $i - 1$ edges were assigned. Intrinsically, all partitioners should work in a distributed way, that is why, knowing where $i - 1$ edges were assigned becomes a non-trivial task. To solve this issue, the authors proposed a distributed implementation of this approach called `Coordinated Greedy Vertex-Cuts` (`Greedy-Coordinated` in what follows). This implementation requires communication among the different instances of the partitioner, however,

it can be too costly. Hence, the authors also introduced a *relaxed* version called `Oblivious Greedy Vertex-Cuts` (`Greedy-Oblivious` in what follows), where no communication is required among the different instances of the partitioner, but each instance remembers its own assignments. Each instance of the partitioner greedily assigns an edge as described above but only considering its own previous choices.

Grid-based Constrained Greedy Vertex-cuts (Grid Greedy)

As the `Grid` partitioner proposed in [49], it relies on a *logical* grid. Instead of randomly selecting one cell from the intersection of cells, it selects a cell using the same greedy criterium as in Section 3.2.3.

The issue here is to remember previous assignments. As in previous case, there can be correct expensive solution, where after each assignment of N edges (because we have N instances of the partitioner) we have to propagate all the information between all the instances, even though it does not support *serializability*.[2] Again, this partitioner can be implemented as the `Greedy-Oblivious` partitioner: each instance remembers only its own assignments.

Torus-based Constrained Greedy Vertex-cuts (Torus Greedy)

It is a greedy version of the `Torus` algorithm. First, like `Torus`, it computes two pairs of row-column in 2D torus T, which correspond to source and destination vertices. Second, it finds an intersection of cells of these two pairs of row-column. Finally, it selects one cell from the intersection according to the greedy heuristic as in Section 3.2.3.

Distributed Funding-based Edge Partitioning (DFEP)

This partitioner was proposed in [51] and implemented for both Hadoop [35] and Spark [13]. In the `DFEP` algorithm each component initially receives a randomly assigned vertex and then tries to progressively grow by including all the edges of the vertices currently in the component that are not yet assigned. In order to avoid

---

[2]*Serializability* property says that concurrent operations applied to a shared object appear as *some* serial execution of these operations.

a dishomogeneous growth of the components, a virtual currency is introduced and each component receives an initial funding that can be used to bid on the edges. Periodically, each component receives additional funding inversely proportional to the number of edges it has.

3.2.4 Hubs Cutting

Most of the real-world graphs are power-law graphs, where a relatively small percentage of nodes (hubs) concentrate most of the edges [54]. This approach moves then from the observation that most probably hubs will need to be cut into N pieces to maintain balance among the components. These partitioners prefer then to cut hubs, trying to spare the large share of nodes that have a small degree

Hybrid-Cut

The `Hybrid-cut` [47] partitioner considers that a vertex is not a hub if its in-degree is below a given threshold. In such case all the incoming edges are partitioned based on the hash value of this vertex and are placed in the same component. Otherwise the algorithm partitions based on their source vertices (assuming that the source vertices are not hubs). The algorithm was implemented for GraphX [55]. It is important to notice that this partitioner starts by calculating the degree of each vertex, which itself can be a time consuming operation.

Ginger

As `Hybrid-cut` this partitioner [47] allocates the incoming edges to a non-hub vertex (v) to the same component. It partitions edges based on destination vertices if the destination vertices are not hubs (otherwise is not specified).

The difference between `Hybrid-Cut` and `Ginger` is that the component E_i is selected based on the following greedy heuristic:

$$i = \operatorname*{argmax}_{i=1,\dots N} \left\{ |\mathcal{N}_{in}(v) \cap V(E_i)| - \frac{1}{2} \left(|V(E_i)| + \frac{|V|}{|E|} |E_i| \right) \right\} \qquad (3.1)$$

The underlying idea is that the partitioner selects the component where there are already neighbors of node v, as far as this component is not too large.

Intrinsically, formula 3.1 has a part related to balance (see formula 3.2). This part represents the cost of adding vertex v to a component i.

$$\frac{1}{2}\left(|V(E_i)| + \frac{|V|}{|E|}|E_i|\right) \tag{3.2}$$

HybridCutPlus

This partitioner is a mix of two anothers: `Hybrid-Cut` and `Grid`. Whenever it is possible (i.e., if one vertex of an edge is a hub and another vertex is not a hub) it works as `Hybrid-Cut` (i.e., partitioning based on non-hub vertices), otherwise it works as a `Grid` partitioner. It was implemented for GraphX [55].

Greedy Bipartite-cut (Aweto)

It is a greedy version of `BiCut` partitioner which is inspired by `Ginger`, and like `BiCut` it is applicable only for *bipartite-oriented* graphs. `Aweto` extends `BiCut` by adding an additional round. In this round it greedily re-locates some edges, according to following rule:

$$i = \underset{i=1,\ldots N}{\operatorname{argmax}} \left\{ |\mathcal{N}(v) \cap V(E_i)| - \sqrt{|E_i|} \right\}, \tag{3.3}$$

where $\mathcal{N}(v)$ denotes the set of vertices which are neighbors of vertex v. Partitioner considers a vertex with all edges attached to it, and tries to find the component where v has the highest number of neighbors including cost of adding edges to this component.

3.2.5 Iterative approach

While the previous partitioners assign once and for all a link to a component, iterative partitioners may iterate multiple times on the partitioning, reassigning an edge to a different component.

DFEPC

It is an iterative variant of `DFEP` that compensates for the possible negative effect
of starting from an initial vertex that is poorly connected to the rest of the graph.
`DFEP` is changed as follows: a component whose size is by a given factor smaller
than the current average component size can also bid for edges that were already
bought by other components, leading to their reassignments.

JA-BE-JA-VC

This partitioner was proposed in [52]. It is a vertex-cut version of an existing edge-
cut partitioner `JA-BE-JA` [56]. The `JA-BE-JA-VC` starts by randomly assigning
colors to the edges. After it improves color assignment by swapping colors of pairs
of edges. Each instance of the partitioner works in parallel, independently, in a
distributed way, without central point with a global knowledge. Finally, each edge
are placed in the component, where color of the edge is considered as an identity
of the component. We will provide more details about `JA-BE-JA-VC` in Chapter 5.

Correct distributed implementation would require expensive synchronization
on each step between all the instances of the partitioner. The authors do not
provide the system where this partitioner can be implemented or even scheme of
synchronization.

In [52] the authors also consider a simple way to adapt `JA-BE-JA` [56] to produce
an edge partitioning. First, `JA-BE-JA` is executed to produce vertex partitions.
Then, the edges that are cut are randomly assigned to one of the two components
their vertices belong to.

3.3   Discussion

Table 3.3 shows which partitioners were directly compared and which metrics were
considered in the comparison ("E" denotes execution metrics, while "P" denotes
partition metrics). Bold fonts indicate that the comparison was performed by
us (see Sec. 3.4). The table shows how many direct comparisons are missing
(e.g., `Hybrid-Cut` was never compared to `Torus`, `JA-BE-JA-VC`, etc.) and our
experiments in Section 3.4 contribute to provide a more complete picture. Even

Table 3.2 – Spark configuration

Property name	Property value
spark.executor.memory	4GB
spark.driver.memory	10GB
spark.cores.max	10
spark.local.dir	"tmp"

when a direct comparison is available, results are not necessarily conclusive. For example, in [52] the authors show that `JA-BE-JA-VC` outperforms `DEFP`, `DFEPC`, and `JA-BE-JA`[3] in terms of *STD*. However in terms of *normalized vertex-cut*, the modified version of `JA-BE-JA` is the best.

Table 3.1 indicates which specific metrics were considered in each paper. We can observe that in many cases execution metrics have not been considered, e.g., in [52] authors do not provide any experiments which shows change in execution time. It happens because they are expensive in terms of computation time. In particular, the lack of information about the partitioning time is problematic because in our experiments we have observed that it can vary by more than one order of magnitude across partitioners and contribute the most to the total execution time. The table also shows that it is difficult to perform an indirect comparison among partitioners using results from different papers, because there is often no common set of metrics considered across them.

In conclusion, it is hard to reach any conclusion regarding the benefits of existing partitioners for multiple reasons. First, not all partitioners have been compared. Second, execution metrics are not always provided and are tied to a specific computing environment. Finally, there is no study which links partitioning metrics to execution metrics, but for [57]. Motivated by these considerations, we decided to conduct experiments using the GraphX framework. Our results partially complete the pairwise comparison in Table 3.3 and are presented in the next section.

---

[3]Actually, they have used modified version of partitioner (original `JA-BE-JA` performs vertex partitioning), where each cut edge replaced with one cut vertex (randomly selected from source or destination vertices of cut edge)
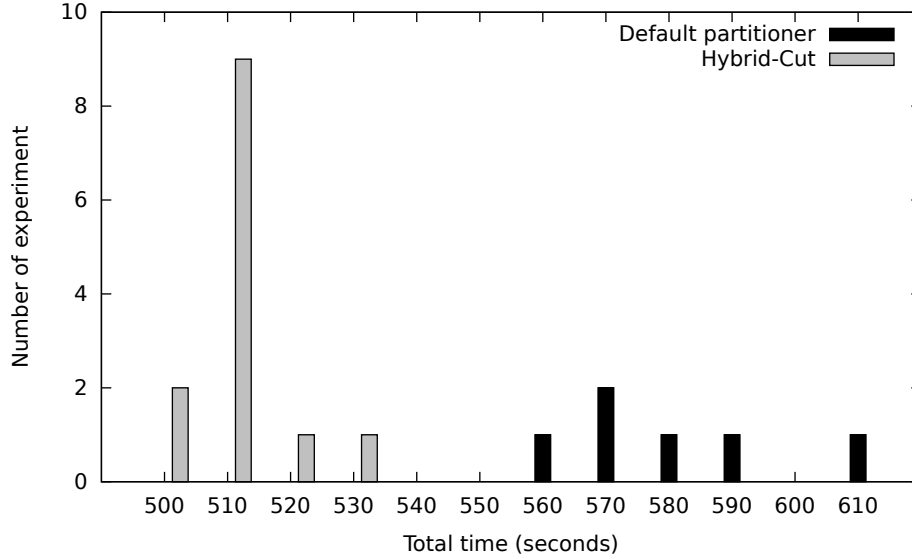
Figure 3.4 – Number of experiments finished with particular time (grouped by 10 seconds), where time is the sum of partitioning and execution time of `PageRank` algorithm executed on 1% snapshot of twitter graph

3.4 Experiments

3.4.1 Partitioning matters

First, we show that, indeed, graph partitioning can affect significantly an execution time. In the experiments we have executed 10 iterations of `PageRank` on partitioned graphs. Graphs were partitioned by two partitioners. The first one is a default partitioner provided by GraphX. When user do not specify some specific partitioner, GraphX sequentially splits the original text file, where each line represents one edge. This default partitioner is not implemented as a partitioner, i.e., by extending *Partitioner* class. In the second case, we used `HybridCut` (see Section 3.2.4). As a dataset we have used two Erdős-Rényi graphs [58] which have 236M edges/25M vertices and 588M edges/64M vertices. We have split the graphs into 2000 components and we used *Sophia nef cluster*[4] to perform the computations. Figures 3.4 and 3.5 show that there is a significant difference in execution time when we use different partitioners.

---

[4]10 worker machines and 1 master machine of dellc6220 (192GB RAM, 20 threads).
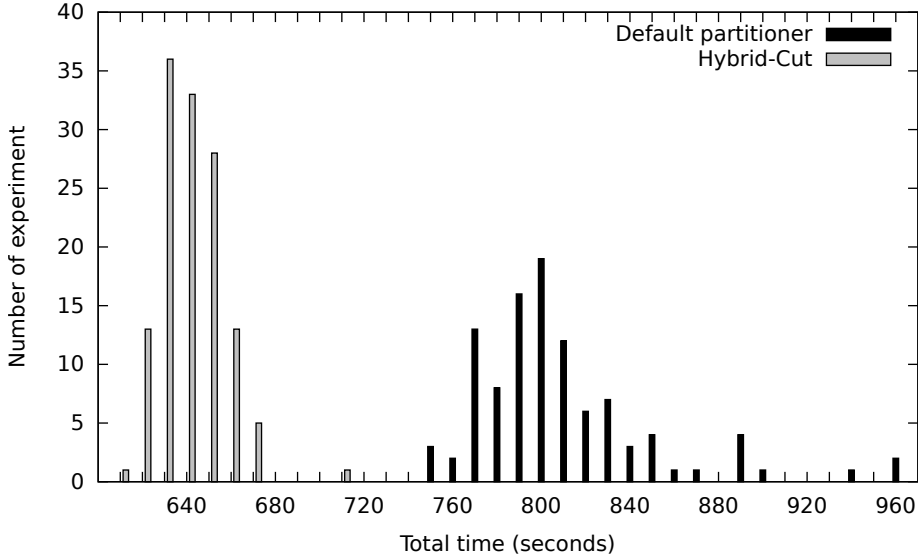
Figure 3.5 – Number of experiments finished with particular time (grouped by 10 seconds), where time is the sum of partitioning and execution time of `PageRank` algorithm executed on 2.5% snapshot of twitter graph

3.4.2 Comparison of different partitioners

We measured *replication factor*, *communication cost*, *balance*, *STD* as partitioning metrics, and the *partitioning time* and the *execution time* of `Connected Components` and `PageRank` (10 iterations) algorithms as execution metrics.

We conducted our experiments on *Nef cluster sophia* by using nodes with dual-Xeon E5-2680@2.80GHz, 192GB RAM and 20 cores. We used Spark version 1.4.0 in standalone cluster mode. Our cluster configuration had eleven machines, one for master and ten for executors. We configured 4 Spark properties as in Table 3.2.

As input we used the undirected *com-Youtube* graph (1,134,890 vertices/2,987,624 edges) from the SNAP project [59].

As a set of partitioners, we used all the GraphX built-in partitioners, i.e., `RandomVertexCut`, `CanonicalRandomVertexCut`, `EdgePartition1D`, `Grid`, the partitioner `DFEP` (whose code was kindly made available by the authors of [51]), `Greedy-Oblivious` (implemented by us), `Hybrid-Cut` and `HybridCutPlus` (both implemented by Larry Xiao [55]).

In each experiment we first randomly selected a partitioner and a graph pro-
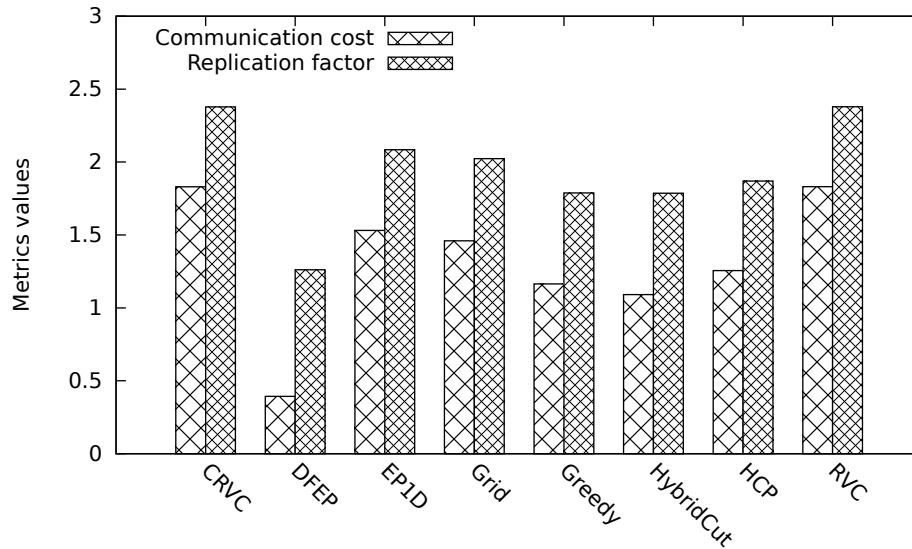
Figure 3.6 – Communication metrics (lower is better) .

cessing algorithm. Then, we applied the selected partitioner to the input graph. Finally, we executed the selected graph processing algorithm. We repeated every combination at least 30 times to obtain 95% confidence intervals for the execution time whose relative amplitude is always less than 10%.

Our experiments confirm that, as expected, the best *balance*, and *STD* metrics are obtained by random partitioners like `RVC` and `CRVC`. In terms of communication metrics, Fig. 3.6 shows that `DFEP` outperforms the other partitioners. This improvement comes at the cost of a much larger partitioning time, indeed in our setting `DFEP` partitions the graph in a few minutes, while the other partitioners are at least 20 times faster. Moreover, these partitioning metrics are not necessarily good predictors for the final execution time. Indeed, Fig. 3.7 shows that while `PageRank` achieves the shortest execution time when the graph is partitioned by `DFEP`, `Hybrid-Cut` provides the best partitioning for `Connected Components` and `HybridCutPlus` performs almost as `DFEP`. This result questions the extent to which partitioning metrics can be used to predict the actual quality of a partition (this aspect are investigated in the next chapter). From the practical point of view, `Hybrid-Cut` appears to achieve the best trade-off between partitioning time and reduction of the execution time.
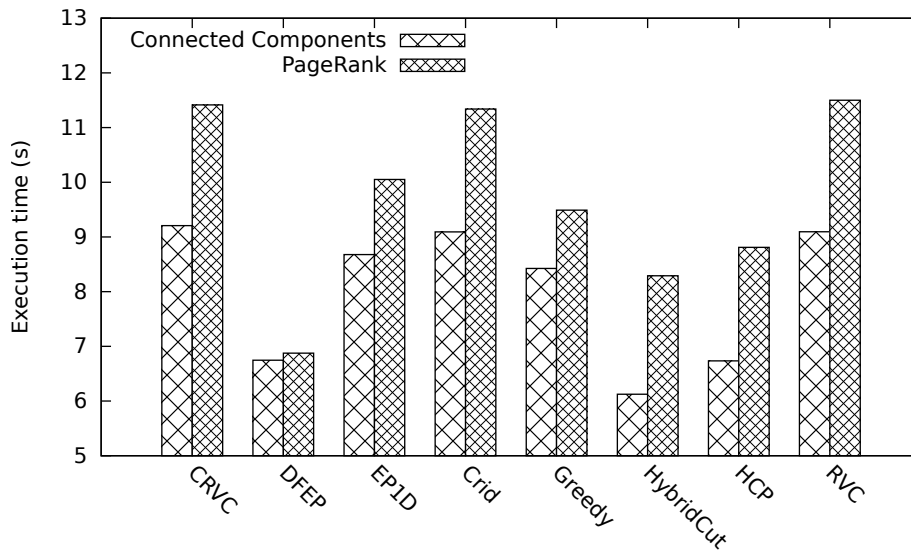
Figure 3.7 – Execution time of algorithms.

3.5 Conclusion

In this chapter we provided an overview of the existing edge partitioners. An analysis of the related literature shows they have been evaluated considering a disparate set of metrics and, moreover, they have been limited compared against each other. We presented some experimental results comparing a large number of edge partitioners for GraphX framework. We observed that partitioning metrics are not always suited to predict which partitioner will provide the shortest execution time and that simple and fast partitioners like `Hybrid-Cut` can outperform more sophisticated ones.

	RandomVertexCut	CRVC	EdgePartition1D	Greedy-Coordinated	Greedy-Oblivious	Grid	Grid Greedy	Torus	Torus Greedy	DFEP	DFEPC	JA-BE-JA-VC	Hybrid-Cut	Ginger	HybridCutPlus	BiCut	Aweto	JA-BE-JA
RandomVertexCut	–																	
CRVC	**EP**	–																
EdgePartition1D	**EP**	**EP**	–															
Greedy-Coordinated	EP	EP	EP	–														
Greedy-Oblivious	**EP**	EP	**EP**	EP	–													
Grid	EP	**EP**	**EP**	EP	EP	–												
Grid Greedy	EP		EP	EP	P	P	–											
Torus	P		P	P	P	P	P	–										
Torus Greedy	EP		EP	EP	EP	EP	EP	P	–									
DFEP	**EP**		**EP**		**EP**	P				–								
DFEPC					P					EP	–							
JA-BE-JA-VC										P	P	–						
Hybrid-Cut	**EP**		**EP**		**EP**	EP	EP			**EP**			–					
Ginger	EP		EP		EP	EP	EP						EP	–				
HybridCutPlus	**EP**		**EP**		**EP**	**EP**				**EP**		**EP**			–			
BiCut					EP	EP										–		
Aweto					EP	EP										EP	–	
JA-BE-JA	P		P		P					EP	EP	P						–

Table 3.3 – Partitioners pairwise comparisons, considering execution metrics (E) or partitioning metrics (P). **Bold** fonts indicate experiments we conducted.

Chapter 4

Predictive power of partition metrics

Contents

In this chapter we investigate how it is possible to evaluate the quality of a partitioning before running the computation. Answering this question would be useful both for the data analysts who need to choose the partitioner appropriate for their graphs and for developers who aim at proposing more efficient partitioners. As discussed in Chapter 2, some metrics have been proposed to this purpose. The survey of the related literature in the previous chapter shows that there is no common agreement about which metrics should be used for a comparison. In this chapter we make a step towards providing an answer by carrying experiments with the widely-used framework for graph processing GraphX and performing an accurate statistical analysis.

The chapter is organized as follows. In Section 4.1 we discuss our statistical methodology to study the dependency between the execution time of different graph-processing algorithms and partitioning metrics. We discuss the experimental setup and illustrate the results in Section 4.2. Finally, we conclude in Section 4.3.

The source code for all experiments is available here [48].

4.1   Statistical analysis methodology

Six partitioning algorithms are considered in this chapter, the GraphX built-in ones (`RandomVertexCut`, `CanonicalRandomVertexCut`, `EdgePartition1D`, `EdgePartition2D`) and two external(`HybridCut`, `HybridCutPlus`). We want to study if the partitioning metrics considered in the literature and described in Section 2.3.2 are good predictors for the final execution time. Remember that an execution time does not include partitioning time. We do not consider partitioning time because it does not depend on the partitions but on how partitioner was implemented.

To this purpose, we would like ideally to design experiments where we could randomly and independently select the five different metrics, generate an input graph with these quintuple of characteristics, evaluate the execution time of the application of interest and finally use some statistical tool like a regression models to identify the contribution of each metric to the execution time. Unfortunately, it is not possible to select first the partitioning metrics and then produce a graph with such characteristics. We can only use a partitioner on a given graph to produce a partition and then compute the metrics. As a consequence, their values will be far from independent and in particular the structure of their correlation can be a function of the specific partitioner used.

For this reason, in order to obtain a variety of different configurations, we used all the six partitioners on the same set of graphs. For each graph this leads to six different quintuples. A statistical model based on 6 points in a five-dimension space would very likely overfit the data. Considering other graphs allow us to obtain other samples. The drawback is that if we use real datasets, they are going to differ for the number of nodes and of edges. Now, these two metrics are very likely to have an effect much more important on the execution time than the partitioning metrics, which are the focus of our study. Remember that our goal is choosing the best partitioner for a given input graph of interest, whose size in terms of number of nodes and edges is out of our control. The contribution of the partition metrics would be dwarfed by the size change.

In order to overcome this difficulty, we generated 10 input graphs with the same

size by simply randomly permutating the ids of the vertices, by replacing vertices ids with the random unique numbers. Even if the different graphs are homeomorphic, components are calculated using the ids, and then each partitioner produces different subsets with different values for the metrics of interest. This approach allowed us to have 60 different quintuples for each graph: the ten permutations of the original graph multiplied by the six partitioners. In this way the risk of an overfitting model is significantly reduced.

To identify the most important metrics, we then used a linear regression model (denoted as LRM) with the five partition metrics as input variables (or predictors) and the execution time as the output variable (or response):

$$\beta_1 BAL + \beta_2 LP + \beta_3 NSD + \beta_4 VC + \beta_5 CC + \epsilon = \text{execution time}$$

where β_i are *regression coefficients*, and ϵ is *error term*. We want to find the most important predictors, but also rank these predictors by their importance. Obviously the more predictors we have in a LRM the smaller is the residual error, but which ones are really important? For this purpose we used the *best subset selection* method [60, Chapter 6]. According *best subset selection* method we have to first compare models with the same number of predictors, in order to find the best one for each number of predictors. And then, compare these best models by using, for example Akaike information criterion [61]. In particular, given the small number of predictors (5), we were able to consider all the possible 5! linear models for each original graph. Models with the same number of predictors were compared through their R^2 value. In this way 5 models were selected, respectively with 1,2,3,4 and 5 predictors. The best model was finally identified as the one with the smallest Akaike information criterion. We have considered another indices as well, such as Bayesian Information Criteria, sample-size corrected AIC, or R^2 adjusted. However, in the most cases the results did not differ. Once the best model was selected, we ordered its predictors by considering those that lead to the largest increase of the R^2 value when added as predictors.

Table 4.1 – Spark configuration

Property name	Property value
spark.executor.memory	4GB (for 10 executors)/ 40GB (for 1 executor)
spark.driver.memory	10GB
spark.cores.max	10
spark.local.dir	"tmp"

4.2   Experiments

Our experiments were performed on the *Nef sophia cluster*. Each machine had nodes two Xeon E5-2680 v2 @2.80GHz with 192GB RAM and 10 cores (20 threads). We used Spark version 1.4.0 and Spark standalone cluster [62] as a resource manager. We used two different cluster configurations. In the first configuration, a master and an executor share the same machine. In the second case, one machine is dedicated to the master and one to each of the ten executors. We configured Spark properties as shown in the Table 4.1.

Two different processing algorithms were evaluated: `Connected Components` and `PageRank` with 10 iterations. `PageRank` exhibits the same computation and communication pattern at each stage (the PageRank of each vertex value is updated according to the same formula and then propagated to the neighbors), while `Connected Components` implements a label propagation mechanism, where as time goes on, less updates are required.

As datasets, we used two undirected graphs: the *com-Youtube* graph (1,134,890 vertices/2,987,624 edges) and the *com-Orkut* graph (3,072,441 vertices/117,185,083 edges) from the SNAP project [59].

For each experiment, first we randomly selected a partitioner, a graph processing algorithm, and a permutation of an input graph. Second, we applied the selected partitioner to the input graph. Finally, we executed the selected graph processing algorithm. To overcome execution time variability (due to a shared network, shared distributed file system, operating system layer, etc.), every combination has been tested at least 30 times, obtaining 95% confidence intervals for the execution time whose relative amplitude is always less than 10%.

As we mentioned earlier, for each graph we obtained 60 different quintuples for

Table 4.2 – Correlation matrix for partition metrics *com-Youtube*

	BAL	LP	NSD	VC	CC
BAL	1	**0.9332**	**0.9445**	0.2070	-0.2448
LP		1	**0.9799**	0.0993	-0.3177
NSD			1	0.1275	-0.2667
VC				1	**0.8737**
CC					1

the partition metrics. Table 4.2 shows their correlation matrix for *com-Youtube* graph.[1] Let us consider all values of the Table 4.2 which are more than 0.8. We can clearly identify the two groups of metrics: those relative to partition balance (BAL, LP NSTDEV) and those related to communication (VC, CC). The high level of collinearity also explains why in the LRM some coefficients are negative [60, Chapter 3].

We computed and selected linear regression models for *com-Youtube*, *com-Youtube doubled*, and *com-Orkut* graph, as it was discussed in Section 4.1. Table 4.4 and Table 4.5 summarize our experimental results respectively for `PageRank` and `Connected Components`. For each input graph and number of machines, they show the best LRM with the factors listed in decreasing order of importance. We note that, although a single node has enough resources to perform all the computation, the results in Table 4.4 and Table 4.5 show that the average execution time decreases as the number of machines increases. A similar result was observed in [63] where it was due to the higher memory contention in case of a single machine. It is possible that the effect has the same cause here.

Below we illustrate our main findings about the partition metrics.

The execution time depends on the partition metrics

For `PageRank` (see Table 4.4) the R^2 value is very high (always above 0.98) while the Root Mean Square Error (RMSE) is less than 5% of mean execution time. This leads to conclude that indeed the execution time depends on these metrics. The dependency is less stronger for `Connected Components`. This can be explained

---

[1]Correlation matrix shows how much partition metrics correlate with each other. 0 means - no correlation, 1 means - maximum correlation.

Figure 4.1 – Execution time for `PageRank` algorithm on *com-Youtube* graph: experimental results vs best LRM predictions

with the fact that `PageRank` roughly does the same operations at each stage, while `Connected Components` is a label propagation algorithm where, very quickly, the values of most of the vertices will not be updated. The execution time likely depends on graph properties (e.g., the graph diameter) that are not well captured by these metrics.

Figures 4.1 , 4.2 and 4.3 confirm these results by comparing the experimental execution time with the one predicted using the best LRM model we found. Results are grouped by partitioners, for each of them results for the 10 graph permutations are shown.

We observe that HC is to be the best partitioner confirming the results in [47] and in Chapter 3 of this thesis. It also outperforms its variant HCP.

Communication metrics are the most important

In all the LRMs, the most important metric is always a communication metric (CC or VC), even when a single machine is used and the network is scarcely used.

This result is also confirmed by comparing the 5 single-predictor LRMs. The single-predictor LRM is model where we use only one metric to predict an execution
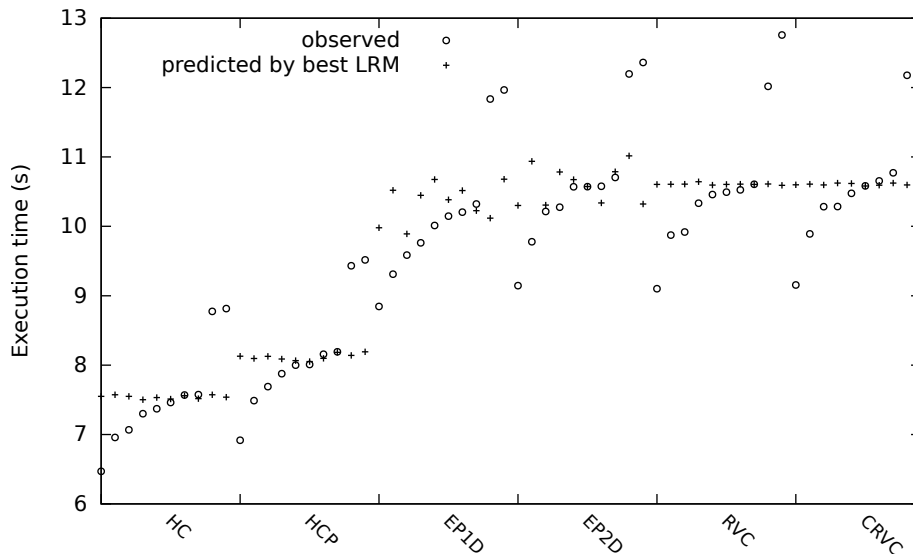
Figure 4.2 – Execution time for `Connected Components` algorithm on *com-Youtube* graph: experimental results vs best LRM predictions

time of the algorithm. The LRMs using VC or CC have larger R^2 value. Figure 4.4 shows how LRM models using only VC or CC are able to produce quite good predictions at least of the relative performance of the different partitioners. On the contrary, the corresponding plot for balance metrics (BAL, LP, NSTDEV) shows an almost horizontal line (see Figure 4.5).

As a side note, we tried to find a setting where balance metrics would have become the most important ones. In particular we considered i) a single machine, ii) very limited memory for each partitioner (70MB), iii) a modified version of `PageRank` where each computation is performed 1000 more times. The purpose was to make communication among executors as fast as possible, while increasing the computational burden on each executor. Even in this settings, communication metrics appeared to be the most important ones.

Results are robust to the partitioners considered

One of the purposes of our analysis is to be able to rank a priori different partitioners before carrying on the experiments. We evaluated how much our results are sensitive to the specific set of partitioners used to tune the LRM. To this purpose,

we carried on the same analysis using only 5 partitioners (we did not use HC). We then used the new LRM model to predict the execution time for the HC partitioner. Figure 4.6 shows that predicted execution time for HC is underestimated. However, the order of the partitioners in terms of execution time is the correct one. Then the LRM model correctly predicts that HC partitioning will lead to a shorter execution time. One could argue that the LRM has been trained using HCP that is a variant of HC. We then performed the same set of experiments removing both HC and HCP (see Figure 4.7). In this case the predicted executed time is really off, but the LRM still correctly predicts the ranking of the different partitioners.

There is space for better partition metrics

While the results above are encouraging, the following experiment suggests that these partition metrics do not capture all the relevant features.

We considered a version of *com-Youtube* graph where we doubled each edge so that both directions are present in the input graph and `PageRank` correctly computes the PageRank of the original undirected graph. We denote the doubled graph as *com-Youtube doubled*.

The execution time of both algorithms on *com-Youtube doubled* is larger, roughly 30% (see Table 4.3). Nevertheless, the communication metrics that we identified as the most important ones may fail to detect the change. This is evident if we compare the CRVC partitioner with the other ones. As shown in Table 4.3 for a specific input graph, the CRVC partitioner provides the same values for all the partition metrics, and in particular for VC and CC metrics, both for *com-Youtube doubled* and *com-Youtube*, since it partitions edges based on the vertex (either source or destination) with the smallest id. For the other partitioners instead, the metrics VC and CC are different. The difference is evident if we compute the LRM including or not CRVC. In the first case the R^2 value of the LRM for `PageRank` significantly decreases from 0.99 for *com-Youtube* (see Table 4.4) to 0.82. In the second case the LRMs are equally good.

We think a more meaningful communication metric could be defined that would permit to identify the difference between CRVC and the other partitioners. We plan to investigate this aspect in the future.
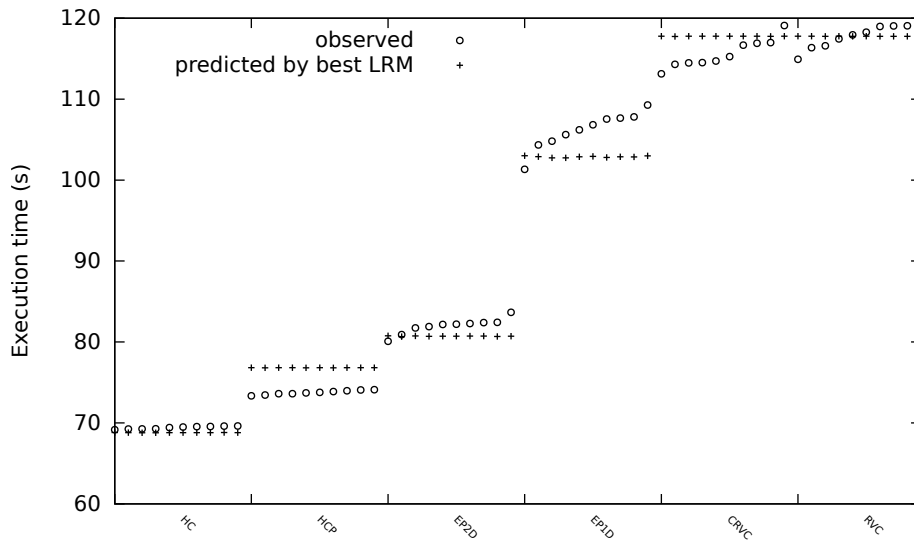
Figure 4.3 – Execution time for `PageRank` algorithm on *com-Orkut* graph: experimental results vs best LRM predictions

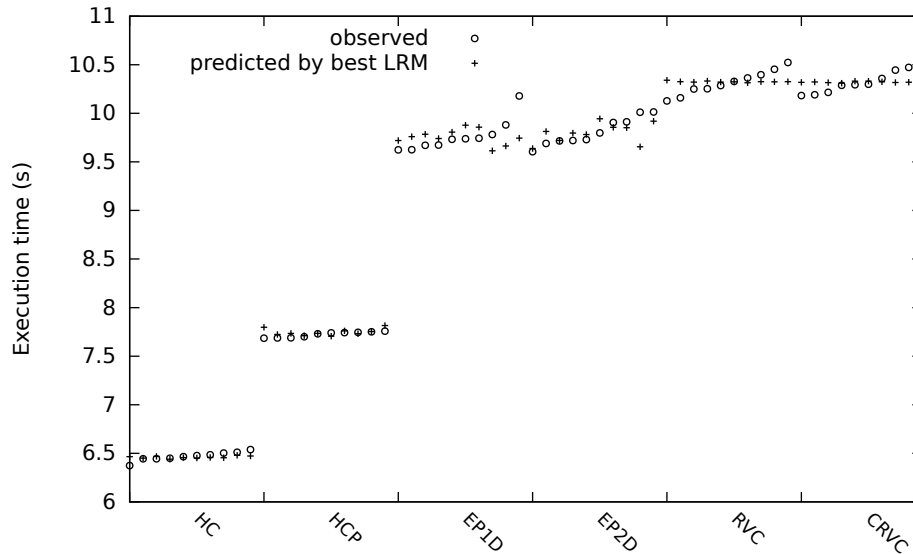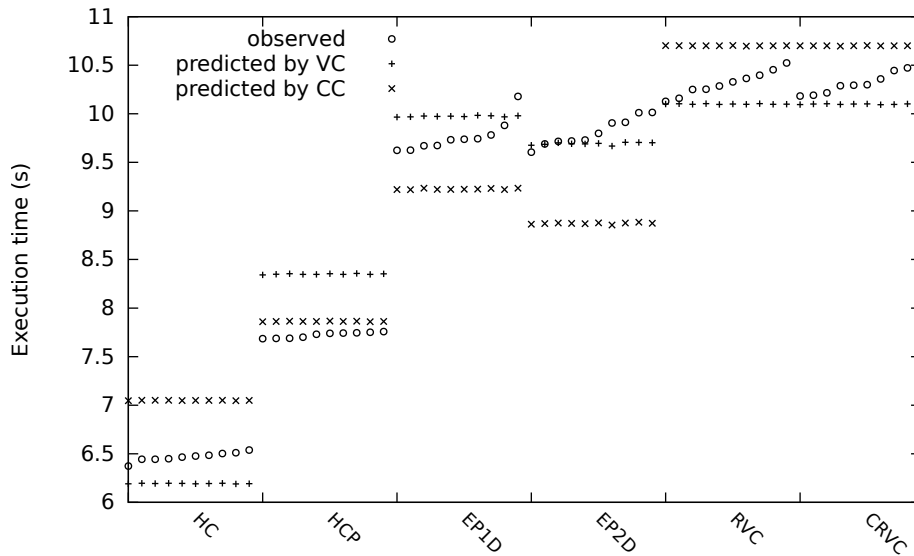Figure 4.4 – Execution time for `PageRank` algorithm on *com-Youtube* graph: experimental results vs LRM predictions using a single communication metrics
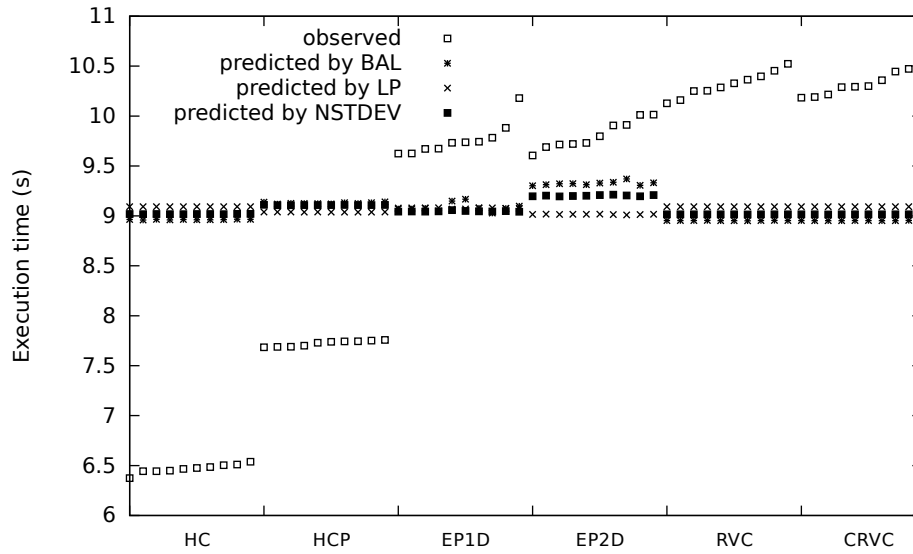
Figure 4.5 – Execution time for `PageRank` algorithm on *com-Youtube* graph: experimental results vs LRM predictions using a single balance metrics
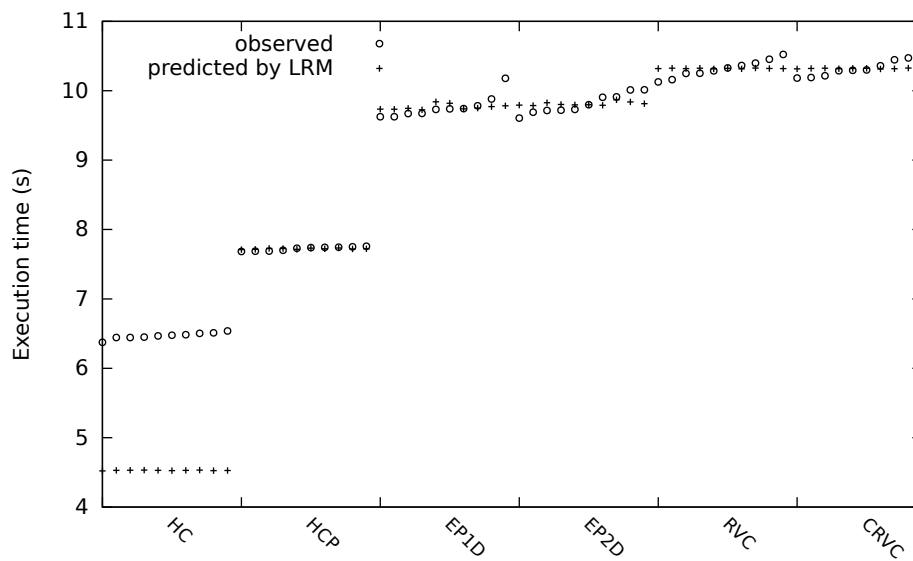
Figure 4.6 – Prediction for HC partitioner (using *com-Youtube* graph, and `PageRank` algorithm)

4.3   Conclusion

We used linear regression models with partitioning metrics as predictors and the average execution time for different graph processing algorithms as the observed
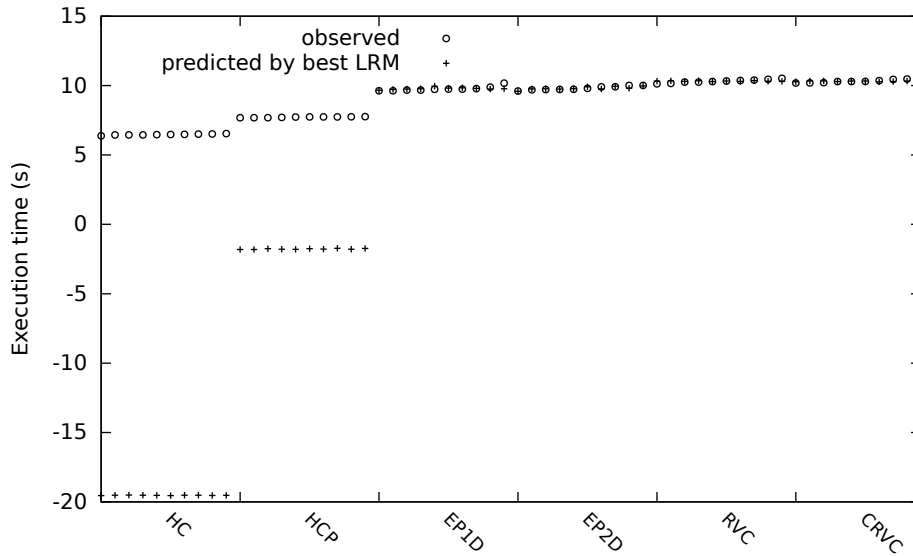
Figure 4.7 – Prediction for HC and HCP parititioners (using *com-Youtube* graph, and `PageRank` algorithm)

Table 4.3 – Metrics and execution time of `PageRank` for HC and CRVC

Graph name	HC			CRVC		
	Average time (ms)	VC	CC	Average time (ms)	VC	CC
com-Youtube	6468	0.304	1.091	10327	0.452	1.831
com-Youtube doubled	8121	0.702	2.204	13404	0.452	1.831

values. The obtained models confirmed that there is an actual dependency between these quantities. More importantly, the most important metrics are CC and VC. Both are an indicator of the amount of communication among the executors. On the contrary, the metrics that quantify load unbalance across the executors are less important. This conclusion holds whether communication is inter-machine or intra-machine, i.e., both if the network is used or not. Our results are robust to the original set of partitioners used to train the model, and the model can correctly rank other partitioners. Moreover, we show that current metrics are not sufficient to evaluate partitions.

Table 4.4 – The best linear regression models for PageRank algorithm

Graph name	Cluster configuration	Mean time (ms)		Metrics (ordered by importance)					RMSE	R^2
com-Youtube	single machine	12,343	metr.	VC	CC	BAL	LP	NSD	111.83	0.996
			coeff.	1.5507	0.3156	0.42743	-0.49504	0.33548		
	1 master + 10 executors	9,068	metr.	VC	CC	BAL	LP	NSD	125.47	0.993
			coeff.	1.2816	0.27261	0.50989	-0.64857	0.49891		
com-Orkut	single machine	122,929	metr.	CC	LP	VC			1199.4	0.998
			coeff.	2.312	5.039	12.942				
	1 master + 10 executors	94,738	metr.	CC	LP	NSD	VC		2222.8	0.989
			coeff.	1.3285	8.3243	-11.486	12.881			

Table 4.5 – The best linear regression models for Connected Components algorithm

Graph name	Cluster configuration	Mean time (ms)		Metrics (ordered by importance)				RMSE	R^2
com-Youtube	single machine	12,429	metrics	VC	LP	NSD		1119.2	0.499
			coefficients	1.7884	-1.3177	1.3861			
	1 master + 10 executors	9,635	metrics	VC	LP	NSD		922.27	0.681
			coefficients	2.1131	-1.7528	2.1043			
com-Orkut	single machine	86,253	metrics	CC	LP	NSD		2628.2	0.959
			coefficients	1.2039	9.771	-8.2634			
	1 master + 10 executors	71,952	metrics	CC	LP	NSD		2235,6	0.973
			coefficients	1.0854	15.484	-17.96			

Chapter 5

A simulated annealing partitioning framework

Contents

This chapter describes how simulated annealing (SA) technique can be used in order to partition a graph with a purpose to minimize a specific partition metric.

We propose a general SA framework for distributed edge partitioning based on simulated annealing [64]. The framework can be used to optimize a large family of partitioning metrics. We provide sufficient conditions for convergence

to the optimum as well as discuss which metrics can be efficiently optimized in a distributed way. We have implemented our partitioners in GraphX and performed a comparison with *JA-BE-JA-VC* [52], a state-of-the-art partitioner that inspired our approach. We show that our approach can provide improvements. We have also developed two version of the proposed framework. The first version — the *SA* framework — is faster but may not converge to the optimum. The second version — the multiopinion *SA* framework — is guaranteed to converge, thanks to some new theoretical results in [65]. Part of the results in this chapter appeared in [66].

5.1   Introduction

A new edge partitioning algorithm, called *JA-BE-JA-VC*, has been proposed in [52] and shown to significantly outperform existing algorithms. The algorithm starts by assigning an initial (arbitrary) color to each edge.[1] Each color represents a component where the edge will be placed after the partitioner has finished. The partitioner iteratively improves on the initial edge colors assignment, by allowing two edges to swap their color if this seems to be beneficial to reduce the number of cuts of the corresponding vertices. In order to avoid getting stuck at local minima, *JA-BE-JA-VC* borrows from simulated annealing (*SA*) the idea to permit apparently detrimentals swaps at early stages of the partitioning.

In this chapter, we develop this initial inspiration and propose two version of graph partitioners based on *SA* for Spark.

To this purpose, we start by reverse engineering *JA-BE-JA-VC* to show which metric it is targeting. After, we propose the first version of our general SA framework that can optimize a large spectrum of objective functions, and for which convergence results can be proven. The naive implementation of this approach (as well as of *JA-BE-JA-VC*), requires a significant number of costly synchronization operations during the partitioning. Then we explain how these algorithms can be efficiently implemented in a distributed architecture as Spark. However, in this case, instances can operate on stale values, which can prevent convergence to the optimum. As a proof of concept, we perform some preliminary experiments con-

---

[1]In this chapter, we refer to edge assignment to components as edge coloring to maintain the original terminology in [52].

sidering an objective function that takes into account both communication cost and computational balance. We show that this objective function may obtain better partitions than *JA-BE-JA-VC*, but this does not happen consistently. Finally, we propose and evaluate a second version of our SA framework, relying on new theoretical results about asynchronous Gibbs sampler [65]. In this version, each instance maintains a different opinion about how the edge should be colored.

The rest of the chapter is organized as follows. We start by introducing the notation and tools used in this work (Section 5.2). Next, we reverse-engineer the *JA-BE-JA-VC* algorithm in Section 5.3. Then, we present the general *SA* framework for edge partitioning in Section 5.4. After, we introduce our first implementation of it — the *SA* framework, in Section 5.5. We compare *JA-BE-JA-VC* and the *SA* framework in Section 5.6. In Section 5.7 we present a second version of our framework — the multi-opinion *SA* framework and we evaluate its performance in Section 5.8. Finally, we conclude in Section 5.9.

5.2 Background and notations

We have to introduce some additional notations. As we have already mentioned in Section 2, we have an undirected graph $\mathcal{G} = (V, E)$. This graph will be partitioned in N distinct components, each of the N component is identified with one of the N colors from the set C. Let $E(c)$ denote the set of edges with color $c \in C$, then $E = \bigcup_{c \in C} E(c)$. Given a vertex $v \in V$, its degree is denoted by d_v and the number of its edges with color c is denoted by $n_v(c)$.

JA-BE-JA-VC [52] is a recently proposed edge partitioner. Given an initial color assignment to edges (e.g., a random one), the algorithm iteratively improves this color assignment. At the end of the partitioning, *JA-BE-JA-VC* distributes all edges to the components by considering the color of the edge as the component identifier. During an algorithm iteration, *JA-BE-JA-VC* selects two vertices u and u'. For each of these two vertices, it then selects an edge among those whose color is less represented in their neighborhood. For example, considering u, it will select an edge of color $\hat{c} \in \text{argmin}\{n_u(c)\}$. Let us denote these two edges as (u, v) and (u', v') with color respectively c and c'. The algorithm always swaps the colors of

the two edges if

$$g(u,v,c) + g(u',v',c') < g(u,v,c') + g(u',v',c)$$
$$+ \frac{1}{d_u} + \frac{1}{d_v} + \frac{1}{d_{u'}} + \frac{1}{d_{v'}}, \qquad (5.1)$$

where $g(u,v,c) \triangleq \frac{n_u(c)}{d_u} + \frac{n_v(c)}{d_v}$. The more links of color c the two nodes u and v have, the larger $g(u,v,c)$ is, and then the two nodes are potentially cut in a smaller number of pieces. In particular, if all edges of u and v have color c, $g(u,v,c)$ attains its maximum value is equal to 2. If we consider that $g(u,v,c)$ is a measure of the quality of the current assignment, (5.1) compares the current quality of the assignment with the quality of an assignment were colors are swapped. The additional terms on the right hand side correspond to the fact that after swapping there is one link more of color c' (resp. c) for u and v (resp. u' and v'). While we have provided an interpretation of $g(u,v,c)$, one may wonder which objective function (if any) *JA-BE-JA-VC* is optimizing by swapping color according to the criterium in (5.1) and if it is related to one of the usual partitioning quality metrics like VC or CC defined above. In Section 5.3 we provide an answer to such questions.

The authors of [52] state that, in order to avoid getting stuck in local optima (of this still unknown objective function), one can introduce the possibility to accept changes that do not satisfy (5.1), especially during the first iterations. To this purpose, inspired by simulated annealing (*SA*) [67, Chapter 7] they introduce a positive parameter T (the temperature) and change condition (5.1) as follows:

$$g(u,v,c) + g(u',v',c') < (1+T)\left[g(u,v,c') + g(u',v',c)\right.$$
$$\left. + \frac{1}{d_u} + \frac{1}{d_v} + \frac{1}{d_{u'}} + \frac{1}{d_{v'}}\right], \qquad (5.2)$$

where T decreases linearly from some initial value to zero. Condition (5.2) accepts all changes that increase the quality of the current assignment, or decrease it no more than a factor $1 + T$. However, it does not accept any changes that decreases the quality of the current assignment by a larger factor. Thus, this condition does not consider a lot of exploration possibilities.

JA-BE-JA-VC is presented in [52] as a distributed algorithm, because an edge swap requires only information available to the nodes involved, i.e., u, v, u' and v'. We observe that this property is not necessarily helpful for performing the partitioning operation on distributed computation frameworks like Spark, because this information is not necessarily local to the instance that processes the two edges. Indeed, while the instance may have access to both the edges (u, v) and (u', v'), it may not know the current value of edges of a given color that each vertex has (e.g., it may not know $n_u(c)$), because these other edges might be assigned to other partitioners. Moreover, the color of these remote edges might be changed concurrently. Hence, expensive communication exchange among instances could be required to implement *JA-BE-JA-VC*. In Section 5.4 we discuss how to modify *JA-BE-JA-VC* in order to significantly reduce communication exchange.

5.3   Reverse Engineering *JA-BE-JA-VC*

The first contribution of this chapter is to identify the global objective function (*energy function* in what follows) *JA-BE-JA-VC* is optimizing when links are swapped according to (5.1). Let m_c be the initial number of edges with color c. Condition (5.1) corresponds to greedily minimizing the function

$$\mathcal{E}_{comm} \triangleq \frac{1}{2|E|(1 - \frac{1}{N})} \left(2|E| - \sum_{v \in V} \sum_{c \in C} \frac{n_v(c)^2}{d_v} \right), \tag{5.3}$$

under the constraint that at each step $|E(c)| = m_c$ for any color c, where m_c is some constant value and $\sum_{c \in C} m_c = |E|$. The constraint is easy to understand, because *JA-BE-JA-VC* simply swaps colors of two edges so that number of edges of a given color is always equal to the initial value. In what follows we show that a swap makes $\mathcal{E}_{comm}$ decrease if and only if condition (5.1) is satisfied.

We have two edges (u, v) and (u', v') with colors respectively c and c'. If we accept to swap them, then the number of colors of the vertices will change as

follows, where the *hat* denotes the quantities after the swap:

$$\begin{cases} \hat{n}_u(c) = n_u(c) - 1, & \hat{n}_u(c') = n_u(c') + 1 \\ \hat{n}_v(c) = n_v(c) - 1, & \hat{n}_v(c') = n_v(c') + 1 \\ \hat{n}_{u'}(c) = n_{u'}(c) + 1, & \hat{n}_{u'}(c') = n_{u'}(c') - 1 \\ \hat{n}_{v'}(c) = n_{v'}(c) + 1, & \hat{n}_{v'}(c') = n_{v'}(c') - 1 \end{cases} \tag{5.4}$$

We want to prove that we have accepted this swap if and only if $\mathcal{E}_{comm}$ decreases, then we want to prove that the acceptance rule (5.1) is equivalent to:

$$\widehat{\mathcal{E}}_{comm} - \mathcal{E}_{comm} < 0,$$

where $\widehat{\mathcal{E}}_{comm}$ denotes the energy value after a swap has occurred. We start from this last inequality and replace with the set of relation in (5.4), and we show that this is indeed equivalent to (5.1).

$$-\frac{\hat{n}_u(c)^2}{d_u} - \frac{\hat{n}_v(c)^2}{d_v} - \frac{\hat{n}_u(c')^2}{d_u} - \frac{\hat{n}_v(c')^2}{d_v} - \frac{\hat{n}_{u'}(c)^2}{d_{u'}} - \frac{\hat{n}_{v'}(c)^2}{d_{v'}} - \frac{\hat{n}_{u'}(c')^2}{d_{u'}} - \frac{\hat{n}_{v'}(c')^2}{d_{u'}} + \frac{n_u(c)^2}{d_u}$$

$$+ \frac{n_v(c)^2}{d_v} + \frac{n_u(c')^2}{d_u} + \frac{n_v(c')^2}{d_v} + \frac{n_{u'}(c)^2}{d_{u'}} + \frac{n_{v'}(c)^2}{d_{v'}} + \frac{n_{u'}(c')^2}{d_{u'}} + \frac{n_{v'}(c')^2}{d_{v'}} < 0$$

$$\frac{-\hat{n}_u(c)^2 - \hat{n}_u(c')^2 + n_u(c)^2 + n_u(c')^2}{d_u} + \frac{-\hat{n}_v(c)^2 - \hat{n}_v(c')^2 + n_v(c)^2 + n_v(c')^2}{d_v}$$

$$+ \frac{-\hat{n}_{u'}(c)^2 - \hat{n}_{u'}(c')^2 + n_{u'}(c)^2 + n_{u'}(c')^2}{d_{u'}} + \frac{-\hat{n}_{v'}(c)^2 - \hat{n}_{v'}(c')^2 + n_{v'}(c)^2 + n_{v'}(c')^2}{d_{v'}} < 0$$

$$\frac{n_u(c)^2 - \left(n_u(c) - 1\right)^2 + n_u(c')^2 - \left(n_u(c') + 1\right)^2}{d_u}$$

$$+ \frac{n_v(c)^2 - \left(n_v(c) - 1\right)^2 + n_v(c')^2 - \left(n_v(c') + 1\right)^2}{d_v}$$

$$+ \frac{n_{u'}(c)^2 - \left(n_{u'}(c) + 1\right)^2 + n_{u'}(c')^2 - \left(n_{u'}(c') - 1\right)^2}{d_{u'}}$$

$$+ \frac{n_{v'}(c)^2 - \left(n_{v'}(c) + 1\right)^2 + n_{v'}(c')^2 - \left(n_{v'}(c') - 1\right)^2}{d_{v'}} < 0$$

$$\frac{2n_u(c) - 2n_u(c') - 2}{d_u} + \frac{2n_v(c) - 2n_v(c') - 2}{d_v}$$

$$+ \frac{2n_{u'}(c') - 2n_{u'}(c) - 2}{d_{u'}} + \frac{2n_{v'}(c') - 2n_{v'}(c) - 2}{d_{v'}} < 0$$

$$2\left(\frac{n_u(c)}{d_u} + \frac{n_v(c)}{d_v} - \frac{n_u(c')}{d_u} - \frac{n_v(c')}{d_v} + \frac{n_{u'}(c')}{d_{u'}} + \frac{n_{v'}(c')}{d_{v'}}\right.$$

$$\left. - \frac{n_{u'}(c)}{d_{u'}} - \frac{n_{v'}(c)}{d_{v'}} - \frac{1}{d_u} - \frac{1}{d_v} - \frac{1}{d_{u'}} - \frac{1}{d_{v'}}\right) < 0$$

$$2\left(g(u, v, c) - g(u, v, c') + g(u', v', c') - g(u', v', c) - \frac{1}{d_u} - \frac{1}{d_v} - \frac{1}{d_{u'}} - \frac{1}{d_{v'}}\right) < 0$$

$$g(u, v, c) + g(u', v', c') < g(u, v, c') + g(u', v', c) + \frac{1}{d_u} + \frac{1}{d_v} + \frac{1}{d_{u'}} + \frac{1}{d_{v'}}$$

We could equivalently, and more succinctly, state that *JA-BE-JA-VC* is maximizing $\sum_{v \in V} \sum_{c \in C} \frac{n_v(c)^2}{d_v}$. The advantage of (5.3) is that $\mathcal{E}_{comm}$ belongs to $[0, 1]$ and *SA* algorithms are usually presented as minimizing an energy function.

Because of the above considerations, *JA-BE-JA-VC* can be thought as a heuristic to solve the following problem:

$$\underset{\mathbf{c} \in C^{|E|}}{\text{minimize}} \quad \mathcal{E}_{comm}(\mathbf{c})$$

$$\text{subject to} \quad |E(\mathbf{c})| = m_c$$

where $\mathbf{c}$ denotes the vectors of colors chosen for all the edges in the network.

While the greedy rule (5.1) would lead, in general, to a local minimum of $\mathcal{E}_{comm}$, one may wonder if rule (5.2), together with the specific criterium to choose the edges to swap in *JA-BE-JA-VC* and to change the temperature, can lead to a solution of the problem stated above. Unfortunately, it is possible to show that this is not the case in general.

A second remark is that (5.3) appears to be a quite arbitrary metric, and is not directly related to metrics like VC or CC. Our experiments show indeed that $\mathcal{E}_{comm}$ can decrease while both VC and CC increase, even if the evaluation in [52] indicates that this is not usually the case.

In the next section we address these two remarks.

5.4 A general *SA* framework for edge partitioning

Let us consider a general optimization problem

$$
\begin{aligned}
& \underset{\mathbf{c} \in C^{|E|}}{\text{minimize}} && \mathcal{E}(\mathbf{c}) \\
& \text{subject to} && \mathbf{c} \in D,
\end{aligned}
\tag{5.5}
$$

where D is a generic set of constraints. We can solve this problem with *SA* as follows.

– given the current solution $\mathbf{c}$, select a possible alternative $\mathbf{c}' \in D$ with probability $q_{\mathbf{c},\mathbf{c}'}$

– if $\mathcal{E}(\mathbf{c}') \leq \mathcal{E}(\mathbf{c})$ accept the change, otherwise accept it with probability $\exp\left(\frac{\mathcal{E}(\mathbf{c})-\mathcal{E}(\mathbf{c}')}{T}\right) < 1$. The probability to accept the change can be also expressed as $\beta_{\mathbf{c},\mathbf{c}'} = \min\left(1, \exp\left(\frac{\mathcal{E}(\mathbf{c})-\mathcal{E}(\mathbf{c}')}{T}\right)\right)$

If the selection probabilities $q_{\mathbf{c},\mathbf{c}'}$ are symmetric ($q_{\mathbf{c},\mathbf{c}'} = q_{\mathbf{c}',\mathbf{c}}$) and if the temperature decreases as $T_0/\log(1 + k)$, where $k \geq 0$ is the iteration number and the initial temperature T_0 is large enough, then this algorithm is guaranteed to converge to the optimal solution of the above problem [67, Chapter 7]. *JA-BE-JA-VC* does

not satisfy any of these conditions, and then it is not guaranteed to converge to the optimal solution.

At a given step the transition probability from state $\mathbf{c}$ to state $\mathbf{c}'$ is $p_{\mathbf{c},\mathbf{c}'} = q_{\mathbf{c},\mathbf{c}'}\beta_{\mathbf{c},\mathbf{c}'}$. The choices for $q_{\mathbf{c},\mathbf{c}'}\beta_{\mathbf{c},\mathbf{c}'}$ and $\beta_{\mathbf{c},\mathbf{c}'}$ correspond to what is called a Metropolis-Hasting sampler. In Section 5.7, we will discuss a different possibility: the Gibbs sampler.

This algorithm is very general and can be applied to any energy function $\mathcal{E}$ including the metrics described in Section 5.2. A practical limit is that the algorithm may not be easy to distribute for a generic function $\mathcal{E}(\mathbf{c})$, because of its dependency on the whole vector $\mathbf{c}$. Nevertheless, we can observe that a *SA* algorithm needs to evaluate only the energy differences $\mathcal{E}(\mathbf{c}') - \mathcal{E}(\mathbf{c})$. Then, as far as such differences depend only on a few elements of the vectors $\mathbf{c}$ and $\mathbf{c}'$, the algorithm has still a possibility to be implemented in a distributed way.

If the function $\mathcal{E}$ can be expressed as a sum of potentials of the cliques of order not larger than r,[2] evaluating the energy difference requires only to evaluate the value of the potentials for the corresponding cliques (see [67, Chapter 7]). The energy function $\mathcal{E}_{comm}$ considered by *JA-BE-JA-VC* falls in this category and in fact at each step the energy difference between two states requires to count only the edges of those colors that u, v, u' and v' have (5.1). As we said, our framework is more general and can accommodate any function that can be expressed as sum of clique potentials. For example in what follows we consider the following function

$$\mathcal{E} = \mathcal{E}_{comm} + \alpha\mathcal{E}_{bal} \tag{5.6}$$

$$\mathcal{E}_{bal} = \frac{1}{|E|^2(1-\frac{1}{N})^2} \sum_{\mathbf{c}\in C}\left(|E(\mathbf{c})| - \frac{|E|}{N}\right)^2, \tag{5.7}$$

that allows to trade off the communication requirements associated to a partition, captured by $\mathcal{E}_{comm}$, and the computational balance, captured by $\mathcal{E}_{bal}$.[3] The term $\mathcal{E}_{bal}$ indeed ranges from 0 for a perfectly balanced partition to 1 for a partition where all the edges have been assigned the same color. The parameter $\alpha > 0$ allows the user to tune the relative importance of the two terms.

---

[2]Cliques of order 1 are nodes, cliques of order 2 are edges, etc..

[3]In Chapter 4 we have shown that linear combinations of similar metrics can be good predictors for the final computation time.

The function $\mathcal{E}$ can be optimized according to the general framework we described above as follows. We select an edge uniformly at random (say it is (u, v) with color c) from E and decide probabilistically if we want to swap its color with another edge $((u', v')$ with color $c')$ or change the color c to another color c'' without affecting other edges. Both the edge (u', v') and the color c'' are selected uniformly at random from the corresponding sets. For a color swapping operation the difference of energy is equal to:

$$\Delta\mathcal{E}^{sw} = \frac{1}{|E|(1 - \frac{1}{N})}\Big(g(u, v, c) - g(u, v, c') + g(u', v', c')$$
$$- g(u', v', c) - \frac{1}{d_u} - \frac{1}{d_v} - \frac{1}{d_{u'}} - \frac{1}{d_{u'}}\Big), \quad (5.8)$$

similarly to the condition (5.1) for *JA-BE-JA-VC*. For a simple color change operation, the change of energy is:

$$\Delta\mathcal{E}^{ch} = \frac{1}{|E|(1 - \frac{1}{N})}\left(g(u, v, c) - g(u, v, c'') - \frac{1}{d_u} - \frac{1}{d_v}\right)$$
$$+ \alpha\frac{2}{|E|^2(1 - \frac{1}{N})^2}\Big(n_u(c'') + n_v(c'') - n_u(c) - n_v(c) + 1\Big). \quad (5.9)$$

Another metrics that can be expressed as sum of clique potentials is the communication cost. Using the notation, in this chapter the communication cost (CC) metric can be defined as:

$$CC = \sum_{v \in V}\sum_{c \in C}\mathbb{1}(0 < n_v(c) < d_v)$$

In what follows we will consider the equivalent metric:

$$\mathcal{E}_{cc} = \frac{\sum\limits_{v \in V}\sum\limits_{c \in C}\mathbb{1}(0 < n_v(c) < d_v)}{|V|N},$$

that has the advantage of being between 0 and 1. Let us consider the color change from c to c' for edge (u, v). The number of colors change as follows:

$$\hat{n}_u(c) = n_u(c) - 1 \qquad\qquad \hat{n}_v(c) = n_v(c) - 1$$
$$\hat{n}_u(c') = n_u(c') + 1 \qquad\qquad \hat{n}_v(c') = n_v(c') + 1$$

The change of the energy of the graph is then equal to:

$$\Delta \mathcal{E}_{cc}^{ch}(u, v) = \widehat{\varepsilon}_{cc}^{ch} - \varepsilon_{cc}^{ch},$$

where ε_{cc}^{ch} and $\widehat{\varepsilon}_{cc}^{ch}$ denote the contribution from the vertices u and v to the total energy of the graph, before and after we have changed the color of the edge respectively. $\widehat{\varepsilon}_{cc}^{ch}$ and ε_{cc}^{ch} are defined as follows:

$$\widehat{\varepsilon}_{cc}^{ch} = \frac{1}{|V|N}(\mathbb{1}(0 < \hat{n}_u(c) < d_u) + \mathbb{1}(0 < \hat{n}_v(c) < d_v)$$
$$+ \mathbb{1}(0 < \hat{n}_u(c') < d_u) + \mathbb{1}(0 < \hat{n}_v(c') < d_v))$$
$$= \frac{1}{|V|N}(\mathbb{1}(0 < n_u(c) - 1 < d_u) + \mathbb{1}(0 < n_v(c) - 1 < d_v)$$
$$+ \mathbb{1}(0 < n_u(c') + 1 < d_u) + \mathbb{1}(0 < n_v(c') + 1 < d_v))$$

$$\varepsilon_{cc}^{ch} = \frac{1}{|V|N}(\mathbb{1}(0 < n_u(c) < d_u) + \mathbb{1}(0 < n_v(c) < d_v)$$
$$+ \mathbb{1}(0 < n_u(c') < d_u) + \mathbb{1}(0 < n_v(c') < d_v))$$

Then $\Delta\mathcal{E}_{cc}^{ch}$ takes values $\frac{-2}{|V|N}, \frac{-1}{|V|N}, 0, \frac{1}{|V|N}, \frac{2}{|V|N}$. In case of color swapping operation, we swaps the colors c and c' of edges (u, v) and (u', v') respectively. Then the energy change is equal to:

$$\Delta\mathcal{E}_{cc}^{sw}(u, v, u', v') = \widehat{\varepsilon}_{cc}^{sw} - \varepsilon_{cc}^{sw}$$

where ε_{cc}^{sw} and $\widehat{\varepsilon}_{cc}^{sw}$ denote contribution from the vertices u, v, u', and v' to the total energy of the graph, before and after we have swapped the color of the edge

respectively.

$$
\begin{aligned}
\widehat{\varepsilon}_{cc}^{sw} = {} & \frac{1}{|V|N}(\mathbb{1}(0 < \hat{n}_u(c) < d_u) + \mathbb{1}(0 < \hat{n}_v(c) < d_v) + \mathbb{1}(0 < \hat{n}_u(c') < d_u) \\
& + \mathbb{1}(0 < \hat{n}_v(c') < d_v) + \mathbb{1}(0 < \hat{n}_{u'}(c) < d_{u'}) + \mathbb{1}(0 < \hat{n}_{v'}(c) < d_{v'}) \\
& + \mathbb{1}(0 < \hat{n}_{u'}(c') < d_{u'}) + \mathbb{1}(0 < \hat{n}_{v'}(c') < d_{v'})) \\
= {} & \frac{1}{|V|N}(\mathbb{1}(0 < n_u(c) - 1 < d_u) + \mathbb{1}(0 < n_v(c) - 1 < d_v) + \mathbb{1}(0 < n_u(c') + 1 < d_u) \\
& + \mathbb{1}(0 < n_v(c') + 1 < d_v) + \mathbb{1}(0 < n_{u'}(c) + 1 < d_{u'}) + \mathbb{1}(0 < n_{v'}(c) + 1 < d_{v'}) \\
& + \mathbb{1}(0 < n_{u'}(c') - 1 < d_{u'}) + \mathbb{1}(0 < n_{v'}(c') - 1 < d_{v'}))
\end{aligned}
$$

$$
\begin{aligned}
\varepsilon_{cc}^{sw} = {} & \frac{1}{|V|N}(\mathbb{1}(0 < n_u(c) < d_u) + \mathbb{1}(0 < n_v(c) < d_v) + \mathbb{1}(0 < n_u(c') < d_u) \\
& + \mathbb{1}(0 < n_v(c') < d_v) + \mathbb{1}(0 < n_{u'}(c) < d_{u'}) + \mathbb{1}(0 < n_{v'}(c) < d_{v'}) \\
& + \mathbb{1}(0 < n_{u'}(c') < d_{u'}) + \mathbb{1}(0 < n_{v'}(c') < d_{v'}))
\end{aligned}
$$

To calculate energy change (due to the change of color of the edge or to the swap of colors of edges) of functions $\mathcal{E}$ and $\mathcal{E}_{cc}$, only information about the nodes involved and their neighborhood is required as it was the case for *JA-BE-JA-VC*. At the same time, the same difficulty noted in Section 5.2 holds. In an edge-centric distributed framework, in general the edges for a node are processed by different instances. First, we have implemented a naive version of our *SA* algorithm of *JA-BE-JA-VC* which requires each instance to propagate color updates (e.g., the new values of $n_u(c)$, $n_v(c)$, etc.) to other instances at each iteration, however it leads to an unacceptable partitioning time. We have thus developed two versions of *SA* framework which overcome this issue.

5.5   The *SA* framework

In order to reduce partitioning time, we implemented the following distributed version of the algorithm. First, edges are randomly distributed among the instances, and each of them executes the general *SA* algorithm described above on the local

set of edges for L swaps. No communication can take place among instances during this phase. After this phase is finished, communication is allowed, the correct values are computed and all the edges are again distributed at random among the instances. This reshuffle guarantees that any pair of edges has a probability to be considered for color swapping.

The larger L, the larger risk that workers operate with stale information. We want then to fix L, so that it is very unlikely that two workers change the color of two different edges of the same vertex. To calculate the upper-bound for L we considered the following situation. When we change the color of an edge in component j (P_j), in average there are $2\bar{d}$ (where $\bar{d}$ is the average degree in the graph) edges attached to this edge. Hence, the probability that all these $2\bar{d}$ edges will not be situated in P_i is the following:

$$\left(1 - \frac{1}{N}\right)^{2\bar{d}}$$

Then, the probability that at least one edge from these $2\bar{d}$ edges will be in P_i is:

$$1 - \left(1 - \frac{1}{N}\right)^{2\bar{d}}$$

The maximum number of vertices in P_i affected by performing swaps in all other $N - 1$ components is the following:

$$4\bar{d}(N - 1)\left(1 - \left(1 - \frac{1}{N}\right)^{2\bar{d}}\right) \tag{5.10}$$

In case we perform L swaps during a *local step*, then in P_i we have two sets of vertices: S_{direct}, $S_{indirect}$. S_{direct} consists of vertices that are directly affected by the L swaps performed in current component, $|S_{direct}| <= 4L$. $S_{indirect}$ is the set of vertices that are affected by the swaps in other components; its size is at most the value in (5.10).

Hence, we need to be sure that these two sets (S_{direct}, $S_{indirect}$) are significantly

Table 5.1 – Spark configuration

Property name	Property value
spark.executor.memory	20GB
spark.driver.memory	40GB
spark.cores.max	10
spark.local.dir	"tmp"
spark.cleaner.ttl	20

smaller than $\frac{|V|}{N}$:

$$max\left(4L, 4L\bar{d}(N-1)\left(1-\left(1-\frac{1}{N}\right)^{2\bar{d}}\right)\right) < 4L\left(1+4\bar{d}Ne^{-2\bar{d}}\right) << \frac{|V|}{N}$$

(5.11)

$$L << \frac{|V|}{4N\left(1+4\bar{d}Ne^{-2\bar{d}}\right)}$$

(5.12)

Given the same number of potential changes considered, this implementation requires L times less synchronization phases among the instances. Due to the large time required for the synchronization phase in comparison to the time required for the *local* step, one can expect the total partitioning time to be reduced by roughly the same factor. Our experiments show that this is the case. In the setting described in the following section, with $L = 200$, there is no difference between the final components produced by the two implementations, but the partitioning time for the naive one is 100 times larger.

The detailed steps are described in Algorithm 2.

5.6 Evaluation of the *SA* framework

All our experiments were performed on a cluster of 2 nodes (1 master and 1 slave) with dual-Xeon E5-2680 v2 @2.80GHz with 192GB RAM and 10 cores (20 threads). We used Spark version 1.4.0 and Spark standalone cluster as a resource manager. We configured Spark properties as in the Table 5.1.

We used two undirected graphs: the *email-Enron* graph (36,692 vertices/ 367,662 edges) and the *com-Amazon* graph (334,863 vertices/ 925,863 edges) provided by SNAP project [59].

1: **procedure** SIMULATEDANNEALING
2:    $G \leftarrow randomlyAssignColors(G)$
3:    $round \leftarrow 0$
4:    **while** $T > 0$ **do**
5:       $G \leftarrow partitionRandomly(G)$
6:       $G \leftarrow propagateValues(G)$
7:       **for** $component \leftarrow components$ **do**   ▷ Executes locally on each component
8:          **for** $i < L$ **do**
9:             **if** $tossCoin(2/3) == "head"$ **then** ▷ swapping with probability 2/3...
10:                $e \leftarrow randomEdge(component)$
11:                $e' \leftarrow randomEdge(component)$
12:                $\Delta\mathcal{E} \leftarrow computeDelta(e, e')$
13:                **if** $\Delta\mathcal{E} < 0$ **then**
14:                   $swapColors(e, e')$
15:                **else**
16:                   $swapColorsWithProb(e, e', e^{-\frac{\Delta\mathcal{E}}{T}})$
17:                **end if**
18:             **else**   ▷ changing...
19:                $e \leftarrow randomEdge(component)$
20:                $c' \leftarrow anotherColor(c)$
21:                $\Delta\mathcal{E} \leftarrow computeDelta(e, c')$
22:                **if** $\Delta\mathcal{E} < 0$ **then**
23:                   $changeColor(e, c')$
24:                **else**
25:                   $changeColorWithProb(e, c', e^{-\frac{\Delta\mathcal{E}}{T}})$
26:                **end if**
27:             **end if**
28:             $i++$
29:          **end for**
30:       **end for**
31:       $round++$
32:       $T \leftarrow T_{init} - round * \Delta T$
33:    **end while**
34:    $G = partitionBasedOnColor(G)$
35: **end procedure**

Algorithm 2 Implementation of *SA* for GraphX

We implemented *JA-BE-JA-VC* and *SA* (Algorithm 2) for GraphX. In both cases we considered the distributed operation described at the end of the previous section: $L(= 200)$ steps are performed locally at each instance before performing a synchronization phase. For a fair comparison between the two algorithms, L corresponds in both cases to the number of alternative configurations considered (i.e., those for which the energy variation is computed). The source code of both versions of our *SA* framework is available online [68].

Each experiment consists of the following steps: i) launch the computational cluster; ii) load the given graph; iii) *color* the graph according to a random partitioner (`CanonicalRandomVertexCut`); iv) *re-color* it with *JA-BE-JA-VC* or *SA*; v) compute the partition metrics.

While *SA* is guaranteed to converge to an optimal solution of problem (5.5) if T decreases as the inverse of the logarithm of the number of iterations, the convergence would be too slow for practical purposes. For this reason and to permit a simpler comparison of *SA* and *JA-BE-JA-VC*, in both cases the initial temperature decreases linearly from T_0 till 0 in 100 or 1000 iterations.

As we said our *SA* partitioner can be used to optimize different functions. We start by comparing *JA-BE-JA-VC* and *SA* when they have the same target $\mathcal{E}_{comm}$ in (5.3). When the objective function is the same, the two main differences between the algorithms are i) the way to choose the edges to swap, and ii) the rule to accept a change. In particular, *JA-BE-JA-VC* chooses edges whose color is the rarest in a neighborhood, while *SA* selects them uniformly at random. *JA-BE-JA-VC* then decides to swap or not the colors according to the deterministic rule (5.2), while *SA* adopts the probabilistic rule (see Section 5.4)

The corresponding results are in Tables 5.2, 5.3, row *I* and *II*, for different values of the initial temperature for *email-Enron*. Both the algorithms reduce the value of $\mathcal{E}_{comm}$, but the decrease is larger for *JA-BE-JA-VC*. This is essentially due to the fact that *JA-BE-JA-VC* performs more swaps, although the number of pairs of links to swap considered is the same (equal to L times the number of iterations). For example for the initial temperature $5 * 10^{-11}$ *SA* swaps the color of 8808 edges, while *JA-BE-JA-VC* swaps the color of 37057 edges. In fact, *SA* random edge selection leads to consider a large number of pairs that is not useful to swap, while *JA-BE-JA-VC* only considers candidates that are more likely to be advantageous

Table 5.2 – Final partitioning metrics obtained by *JA-BE-JA-VC* partitioner. Temperature decreases linearly from T_0 till 0.0 by given number of iterations.

# iterations	T_0	Final $\mathcal{E}_{comm}$	Vertex-cut	Comm. cost	Balance	STD
	5.00E-11	0.888788	25091	122477	1.0091	0.0055
100	1.00E-10	0.888638	25096	122572	1.0091	0.0055
	5.00E-10	0.888634	25085	122350	1.0091	0.0055
	5.00E-11	0.8197	25685	118453	1.0091	0.0055
1000	1.00E-10	0.8202	25656	118588	1.0091	0.0055
	5.00E-10	0.8193	25603	118455	1.0091	0.0055

Table 5.3 – Final partitioning metrics obtained by *SA* using only E_{comm} as energy function. Temperature decreases linearly from T_0 till 0.0 by given number of iterations.

# iterations	T_0	Final $\mathcal{E}_{comm}$	Vertex-cut	Comm. cost	Balance	STD
	5.00E-11	0.900026	25046	120083	1.0091	0.0055
100	1.00E-10	0.900027	25046	120087	1.0091	0.0055
	5.00E-10	0.900006	25046	120080	1.0091	0.0055
	5.00E-11	0.8989	25048	120648	1.0091	0.0055
1000	1.00E-10	0.8990	25049	120634	1.0091	0.0055
	5.00E-10	0.8989	25046	120664	1.0091	0.0055

to swap. In this sense *JA-BE-JA-VC* is greedier than *SA*: *JA-BE-JA-VC* exploits more, while *SA* explores more. Adopting the same choice for *SA* would lead to lose the condition $q_{\mathbf{c},\mathbf{c}'} = q_{\mathbf{c}',\mathbf{c}}$, that is required to guarantee convergence to the global minimum of the function. We plan to investigate in the future how to bias the selection process so that edges whose color is less represented are more likely to be selected, but still the condition $q_{\mathbf{c},\mathbf{c}'} = q_{\mathbf{c}',\mathbf{c}}$ is satisfied.

Although *SA* seems to be less effective to reduce the energy, the results in Tables 5.2, 5.3 also show that the function $\mathcal{E}_{comm}$ is not necessarily a good proxy for the usual partition metrics like VC or CC. In fact, we see that for 100 iterations *SA* slightly outperforms *JA-BE-JA-VC* both in terms of VC and CC for the initial temperature values, even if its final energy is always larger. For 1000 iterations *JA-BE-JA-VC* performs better in terms of VC and worse in terms of CC. What is even more striking is that the increase in the number of iterations leads to a decrease of the energy value (as expected), but not necessarily to a decrease of

Table 5.4 – Final partitioning metrics obtained by SA using $E_{comm} + 0.5E_{bal}$ as energy function). Temperature decreases linearly from T_0 till 0.0 by given number of iterations.

# iterations	T_0	Final $\mathcal{E}_{comm}$	Vertex-cut	Comm. cost	Balance	STD
	5.00E-11	0.894742	25044	120768	1.0088	0.0058
100	1.00E-10	0.894692	25043	120751	1.0079	0.0058
	5.00E-10	0.894617	25043	120782	1.0084	0.0061
	5.00E-11	0.8466	24795	113008	1.0144	0.0114
1000	1.00E-10	0.8467	24794	112951	1.0178	0.0099
	5.00E-10	0.8466	24771	112946	1.0332	0.0211
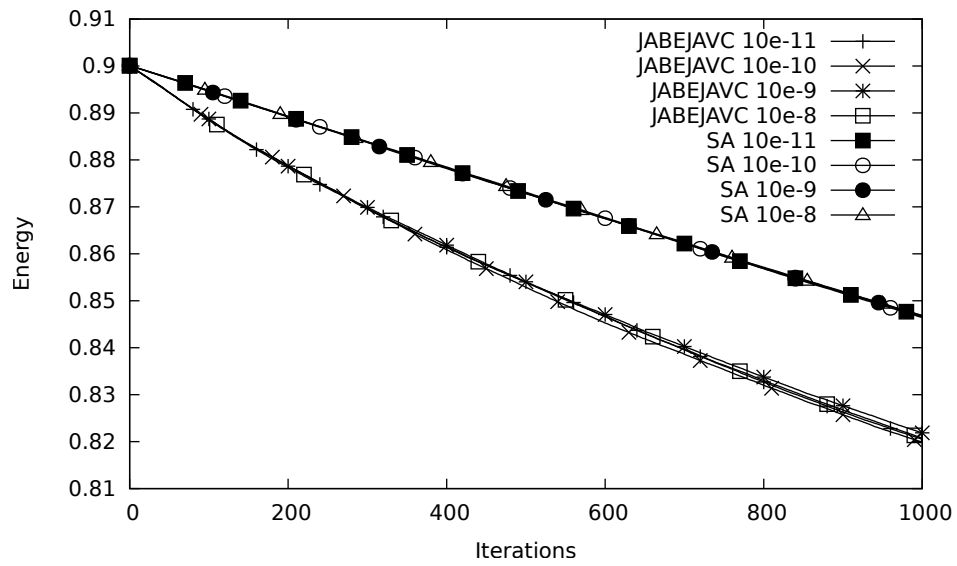
Figure 5.1 – $\mathcal{E}_{comm}$ value for $JA\text{-}BE\text{-}JA\text{-}VC$ and $\mathcal{E}$ value for SA using *email-Enron* graph (1000 iterations were performed)

VC and CC. These results suggest that more meaningful energy functions should probably be considered and our framework has the advantage to work for a large family of different objectives.

We now move to compare $JA\text{-}BE\text{-}JA\text{-}VC$ with SA when the function $\mathcal{E} = \mathcal{E}_{comm} + \alpha\mathcal{E}_{bal}$ is considered. Figure 5.1 shows the evolution of the energy after each local phase and then every $L = 200$ local iterations. Note that after a given iteration the energy can increase both for $JA\text{-}BE\text{-}JA\text{-}VC$ and SA, but the figure shows that every L iterations, the energy always decrease. While the two
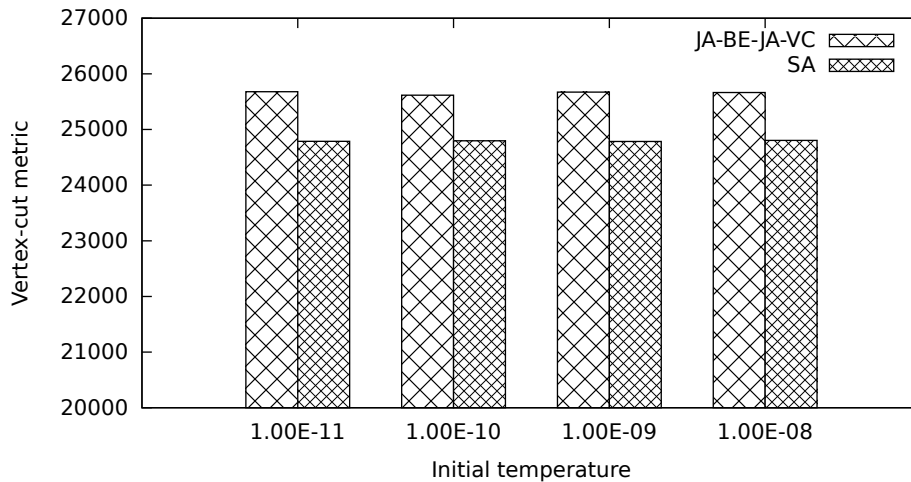
Figure 5.2 – Vertex-cut metric for *JA-BE-JA-VC* and *SA* using *email-Enron* graph (1000 iterations were performed)

energies have different expressions, the initial energy values are indistinguishable, because the starting point is an almost balanced partition and then $\mathcal{E}_{bal} \ll \mathcal{E}_{comm}$ and $\mathcal{E} \approx \mathcal{E}_{bal}$. As in the previous case, *JA-BE-JA-VC* appears to be greedier in reducing the energy function. Tables 5.2, 5.4 show that this does not lead necessarily to a better partitioning. Indeed, after 100 iterations, *SA* minimizing $\mathcal{E}$ provides the best partition in terms of VC, CC and BAL, while STD is slightly worse. After 1000 iterations, *SA* has further improved VC and CC at the expenses of the balance metrics like BAL and STD.

Figures 5.2 and 5.3 show similar results comparing the final metrics VC and CC for an even larger range of initial temperatures.

While for *email-Enron* we have shown how *SA* can improve communication metrics at the expenses of balance metrics, we show that the opposite result can be obtained on a different graph (*com-Amazon*) in Figures 5.4 and 5.5. Remember that in any case, for a given graph, it is possible to tune the relative importance of the different metrics by varying the parameter α.
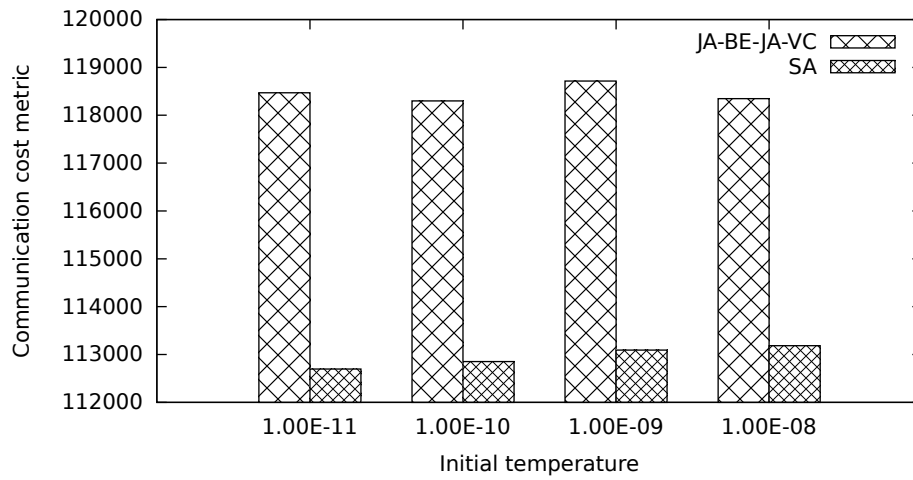
Figure 5.3 – *Communication cost* metric for *JA-BE-JA-VC* and *SA* using *email-Enron* graph (1000 iterations were performed)
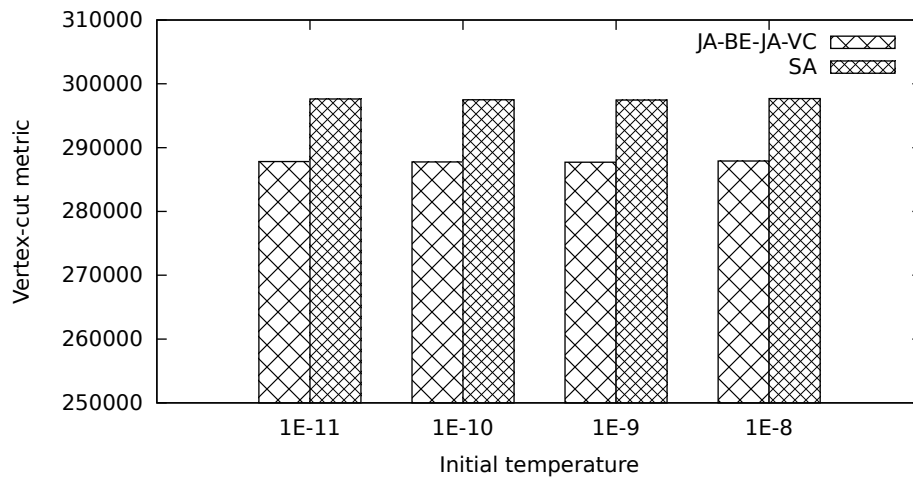
Figure 5.4 – *Vertex-cut* metric value for *JA-BE-JA-VC* and *SA* using *com-Amazon* graph (1000 iterations were performed)
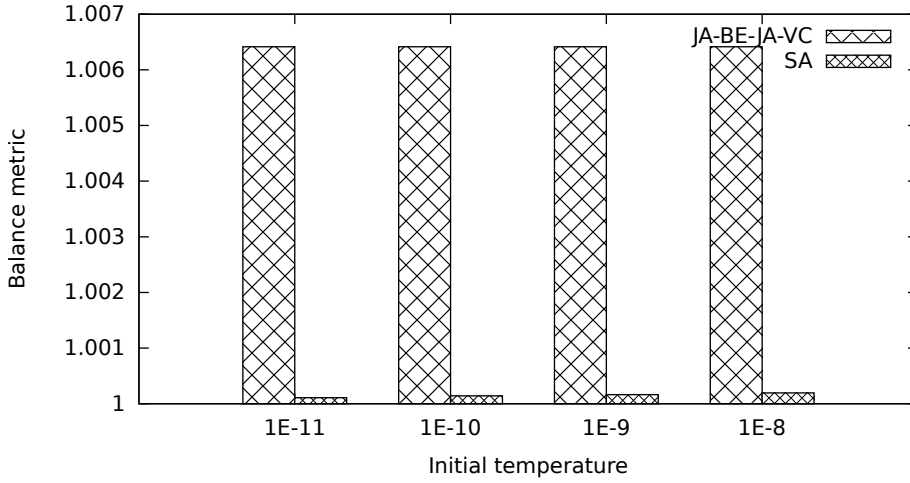
Figure 5.5 – *Balance* metric value for *JA-BE-JA-VC* and *SA* using *com-Amazon* graph (1000 iterations were performed)

5.7 The multi-opinion *SA* framework

In this section, we provide an enhanced version of our framework — the multi-opinion *SA* framework, which relies on some ideas from the asynchronous Gibbs sampler proposed in [65].

A Gibbs sampler is another possible set of rules to determine the next state, i.e., the next color assignment in our case. Under Gibbs sampler, a subvector $\mathbf{c}_s$ of $\mathbf{c}^4$ is selected with probability $q_{\mathbf{c}_s}$. Let $\mathbf{c}_{-s}$ denote the other elements of $\mathbf{c}$, so that $\mathbf{c} = (\mathbf{c}_s, \mathbf{c}_{-s})$. A new random subvector $\mathbf{c}'_s$ is randomly generated so that the probability to move to $\mathbf{c}' = (\mathbf{c}'_s, \mathbf{c}_{-s})$ is:

$$\frac{e^{-\frac{\mathcal{E}(\mathbf{c}'_s, \mathbf{c}_{-s})}{T}}}{\sum_{\mathbf{d}_s \in C^{|\mathbf{c}_s|}} e^{-\frac{\mathcal{E}(\mathbf{d}_s, \mathbf{c}_{-s})}{T}}}. \tag{5.13}$$

Gibbs samplers can be considered as a special case of Metropolis-Hasting samplers where the new candidate states are selected with probabilities $q_{\mathbf{c},\mathbf{c}'}$ as in (5.13) and the acceptance probabilities $\beta_{\mathbf{c},\mathbf{c}'}$ are all equal to one. Practically speaking

---

[4]$\mathbf{c}$ is the solution for (5.5)

one talks about a Metropolis-Hasting sampler, if the probabilities $q_{\mathbf{c},\mathbf{c}'}$ are fixed (independently from the energy function) and the acceptance probabilities $\beta_{\mathbf{c},\mathbf{c}'}$ can be smaller than 1. The Gibbs sampler has the advantage that no change is refused (but it may be $\mathbf{c}'_s = \mathbf{c}$) but it requires to be able to sample according to (5.13), that corresponds, in general, to knowing the full conditional distribution. This may limit the size of the state vector that can be modified at a given time. Often, a single vector element (the color of a single edge in our case) is modified by a Gibbs sampler.

Also for the Gibbs sampler, if the temperature decreases logarithmically to 0, the state will converge almost surely to a global minimizer of the function $\mathcal{E}$. Sometimes the expression annealed Gibbs sampler is used for this specific SA algorithm.

In a distributed setting, one would split the vector $\mathbf{c}$ among the N workers: $\mathbf{c} = (\mathbf{c}_1, \mathbf{c}_2, \ldots \mathbf{c}_N)$. While every instance, say it i, could independently modify its subvector $\mathbf{c}_i$ (i.e., the colors of its component), it would need to know the current value of all the other variables $\mathbf{c}_{-i}$. The same difficulties we exposed above hold then. Recently, the authors of [65] have shown that it is possible to circumvent this problem. Their asynchronous Gibbs sampler allow workers to proceed in parallel without synchronization or locking. We briefly describe the algorithm using our notation.

The algorithm requires each instance to maintain an *opinion* about the color assignment for all the edges. We use the superscript i to denote the opinion of instance i, that we can write as $(\mathbf{c}_1^i, \mathbf{c}_2^i, \ldots \mathbf{c}_N^i)$. Each iteration of the proposed algorithm consists of two steps: local and global. During a local step each instance of the algorithm improves its own component of the graph. Instance i selects a subset $\mathbf{c}_{i,s}^i$ of its subvector $\mathbf{c}_i^i$ and generate $\tilde{\mathbf{c}}_{i,s}^i$ with probability

$$\frac{e^{-\frac{\mathcal{E}(\tilde{\mathbf{c}}_{i,s}^i, \mathbf{c}_{-i}^i)}{T}}}{\sum_{\mathbf{d}_{i,s} \in C^{|\mathbf{c}_{i,s}^i|}} e^{-\frac{\mathcal{E}(\mathbf{d}_{i,s}, \mathbf{c}_{-s}^i)}{T}}}, \tag{5.14}$$

that depends only on the current opinion of instance i. Then, during the global step, each instance, decides whether to update its opinion according to what other

instances think about their components or not. In particular an instance j updates its opinion about component i, according to what i thinks about it with probability $\alpha_{i,j}$:

$$\alpha_{i,j} = \min\left(1, \exp\left(-\frac{1}{T}(\mathcal{E}(\mathbf{c}_i^i, \mathbf{c}_{-i}^j) - \mathcal{E}(\mathbf{c}_i^j, \mathbf{c}_{-i}^j) + \mathcal{E}(\mathbf{c}_i^j, \mathbf{c}_{-i}^i) - \mathcal{E}(\mathbf{c}_i^i, \mathbf{c}_{-i}^i))\right)\right)$$

(5.15)

In [65] it is proven that the probability distribution of each opinion $\mathbf{c}^i$ converges to the same distribution the centralized Gibbs sampler would converge. It follows then that if we gradually decrease the temperature according to the usual law, each opinion will converge almost surely to a global minimizer of the energy function.

The next section describes how we have modified our original simulated algorithm according to the results in [65] and how we have implemented it in GraphX.

5.7.1 Distributed implementation

Our new algorithm borrows from [65] the idea to maintain potentially different opinions at each instance, and to use the probabilities in (5.15) to accept the opinions of other instances. At the same time, instance i updates its subvector $\mathbf{c}_i^i$ according to Metropolis-Hasting sampling described in Section 5.4, because it is computationally simpler than Gibbs sampling. Moreover, the stationary distribution corresponding to the local Metropolis-Hasting sampling steps is (5.14). Hence a "large" number of Metropolist-Hasting steps correspond to draw a single Gibbs sample. We suspect that the results in [65] hold also when a finite number of Metropolis-Hasting sampling steps are performed, but we do not have yet a formal proof. At the same time, implementing a simulated annealing algorithm based on the asynchronous Gibbs sampler in [65] requires minor changes to the Spark implementation of our algorithm described in what follows, as far as Gibbs samples can be drawn efficiently.

We assume that the energy can be decomposed as sum of vertex energies that depend only on the number of edges of each color the vertex has:

$$\mathcal{E}(\mathbf{c}) = \sum_{v \in V} \varepsilon_v(\mathbf{c}) = \sum_{v \in V} \varepsilon_v(\{n_v(c), c \in C\}).$$

This is for example the case of both $\mathcal{E}_{comm}$ and $\mathcal{E}_{cc}$. This assumption allows us to simplify the computational requirement of the algorithm, but it is not necessary. It will be convenient to define the energy associated to a subset A of the vertices:

$$\mathcal{E}_A(\mathbf{c}) \triangleq \sum_{v \in A} \varepsilon_v(\mathbf{c}).$$

Remember that we have N instances of the partitioner algorithm, where each instance has its own subset of edges E_i, whose set of vertices is $V(E_i)$. Let E_{-i} denote all the edges except those in E_i Each edge has two values attached to it: the index of the instance to whom this edges belongs, and an array of colors of length N: $c_k^0, c_k^1, ..., c_k^N$ which represents the colors of edge k according to the N different instances. The different opinions the instances have about what the color of edges k should be. When an instance i changes the color of edge k, it changes c_k^i. A value attached to a vertex is an array which contains N different maps. Each of these maps contains an information about the colors of the edges attached to this vertex according to some instance opinion, e.g., a map says there are n_0 edges of color c_0, n_1 edges of color c_1, etc.

Each iteration of this distributed algorithm consists of two steps: a local step and global step. Each instance updates its opinion during the local step performing L attempts to swap/change colors as in the first version. No communication between instances is required. Then during a global step, it performs a *shuffle*, which propagates vertex values to all the instances, and after it computes the $N(N-1)$ values of $\alpha_{i,j}$, which are used to accept the opinions of the other instances. A naive computation of the probabilities $\alpha_{i,j}$ requires computing four times the energy of the whole graph in our case. Computing the energy of the whole graph in GraphX, requires using all N instances, because each instance has only a subset of the graph. Thus, each instance i needs to compute the $N-1$ acceptance probabilities $\alpha_{k,i}$ for k different from i. To compute all α for each instance, we will need to compute sequentially $4N(N-1)$ times energy of different graphs.

In order to speed up the computation of the probabilities $\alpha_{i,j}$, we propose the following procedure that makes possible to calculate the four energies appearing in (5.15) as sum of two differences, where each difference can be computed locally by instance i, thanks to our assumption on the energy function.

First we consider the difference between the third and forth energy terms in (5.15):

$$\mathcal{E}(\mathbf{c}_i^j, \mathbf{c}_{-i}^i) - \mathcal{E}(\mathbf{c}_i^i, \mathbf{c}_{-i}^i).$$

Both these energies are computed as function of the vertices of the whole graph, but these graphs are different. The two energies are different because i and j have in general different opinions about what colors assign to the edges E_i: $\mathbf{c}_i^i \neq \mathbf{c}_i^j$. It is important to notice that $\mathbf{c}_i^j$ did not change during the local step: instance j may only have changed $\mathbf{c}_j^j$. Instance i has then all the information required to compute this difference. Moreover, because of our assumption on the energy function, the difference of the two energies can be reduced to computing the difference between energies attached to $V(E_i)$ according to j and i opinions:

$$\mathcal{E}(\mathbf{c}_i^j, \mathbf{c}_{-i}^i) - \mathcal{E}(\mathbf{c}_i^i, \mathbf{c}_{-i}^i) = \mathcal{E}_{V(E_i)}(\mathbf{c}_i^j, \mathbf{c}_{-i}^i) - \mathcal{E}_{V(E_i)}(\mathbf{c}_i^i, \mathbf{c}_{-i}^i). \qquad (5.16)$$

As we said above, this difference can be computed immediately after the local step, without any need for the nodes to communicate.

Now, we consider the difference between the first two energies appearing in the formula (5.15):

$$\mathcal{E}(\mathbf{c}_i^i, \mathbf{c}_{-i}^j) - \mathcal{E}(\mathbf{c}_i^j, \mathbf{c}_{-i}^j)$$

However, $\mathbf{c}_j^j \subset \mathbf{c}_{-i}^j$ and the updated values of $\mathbf{c}_j^j$ are located on instance j. That it why, it is necessary to perform a shuffle first to propate the new set of opinions. We observe that, because of our assumption on the energy function:

$$\mathcal{E}(\mathbf{c}_i^i, \mathbf{c}_{-i}^j) - \mathcal{E}(\mathbf{c}_i^j, \mathbf{c}_{-i}^j) = \mathcal{E}_{V(E_i)}(\mathbf{c}_i^i, \mathbf{c}_{-i}^j) - \mathcal{E}_{V(E_i)}(\mathbf{c}_i^j, \mathbf{c}_{-i}^j). \qquad (5.17)$$

Moreover, we need to know only the colors of $E(V(E_i))$ (all neighbors edges of $V(E_i)$)). We calculate $\mathcal{E}_{V(E_i)}(\mathbf{c}_i^i, \mathbf{c}_{-i}^j)$ in the following manner. First, instance i collects all the triplets (edges with their vertices) that correspond to E_i. Next, it takes all vertices attached to these triplets and reduce it to a set of vertices (because some vertices may be repeated). After, instance i takes vertex values (mapping from color to the number of times edges of this color are connected to this vertex) according to j opinion. Then, it traverses all triplets and compare

color of the edges according to i and j. In case the colors of edge $e = (u, v)$ are different for i and j we modify vertex values of u and v (by removing from both vertex data one appearance of color c_e^j and adding one appearance of color c_e^i).

Formulas (5.17) and (5.16) simplify the computation of $\alpha_{i,j}$: instead of computing four times an energy of the four different graphs (which cannot be done in local way), it is necessary to compute locally difference in energy related to the local vertices between what the owner instance thinks and remote instance thinks. Finally, computing $\alpha_{i,j}$ is reduced to (5.18):

$$
\begin{aligned}
\alpha_{i,j} = \min\Big(1, \exp\Big(& -\frac{1}{T}(\mathcal{E}_{V(E_i)}(\mathbf{c}_i^i, \mathbf{c}_{-i}^j) - \mathcal{E}_{V(E_i)}(\mathbf{c}_i^j, \mathbf{c}_{-i}^j) \\
& +\mathcal{E}_{V(E_i)}(\mathbf{c}_i^j, \mathbf{c}_{-i}^i) - \mathcal{E}_{V(E_i)}(\mathbf{c}_i^i, \mathbf{c}_{-i}^i))\Big)\Big)
\end{aligned}
\tag{5.18}
$$

The probability $\alpha_{i,j}$ (the probability to assign $\mathbf{c}_i^j := \mathbf{c}_i^i$) can be computed then by instance i in two phases requiring only one shuffle. Once $\alpha_{i,j}$ has been computed for all j different from i, instance i can generate the corresponding Bernoulli random variable and decide if $\mathbf{c}_i^j$ should be updated to $\mathbf{c}_i^i$. Note that the values $\mathbf{c}_i^j$ are associated the links E_i and are then stored at instance i. Hence, no communication is required for this update. Finally, instance i computes for each vertex in $V(E_i)$ how many edges in E_i of a given color it has according to the different N opinion. A second shuffle is needed to aggregate this information and update the array of maps associated to each vertex.

Algorithm 3 shows the pseudo-code of the distributed implementation of our algorithm.

5.8 Evaluation of the multi-opinion *SA* framework

As a cluster we used 2 machines of *Nef Sophia cluster* (1 master and 1 slave) with dual-Xeon E5-2680 v2 @2.80GHz with 192GB RAM and 10 core (20 threads). We used Spark version 1.4.0 and Spark standalone cluster as a resource manager. We have configured Spark properties as in the Table 5.5. We used the undirected graph

1: **procedure** SIMULATEDANNEALING
2: $\quad G \leftarrow randomlyAssignColors(G)$
3: $\quad G \leftarrow partitionRandomly(G)$
4: $\quad round \leftarrow 0$
5: $\quad$ **while** $T > 0$ **do**
6: $\quad\quad G \leftarrow propagateValues(G)$
7: $\quad\quad$ **for** $component \leftarrow components$ **do** $\qquad \triangleright$ Executes locally on each component
8: $\quad\quad\quad$ **for** $i < L$ **do**
9: $\quad\quad\quad\quad$ **if** $tossCoin(probabillityToSwap) == "head"$ **then** $\qquad \triangleright$ swap
10: $\quad\quad\quad\quad\quad e \leftarrow randomEdge(component)$
11: $\quad\quad\quad\quad\quad e' \leftarrow randomEdge(component)$
12: $\quad\quad\quad\quad\quad \Delta\mathcal{E} \leftarrow computeDelta(e, e')$
13: $\quad\quad\quad\quad\quad$ **if** $\Delta\mathcal{E} < 0$ **then**
14: $\quad\quad\quad\quad\quad\quad swapColors(e, e')$
15: $\quad\quad\quad\quad\quad$ **else**
16: $\quad\quad\quad\quad\quad\quad swapColorsWithProb(e, e', e^{-\frac{\Delta\mathcal{E}}{T}})$
17: $\quad\quad\quad\quad\quad$ **end if**
18: $\quad\quad\quad\quad$ **else** $\qquad\qquad\qquad\qquad\qquad\qquad \triangleright$ change
19: $\quad\quad\quad\quad\quad e \leftarrow randomEdge(component)$
20: $\quad\quad\quad\quad\quad c' \leftarrow anotherColor(c)$
21: $\quad\quad\quad\quad\quad \Delta\mathcal{E} \leftarrow computeDelta(e, c')$
22: $\quad\quad\quad\quad\quad$ **if** $\Delta\mathcal{E} < 0$ **then**
23: $\quad\quad\quad\quad\quad\quad changeColor(e, c')$
24: $\quad\quad\quad\quad\quad$ **else**
25: $\quad\quad\quad\quad\quad\quad changeColorWithProb(e, c', e^{-\frac{\Delta\mathcal{E}}{T}})$
26: $\quad\quad\quad\quad\quad$ **end if**
27: $\quad\quad\quad\quad$ **end if**
28: $\quad\quad\quad\quad i++$
29: $\quad\quad\quad$ **end for**
30: $\quad\quad\quad D2 = computeDifferenceD2(component) \qquad \triangleright$ See 5.16
31: $\quad\quad$ **end for**
32: $\quad\quad G \leftarrow propagateValues(G)$
33: $\quad\quad$ **for** $component \leftarrow components$ **do** $\qquad \triangleright$ Executes locally on each component
34: $\quad\quad\quad D1 = computeDifferenceD1(component) \qquad \triangleright$ See 5.17
35: $\quad\quad\quad \alpha_{i,j} = computeAlpha(D1, D2)$
36: $\quad\quad\quad propagateWithPtob(i, j, \alpha_{i,j})$
37: $\quad\quad$ **end for**
38: $\quad\quad round++$
39: $\quad\quad T \leftarrow T_{init} - round * \Delta T$
40: $\quad$ **end while**
41: $\quad G = partitionBasedOnColor(G)$
42: **end procedure**

Algorithm 3 Asynchronous *SA* for GraphX

Table 5.5 – Spark configuration

Property name	Property value
spark.executor.memory	150GB
spark.driver.memory	150GB
spark.cores.max	10
spark.local.dir	"tmp"
spark.cleaner.ttl	20

email-Enron (36,692 vertices/367,662 edges) provided by the SNAP project [59]. However, this graph is represented as a text file where each line is a direct edge. Hence each undirected edge is represented as a two opposite directed edges.

Both our distributed algorithms starts from some initial partitioning provided by some simple partitioner. In order to find out which initial partitioner we have to use we have conducted experiments with the following partitioners: `RandomVertexCut`, `CanonicalRandomVertexCut`, `EdgePartition1D`, `EdgePartition2D`, `HybridCut`, `HybridCutPlus`, `Greedy-Oblivious`. In each experiment we partitioned original graph by one of these partitioners and measured $\mathcal{E}_{cc}$ value. Figure 5.6 shows that for the original graph the best $\mathcal{E}_{cc}$ value was provided by `HybridCutPlus` partitioner. Moreover, the value for `CanonicalRandomVertexCut` is smaller (better) than for `HybridCut`, and we know that `CanonicalRandomVertexCut` performs random partitioning but keeps edges that connect the same vertices in the same partition. That is why, `CanonicalRandomVertexCut` outperforms `HybridCut` just because of the way the original graphs are represented, i.e., two direct edges represent one undirected edge. Thus we have pre-processed original graphs, by randomly removing one out of two directed edges. In the same Figure 5.6 we can see that for pre-processed graphs the best $\mathcal{E}_{cc}$ values were provided by `HybridCut`. Hence, all our next experiments will be performed on the pre-processed graphs with `HybridCut` as initial partitioner.

Figure 5.7 shows an evolution of $\mathcal{E}_{cc}$ energy, after each iteration of the multi-opinion *SA* algorithm. In each experiment temperature linearly decreases from some given initial temperature till zero. *Composite graph* refers to energy of the graph, where each edge is taken with color according to an opinion of instance which owns this edge. *Best instance* denotes the minimal energy of the graph
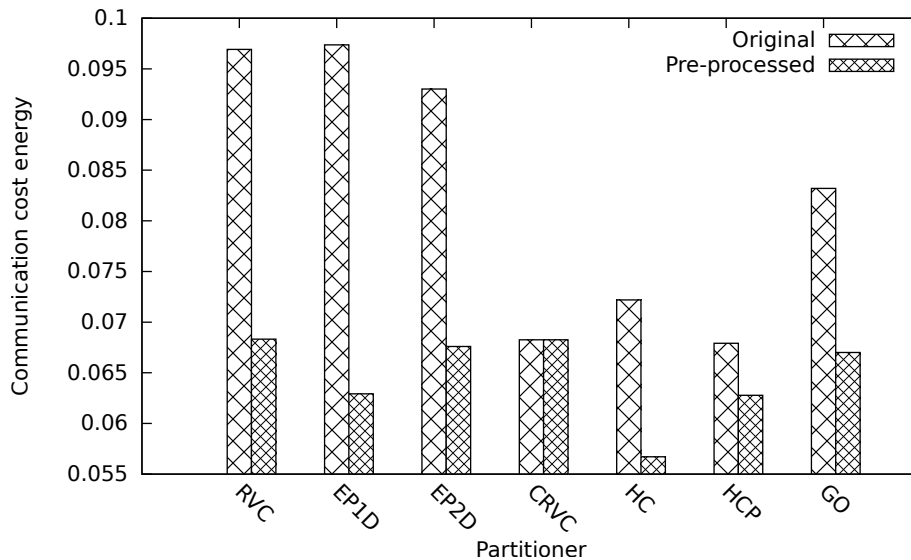
Figure 5.6 – *Energy* value for $\mathcal{E}_{cc}$ function for original and pre-processed *email-Enron* graphs

among N different instances. In the Figure 5.7 we can see that energy of the graph is not improved significantly, in the best case, it is roughly 2% of improvement. It happens, because every instance stuck in improvement of its set of edges. To overcome this stuck, we decided to shuffle partitioned graph every 3 iterations. By shuffle, we mean that we randomly reassign edges among the instances, without affecting opinion of any instance about any edge. In this case (see Figure 5.8), energy of the *best instance* decreases from 0.056 till 0.047.

5.9   Conclusion

In this chapter, we have analyzed and reverse engineered *JA-BE-JA-VC* edge partitioner. We have shown which objective function it optimizes. *JA-BE-JA-VC* uses ideas inspired by simulated annealing. However, we have explained that it cannot be considered as a correct simulated annealing implementation. That is why, we have proposed a framework for distributed edge partitioning based on simulated annealing which can be used to optimize a large family of partitioning metrics. We have implemented and evaluated on GraphX two versions of this
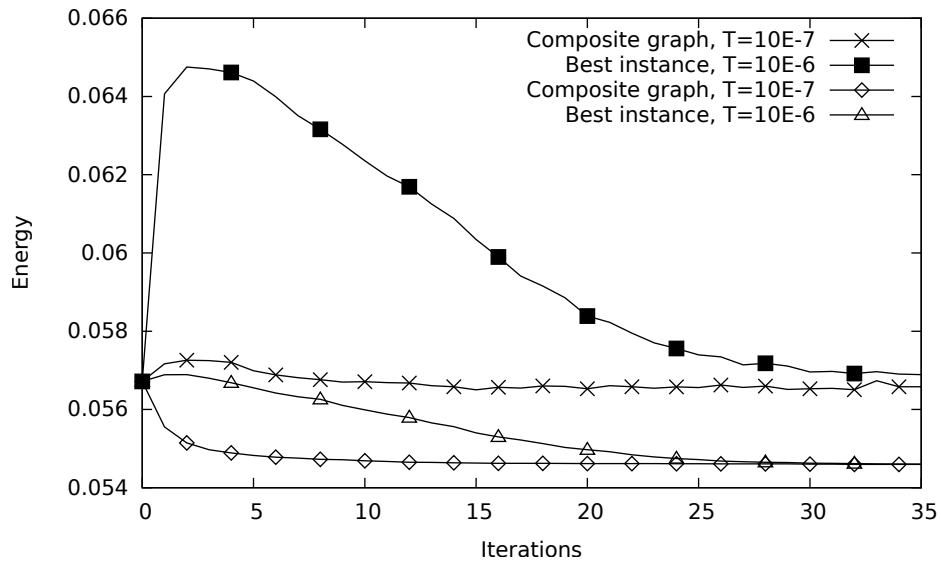
Figure 5.7 – *Energy* value for $\mathcal{E}_{cc}$ function for pre-processed *email-Enron* graph (`HybridCut` is initial partitioner, L equals to 10^5).
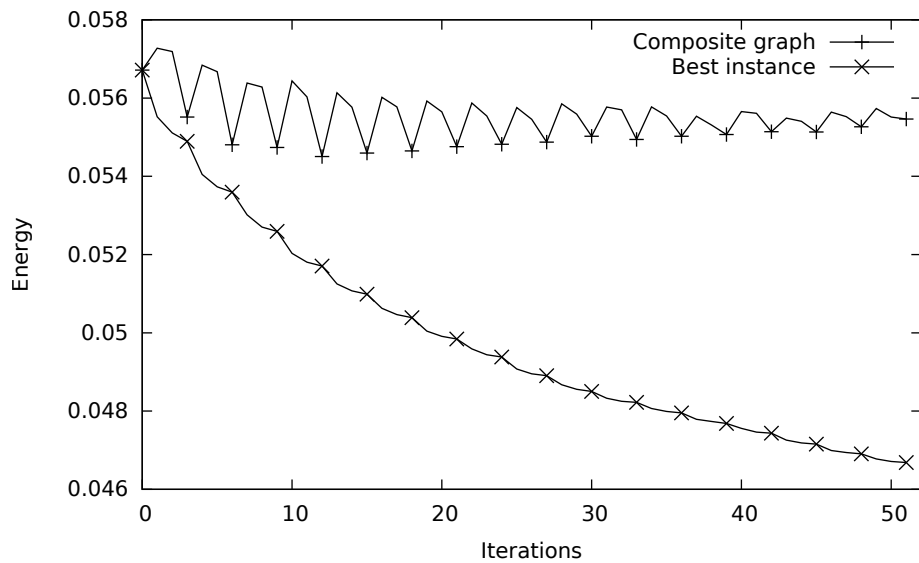
Figure 5.8 – *Energy* value for $\mathcal{E}_{cc}$ function for pre-processed *email-Enron* graph (`HybridCut` is initial partitioner, L equals to 10^5, initial temperature is 10^{-7}).

framework. The first implementation uses a fast but quite naive approach and that is why, it is not guaranteed to converge. The second implementation uses the

same multi-opinion approach for which [65] proves that a Gibbs-sampler would converge. We believe convergence holds also in our case, even if we have not proved yet. Our experimental results show that our framework is quite flexible, but at the same time it is difficult to provide rules for parameter tuning and greedier algorithms (as *JA-BE-JA-VC*) can provide a better partitioning when the number of iterations is limited.

Chapter 6

Conclusion

In this thesis we addressed the problem of how to partition a graph in order to speed up distributed algorithms to be run on the partitioned graph. This is a difficult problem. First, from a computational point of view, the problem to find the optimal partition is NP-hard for most of the natural objective functions one can think about. Moreover, it is not even clean which objective function should be considered to reduce the final computational time. We have dug in graph partitioning by overviewing the common approaches, solutions, and frameworks that have been proposed in literature, with a special attention to those for which running code is available. All partitioners can be classified into two approaches: *edge* and *vertex* partitioners. Based on the current study, we decided to work with the *edge* partitioning approach as more suitable for real-world graphs. Among the different graph processing frameworks available, we selected GraphX for our experiments.

In order to better understand what is the current progress in the area of distributed edge-partitioning and what are the commonly accepted solutions, we made a survey of all the existing algorithms. Moreover, we provided a new taxonomy for partitioners. It was important for us to see how partitioners are compared. However, during this process we have noticed that i) there is no commonly accepted solution for graph partitioning, ii) different partitioners are rarely compared to each other, iii) it is not even clear how to compare them the best. To fulfill this lack of comparison we conducted series of experiments on GraphX with all

existing partitioners available for GraphX plus some other ones which we have implemented. In these experiments we compared partitioners using existing metrics. Our results suggest that the `Hybrid-Cut` partitioner provides a partition on which graph algorithms perform the fastest.

This analysis was carried out by directly comparing the final execution time of different typical graph algorithms like `Connected Components` or `PageRank`. This approach provides the definitive comparison among different partitioners, but we would like to be able to compare two partitions and choose the best one for the purposes of our computation without running actual the computation itself. For this reason, we are interested in partition metrics, i.e., metrics that can be easily evaluated considering the partitioned graph. That is why we decided to conduct a deeper study of existing partition metrics which would allow us to argue about their importance. For this reason, we have conducted another series of experiments and used a sound statistical methodology. One of the difficulties was to handle huge variability of execution time which came from multiple sources,[1] and still get statisically significant conclusions. Finally, we have shown that there is a linear dependency between partition metrics and the execution time of graph processing algorithms. Our results show that *communication* metrics are more important than *balance* metrics. This important finding as well as *JA-BE-JA-VC* [52] partitioner inspired us for the next step.

We have decided to develop a new approach for distributed edge partitioning, based on simulated annealing that can be used to optimize a large family of partition metrics, including the communication ones. The challenge was to implement distributed simulated annealing in GraphX. The naive implementation of the algorithm would perform only one swap during an iteration and would then require an unacceptable computation time, because of the frequent data shuffles. After, we enhanced it by showing that each instance can perform up to L swaps during iteration without significantly affecting other instances. The recent results [65] allowed us to implement a second version of the partitioner based on Gibbs sampler. Nevertheless, also in this case the most natural implementation would lead to enormous amount of communication between iteration of the algorithm. We found out how to reduce this amount of communication from $4N(N-1)$ to 2 shuffles.

---

[1]Variability comes from operation system, newtwork, and distributed file system layers.

We conducted experiments to show the efficiency as well as the flexibility of our approach compared to state-of-the-art *JA-BE-JA-VC*.

6.1 Perspectives

In our experiments we have used relatively small graphs, for the reason that it is not be possible to conduct thousands of experiments with larger graphs due to the unacceptable execution time, but also because GraphX has implicit limitation to the graph size it can process. It is easy to observe failure while loading graph in GraphX with no apparent explanation. Thus, one of the perspectives is to perform on the short term some limited experiments on larger graphs.

Naturally the more time is allocated to partitioning the better the partitions are. However, sophisticated partitioners may require 100 times longer partitioning time while providing $1 - 2\%$ of improvement in terms of metrics. Thus, another perspective is to provide *partitioning service*, where user of this service provides a graph, graph processing algorithm (such as `PageRank`), number of time this algorithm will be executed (with different initial settings), and desired number of components N. *Partitioning service* selects and runs appropriate partitioner (if any partitioner is required) itself.

Partitioning service may be implemented using GraphX, however, it can be implemented also on other frameworks, including implementing it without using any framework.

The development of our simulated-annealing partitioning framework is illustrative of the general difficulty of adapting distributed algorithms, which require some form of shared state, to the bulk synchronous parallel model. Indeed, the communication cost of the synchronization phase and the need to wait for the slowest instances can significantly slow down computation. This problem is nowadays particularly evident in machine learning. Indeed, a basic step in machine learning is to compute parameter models using some stochastic gradient method in a distributed way. The dataset is split among different executors, each using its data subset to compute a noisy estimation of the gradient of the loss function. The gradient estimates are then averaged during a synchronization phase and this improved estimate is used to update the parameter models. The synchro-

nization phase is time consuming because of the reasons provided above, so that asynchronous solutions have been proposed, where nodes may work on stale data and read-write race conditions may arise. Empirically, on single-node systems, these asynchronous algorithms have yielded order-of-magnitude improvements in performance (see e.g., [69]).

Our goal in the future is to investigate how these algorithms can be adapted to Spark, for example averaging the intrinsically low time requirement of local operations. As in our implementations of the *SA* partitioner framework, we can perform many local operations on the basis of potentially "wrong" local data as far as we keep the number of inconsistencies bounded (as in our single-opinion implementation) or we can embrace inconsistencies maintaining potentially different coupled versions of the shared state (as in our multi-opinion implementation).

Appendix A

Extended Abstract in French

Partitionnement réparti basé sur les sommets

A.1 Introduction

La taille des graphes du monde réel obligent de les traiter d'une manière distribuée. C'est pourquoi, le partitionnement de graphe est la première étape indispensable avant le traitement des graphes. En plus, car le partitionnement de graphe est un problème NP-difficile, il y a clairement un manque de recherche consacré au partitionnement de graphe, par ex. Il n'est pas clair comment évaluer la qualité des méthodes de partitionnement (partitionneurs) de graphe, comment comparer des méthodes de partitionnement différentes et comment le partitionnement affecte le temps final de calcul. En outre, il existe toujours un compromis entre les partitionneurs simples et complexes: partitionneurs complexes peuvent avoir besoin d'un temps de partitionnement trop long pour annuler les économies de temps d'exécution.

Dans ce travail, nous avons essayé de résoudre ces problèmes. En particulier, nos objectifs étaient: trouver un moyen correct de comparer les partitionneurs (en particulier, avant d'exécuter les algorithmes de traitement de graphe actuel), identifier une fonction objective que le partitionneur devrait optimiser et concevoir un partitionneur capable d'optimiser cette fonction.

A.2   Résumé des développements

L'analyse des grands graphes est une opération qui demande beaucoup d'espace, qui ne peut normalement pas être effectué sur une seule machine. Il y a deux raisons pour lesquelles un graphe doit être distribué: des problèmes de la mémoire et de calcul. Le problème de la mémoire se produit lorsque tout le graphe doit être chargé dans la RAM. Par exemple, un graphe avec un milliard des arêtes nécessiteraient au moins $8|E|$ octets d'espace pour stocker des informations sur les bords, où E est l'ensemble des arêtes, et cela ne comprend pas le calcul frais généraux - en pratique, le traitement du graphe nécessiterait plusieurs fois plus d'espace. Même si une machine a suffisamment de RAM pour stocker et traiter un graphe, elle peut prendre un inacceptablement longtemps si un graphe n'est pas partitionné, mais est plutôt traité en utilisant un seul thread d'exécution.

Afin de surmonter les problèmes de mémoire et de calcul, nous devons partitionner un graphe en plusieurs composants. Ensuite, un graphe partitionné peut être traité en parallèle sur plusieurs coeurs indépendamment du fait qu'ils soient sur la même machine ou pas. Naturellement, la taille de chaque composant est plus petite que le graphe original, ce qui conduit à des exigences de mémoire plus petites.

Naturellement, pour trouver une partition optimale, des problèmes de partitionnement de graphe apparaissent. Le partitionnement divise un graphe en plusieurs sous-graphes afin d'obtenir le meilleur temps de calcul d'un algorithme de traitement de graphe sous deux aspects conflictuels. Le premier aspect - équilibre - dit que la taille de chaque composant devrait être presque la même. Il provient du fait que les graphes sont traités par des clusters de machines et si une machine a aussi grande composante, cela ralentira l'exécution complète. Le deuxième aspect - communication - indique que le partitionnement devrait réduire la quantité de composants en commune. Comme un exemple trivial, si un graphe a composants non connexe et chaque exécuteur testamentaire reçoit un composant, les exécuteurs peuvent, dans de nombreux cas, fonctionner de manière presque indépendante.

Les algorithmes de partitionnement (partitionneurs) prennent divisent un graphe dans les N composants. En particulier, nous sommes intéressés par les divisions qui peuvent être exécuté de façon distribuée. Un partitionneur distribué est un

algorithme qui se compose de plusieurs instances, où chaque instance effectue le partitionnement en utilisant le même algorithme mais sur des composants différents du graphe. Chaque instance représente une copie de l'algorithme avec le composant unique du graphe et certains ressources qui lui sont affectées, comme les threads informatiques et la RAM. Instances de la partitionneur distribué peut communiquer entre eux ou pas. Dans ce qui suit, nous supposons que le nombre d'instances d'un partitionneur distribué est égal à N, le nombre de composants du graphe.

Deux approches ont été développées pour résoudre le problème de partitionnement de graphe: le partitionnement des sommets et le partitionnement des arêtes. Une façon classique de distribuer un graphe est le partitionnement des sommets où les sommets sont affectés aux composants différents. Un arête est coupé, si ses sommets appartiennent à deux composants différents. Les partitionneurs des sommets essaient alors de minimiser le nombre d'arêtes coupées. Plus récemment, le partitionnement des arêtes a été proposé et préconisé [2] comme une meilleure approche pour traiter les graphes avec la distribution d'une loi de puissance [3] (les graphes de loi de puissance sont communs dans des données du monde réel plaw, plaw2). Dans ce cas, les arêtes sont mappés aux composants et les sommets sont coupés si leurs arêtes sont attribués aux composants différents. L'amélioration peut être expliqué qualitativement avec la présence, dans un graphe de loi de puissance, de centres, c.a.d. des sommets de degré beaucoup plus grand que la moyenne. Dans un partitionnement de sommet, l'attribution d'un concentrateur à une partition donnée conduit facilement à i) déséquilibre de calcul, si ses voisins sont également affectés au même composant, ou ii) à un grand nombre d'arêtes coupées et à des exigences de communication fortes. Un partitionneur des arêtes peut plutôt obtenir un meilleur compromis, en coupant uniquement un nombre limité de hubs. Le support analytique de ces résultats est présenté dans [6]. Pour cette raison, de nombreux nouveaux cadres de calcul graphe, comme GraphX [7] et PowerGraph [2], reposent sur le partage des arêtes.

Les partitionneurs différents fournissent des partitions différentes, mais il n'est pas évident quelle partition est meilleure. La qualité de la partition peut être évaluée de deux façons. Une façon est pour évaluer l'effet de la partition sur l'algorithme que nous voulons exécuter sur le graphe, par ex. en termes de temps total d'exécution ou de frais généraux de communication. Bien que cette analyse

fournisse la réponse définitive, il est clair que nous aimerions choisir la meilleure partition avant d'exécuter un algorithme. Autrement les mesures peuvent être calculée directement à partir de la partition sans avoir besoin d'exécuter l'algorithme cible. Nous appelons le premier ensemble des paramètres - métriques d'exécution et les deuxièmes - partition métriques.

Nous commençons notre étude de partitionnement des arêtes par un sondage des partitionneurs existants, pour lesquels nous fournissons une taxonomie. Nous examinons les travaux publiés, en comparant les partitionneurs. Nous distinguons 5 classes de partitionneurs: assignation aléatoire, segmentation de l'espace de hachage, approche glouton, coupe de moyeu, approche itérative.

Nous avons mené des expériences qui ont montré que, en effet, le partitionnement de graphe peut affecter un temps d'exécution de manière significative. Cependant, notre étude suggère qu'il n'est pas possible de tirer une conclusion claire sur leur performance relative.

Ensuite, nous étudions comment il est possible d'évaluer la qualité d'un partitionnement avant d'exécuter le calcul. Répondre à cette question serait utile pour les analystes de données qui doivent choisir le partitionneur approprié à leurs graphes et pour les développeurs qui souhaitent proposer des partitionneurs plus efficaces. Nous faisons un pas vers une réponse en menant des expériences avec le cadre largement utilisé pour le traitement de graphe - GraphX et l'analyse statistique précise.

Nous avons utilisé des modèles de régression linéaire avec des paramètres de partitionnement comme prédicteurs et le temps d'exécution moyen pour les algorithmes de traitement de graphe différents comme les valeurs observées. En outre, nous avons utilisé la méthode meilleure sélection de sous-ensemble pour trouver le meilleur modèle parmi tous les modèles possibles. Les modèles obtenus confirment qu'il existe une dépendance réelle entre ces quantités. Plus important, les mesures les plus importantes sont les coûts de communication et les coupures de sommets. Les deux sont un indicateur de la quantité de communication entre les exécuteurs. Au contraire, les mesures qui quantifient le déséquilibre de la charge dans les exécuteurs sont moins importantes. Cette conclusion confirme si la communication est inter-machine ou intra-machine, c.a.d. si le réseau est utilisé ou non. Nos résultats sont robustes à l'ensemble d'éléments de partition utilisés pour

former le modèle, et le modèle peut classer correctement d'autres partitionneurs.

Un nouveau algorithme de partitionnement des arêtes, appelé *JA-BE-JA-VC*, a été proposé dans [52] et a montré qu'il dépassait considérablement les algorithmes existants. L'algorithme commence par attribuer une couleur initiale (arbitraire) à chaque arête. Chaque couleur représente un composant où l'arête sera placé après la partitionnement. Le partitionneur s'améliore itérativement sur l'affectation des couleurs des arêtes initial, en permettant à deux arêtes d'échanger leur couleur si cela semble être bénéfique pour réduire le nombre de coupures des sommets correspondants. Afin d'éviter de se coincer à des minima locaux, *JA-BE-JA-VC* emprunt d'un recuit simulé (*SA*) l'idée de permettre apparemment des compromis swaps aux premiers stades du partitionnement.

Nous développons cette inspiration initiale et proposons deux versions de partition de graphe basées sur *SA* for Spark.

A cet effet, nous commençons par l'ingénierie inverse de *JA-BE-JA-VC* pour montrer la métrique ciblée. Ensuite, nous proposons la première version de notre cadre général de *SA* qui peut optimiser un large éventail de fonctions objectives et pour lesquelles les résultats de convergence peuvent être prouvés. La mise en oeuvre naïve de cette approche (ainsi que de *JA-BE-JA-VC*) nécessite un nombre important d'opérations de synchronisation coûteuses pendant le partitionnement. Ensuite, nous expliquons comment ces algorithmes peuvent être mis en oeuvre efficacement dans une architecture distribuée comme Spark. Cependant, dans ce cas, les instances peuvent fonctionner sur des valeurs périmées, ce qui peut empêcher la convergence à l'optimum.

Ensuite, nous avons fourni une version améliorée de notre cadre - le cadre multi-opinion *SA*, qui repose sur certaines idées de l'échantillonneur asynchrone de Gibbs proposé dans [65].

A.3   Conclusion

Dans cette thèse, nous avons abordé le problème de la partition d'un graphe afin d'accélérer les algorithmes distribués à exécuter sur le graphe partitionné. C'est un problème difficile. Tout d'abord, d'un point de vue informatique, le problème pour trouver la partition optimale est NP-difficile pour la plupart des fonctions ob-

jectives naturelles auxquelles on peut penser. En outre, il n'est même pas évident quelle fonction objective doit être considérée comme réduisant le temps de calcul final. Nous avons creusé dans le partitionnement de graphe en abordant les approches, solutions et cadres communs qui ont été proposés dans la littérature, en accordant une attention particulière à ceux pour lesquels le code d'exécution est disponible. Tous les partitionneurs peuvent être classés en deux approches:le partitionnement des sommets et le partitionnement des arêtes. Sur la base de l'étude actuelle, nous avons décidé de travailler avec l'approche de partitionnement des arêtes comme plus adapté aux graphes du monde réel. Parmi les différents cadres de traitement graphe disponibles, nous avons sélectionné GraphX pour nos expériences.

Afin de mieux comprendre quel est le progrès actuel dans le domaine du partitionnement des arêtes distribué et quelles sont les solutions couramment acceptées, nous avons mener un sondage sur tous les algorithmes existants. En outre, nous avons fourni une nouvelle taxonomie pour les partitionneurs. Il était important pour nous de voir comment les partitionneurs sont comparés. Cependant, au cours de ce processus, nous avons remarqué que i) il n'existe pas de solution généralement acceptée pour le partitionnement de graphe, ii) des partitionneurs différents sont rarement comparés les uns aux autres, iii) il n'est même pas clair comment les comparer au mieux. Pour réaliser ce manque de comparaison, nous avons mené des séries d'expériences sur GraphX avec tous les partitionneurs existants et disponibles pour GraphX plus d'autres que nous avons mis en oeuvre. Dans ces expériences, nous avons comparé les partitionneurs à l'aide de métriques existantes. Nos résultats suggèrent que le partitionneur Hybrid-Cut fournit une partition sur laquelle les algorithmes graphes exécutent le plus rapidement.

Cette analyse a été effectuée en comparant directement le temps d'exécution final des algorithmes de graphe différents comme `Connected Components` ou `PageRank`. Cette approche fournit une comparaison définitive entre les partitionneurs différents, mais nous aimerions pouvoir comparer deux partitions et choisir la meilleure pour les besoins de notre calcul sans exécuter le calcul. Pour cette raison, nous sommes intéressés par les paramètres de partition, c'est-à-dire des mesures qui peuvent être facilement évaluées compte tenu du graphe partitionné. C'est pourquoi nous avons décidé de mener une étude plus approfondie des paramètres de partition existants

qui nous permettrait de discuter de leur importance. Pour cette raison, nous avons effectué une autre série d'expériences et utilisé une méthodologie statistique solide. L'une des difficultés était de gérer une grande variabilité du temps d'exécution provenant de sources multiples, et obtient toujours des conclusions statistiquement significatives. Enfin, nous avons montré qu'il existe une dépendance linéaire entre les paramètres de partition et le temps d'exécution des algorithmes de traitement de graphe. Nos résultats montrent que les métriques communication sont plus importantes que les métriques d'équilibre. Cette constatation importante ainsi que le partitionneur *JA-BE-JA-VC* [52] nous ont inspiré pour la prochaine étape.

Nous avons décidé de développer une nouvelle approche pour le partitionnement des arêtes distribué, basé sur un recuit simulé qui peut être utilisé pour optimiser une grande famille de paramètres de partition, y compris la communication. Le défi était de mettre en place un recuit simulé distribué dans GraphX. La mise en oeuvre naïve de l'algorithme effectuera un seul échange lors d'une itération et nécessiterait alors un temps de calcul inacceptable, en raison des mélanges de données fréquents. Ensuite, nous l'avons amélioré en montrant que chaque instance peut effectuer jusqu'à L swaps pendant l'itération sans affecter de manière significative d'autres instances. Les résultats récents [65] nous ont permis de mettre en oeuvre une deuxième version du partitionneur basé sur l'échantillonneur de Gibbs. Néanmoins, dans ce cas, la mise en oeuvre la plus naturelle entraînerait une énorme quantité de communication entre l'itération de l'algorithme. Nous avons découvert comment réduire cette quantité de communication de $4N(N-1)$ à 2 mélangés. Nous avons mené des expériences pour montrer l'efficacité ainsi que la flexibilité de notre approche par rapport à l'état de l'art *JA-BE-JA-VC*.

A.3.1   Perspectives

Dans nos expériences, nous avons utilisé des graphes relativement petits, car il n'est pas possible de mener des expériences avec des graphes plus grands parce que le temps d'exécution est inacceptable, mais aussi parce que GraphX a une limitation implicite à la taille du graphe qu'il peut traiter. Il est facile d'observer les erreurs lors du chargement du graphe dans GraphX sans explication évident. Ainsi, l'une des perspectives est d'effectuer à court terme des expériences sur des

graphes plus grands.

Naturellement, les partitions sont mieux si plus du temps est alloué au partitionner. Cependant, les partitionneurs sophistiqués peuvent nécessiter 100 fois plus de temps de partitionnement, tout en offrant une amélioration de $1-2\%$ par rapport à la valeur mesurée. Ainsi, une autre perspective est de créer un service de partitionnement, où l'utilisateur de ce service fournit un graphe, un algorithme de traitement de graphe (tel que `PageRank`), le quantité de temps que cet algorithme sera être exécuté (avec paramètres initiaux différents) et souhaité Nombre de composants N. Le service de partitionnement sélectionne et exécute le partitionneur approprié (si un partitionneur est requis) lui-même.

Le service de partitionnement peut être implémenté à l'aide de GraphX, mais il peut être implémenté également sur des autres frameworks.

Le développement de notre cadre de partitionnement de recuit simulé illustre la difficulté générale d'adaptation d'algorithmes distribués, qui nécessitent une forme d'état partagé, au modèle en parallèle synchrone en vrac (BSP model). En effet, le coût de communication de la phase de synchronisation et la nécessité d'attendre les instances les plus lentes peuvent considérablement ralentir le calcul. Ce problème est aujourd'hui particulièrement évident à l'apprentissage automatique. En effet, une étape de base à l'apprentissage automatique consiste à calculer des modèles de paramètres utilisant une méthode de gradient stochastique de manière distribuée. Les données sont divisé entre exécuteurs différents, chaque exécuteur utilise son partie de données pour calculer une estimation bruyante du dégradé de la fonction de perte. Les estimations de gradient sont calculées en moyenne au cours d'une phase de synchronisation et cette estimation améliorée est utilisée pour mettre à jour les modèles de paramètres. La phase de synchronisation prend du temps en raison expliquée ci-dessus, de sorte que des solutions asynchrones ont été proposées, où les sommets peuvent fonctionner sur des données périmées et des conditions de course de lecture et d'écriture peuvent survenir. Empiriquement, sur les systèmes à un seul noeud, ces algorithmes asynchrones ont donné des améliorations de performance de l'ordre de la grandeur (voir par exemple [69]).

Notre objectif est d'étudier comment ces algorithmes peuvent être adaptés à Spark, par exemple en moyenne des exigences de temps intrinsèquement bas des opérations locales. Comme dans nos implémentations du framework de partition-

nement SA, nous pouvons effectuer de nombreuses opérations locales sur la base de données locales potentiellement "incorrectes" dans la mesure où nous gardons le nombre d'incohérences limitées (comme dans notre implémentation d'opinion unique) ou nous peuvent adopter des incohérences en maintenant des versions couplées potentiellement différentes de l'état partagé (comme dans notre mise en oeuvre multi-opinion).

Bibliography

[1] Jesun Sahariar Firoz, Thejaka Amila Kanewala, Marcin Zalewski, Martina Barnas, and Andrew Lumsdaine. "The anatomy of large-scale distributed graph algorithms". In: *arXiv preprint arXiv:1507.06702* (2015) (cit. on p. 7).

[2] Joseph E Gonzalez, Yucheng Low, Haijie Gu, Danny Bickson, and Carlos Guestrin. "Powergraph: Distributed graph-parallel computation on natural graphs". In: *Presented as part of the 10th USENIX Symposium on Operating Systems Design and Implementation (OSDI 12)*. 2012, pp. 17–30 (cit. on pp. 8, 21, 26, 32, 97).

[3] *Power Law.* http://www.necsi.edu/guide/concepts/powerlaw.html (cit. on pp. 8, 97).

[4] Lada A Adamic, Rajan M Lukose, Amit R Puniyani, and Bernardo A Huberman. "Search in power-law networks". In: *Physical review E* 64.4 (2001), p. 046135 (cit. on p. 8).

[5] Michalis Faloutsos, Petros Faloutsos, and Christos Faloutsos. "On power-law relationships of the internet topology". In: *ACM SIGCOMM computer communication review*. Vol. 29. 4. ACM. 1999, pp. 251–262 (cit. on p. 8).

[6] Florian Bourse, Marc Lelarge, and Milan Vojnovic. "Balanced graph edge partition". In: *Proceedings of the 20th ACM SIGKDD international conference on Knowledge discovery and data mining*. ACM. 2014, pp. 1456–1465 (cit. on pp. 8, 97).

[7] Reynold S. Xin, Joseph E. Gonzalez, Michael J. Franklin, and Ion Stoica. "GraphX: A Resilient Distributed Graph System on Spark". In: *First International Workshop on Graph Data Management Experiences and Systems*.

GRADES '13. New York, New York: ACM, 2013, 2:1–2:6 (cit. on pp. 8, 19, 30, 32, 34, 97).

[8]   *GraphX programming guide.* `http://spark.apache.org/docs/latest/graphx-programming-guide.html` (cit. on p. 9).

[9]   Ravi Kannan, Santosh Vempala, and Adrian Vetta. "On clusterings: Good, bad and spectral". In: *Journal of the ACM (JACM)* 51.3 (2004), pp. 497–515 (cit. on pp. 11, 12).

[10]   Gary William Flake, Robert E Tarjan, and Kostas Tsioutsiouliklis. "Graph clustering and minimum cut trees". In: *Internet Mathematics* 1.4 (2004), pp. 385–408 (cit. on pp. 11, 12).

[11]   Mijung Kim and K Selçuk Candan. "SBV-Cut: Vertex-cut based graph partitioning using structural balance vertices". In: *Data & Knowledge Engineering* 72 (2012), pp. 285–303 (cit. on p. 12).

[12]   Grzegorz Malewicz, Matthew H Austern, Aart JC Bik, James C Dehnert, Ilan Horn, Naty Leiser, and Grzegorz Czajkowski. "Pregel: a system for large-scale graph processing". In: *Proceedings of the 2010 ACM SIGMOD International Conference on Management of data.* ACM. 2010, pp. 135–146 (cit. on pp. 12, 13, 23).

[13]   Matei Zaharia, Mosharaf Chowdhury, Michael J Franklin, Scott Shenker, and Ion Stoica. "Spark: cluster computing with working sets." In: *HotCloud* 10 (2010), pp. 10–10 (cit. on pp. 14, 37).

[14]   Matei Zaharia, Mosharaf Chowdhury, Tathagata Das, Ankur Dave, Justin Ma, Murphy McCauley, Michael J Franklin, Scott Shenker, and Ion Stoica. "Resilient distributed datasets: A fault-tolerant abstraction for in-memory cluster computing". In: *Proceedings of the 9th USENIX conference on Networked Systems Design and Implementation.* 2012 (cit. on p. 14).

[15]   *Java Vitrual Machine.* `http://docs.oracle.com/javase/specs/` (cit. on p. 14).

[16]   *Scala programming language.* `http://www.scala-lang.org/` (cit. on p. 14).

[17]   *Apache Mesos.* `http://mesos.apache.org/` (cit. on p. 14).

[18] Vinod Kumar Vavilapalli, Arun C Murthy, Chris Douglas, Sharad Agarwal, Mahadev Konar, Robert Evans, Thomas Graves, Jason Lowe, Hitesh Shah, Siddharth Seth, et al. "Apache hadoop yarn: Yet another resource negotiator". In: *Proceedings of the 4th annual Symposium on Cloud Computing*. ACM. 2013, p. 5 (cit. on pp. 14, 22).

[19] *Akka toolkit.* `http://akka.io/` (cit. on p. 14).

[20] *RDD Lineage.* `https://jaceklaskowski.gitbooks.io/mastering-apache-spark/content/spark-rdd-lineage.html` (cit. on p. 14).

[21] *Spark cluster mode overview.* `http://spark.apache.org/docs/latest/cluster-overview.html` (cit. on p. 15).

[22] *The Pathologies of Big Data.* `http://queue.acm.org/detail.cfm?id=1563874` (cit. on p. 15).

[23] *Narrow and wide transformations.* `http://horicky.blogspot.fr/2015/02/big-data-processing-in-spark.html` (cit. on p. 17).

[24] *LRU policy.* `https://en.wikipedia.org/wiki/Cache_replacement_policies#LRU` (cit. on pp. 18, 24).

[25] *Pure function.* `https://en.wikipedia.org/wiki/Pure_function` (cit. on p. 18).

[26] *Under The Hood: DAS Scheduler.* `http://slideplayer.com/slide/5892719/` (cit. on p. 19).

[27] Leslie G Valiant. "A bridging model for parallel computation". In: *Communications of the ACM* 33.8 (1990), pp. 103–111 (cit. on p. 18).

[28] Maurice Herlihy and Nir Shavit. *The art of multiprocessor programming.* Morgan Kaufmann, 2011 (cit. on pp. 18, 25).

[29] *Bulk synchronous parallel model.* `https://en.wikipedia.org/wiki/Bulk_synchronous_parallel` (cit. on p. 20).

[30] Lawrence Page, Sergey Brin, Rajeev Motwani, and Terry Winograd. "The PageRank citation ranking: bringing order to the web." In: *Technical report, Stanford InfoLab, Stanford, CA* (1999) (cit. on p. 20).

[31] Yucheng Low, Danny Bickson, Joseph Gonzalez, Carlos Guestrin, Aapo Ky-
      rola, and Joseph M Hellerstein. "Distributed GraphLab: a framework for ma-
      chine learning and data mining in the cloud". In: *Proceedings of the VLDB
      Endowment* 5.8 (2012), pp. 716–727 (cit. on pp. 21, 25).

[32] Ching Avery. "Giraph: Large-scale graph processing infrastructure on hadoop".
      In: *Proceedings of the Hadoop Summit. Santa Clara* 11 (2011) (cit. on pp. 21,
      23, 31).

[33] Yuanyuan Tian, Andrey Balmin, Severin Andreas Corsten, Shirish Tatikonda,
      and John McPherson. "From think like a vertex to think like a graph". In:
      Proceedings of the VLDB Endowment 7.3 (2013), pp. 193–204 (cit. on pp. 21,
      24).

[34] Niels Doekemeijer and Ana Lucia Varbanescu. "A survey of parallel graph
      processing frameworks". In: *Delft University of Technology* (2014) (cit. on
      p. 21).

[35] Andrzej Bialecki, Michael Cafarella, Doug Cutting, and Owen O'Malley.
      "Hadoop: a framework for running applications on large clusters built of com-
      modity hardware". In: *Wiki at http://lucene. apache. org/hadoop* 11 (2005)
      (cit. on pp. 21, 23, 37).

[36] Jeffrey Dean and Sanjay Ghemawat. "MapReduce: simplified data processing
      on large clusters". In: *Communications of the ACM* 51.1 (2008), pp. 107–113
      (cit. on p. 21).

[37] *Higher-order function.* `https://en.wikipedia.org/wiki/Higher-order_`
      `function` (cit. on p. 21).

[38] Konstantin Shvachko, Hairong Kuang, Sanjay Radia, and Robert Chansler.
      "The hadoop distributed file system". In: *Mass storage systems and technolo-
      gies (MSST), 2010 IEEE 26th symposium on.* IEEE. 2010, pp. 1–10 (cit. on
      p. 22).

[39] *Different consistencu model in Distributed GraphLab.* `http://slideplayer.`
      `com/slide/8912832/` (cit. on p. 26).

[40] *Nef Inria Cluster.* `http://nef.inria.fr/` (cit. on p. 27).

[41] Raphaël Bolze, Franck Cappello, Eddy Caron, Michel Daydé, Frédéric Desprez, Emmanuel Jeannot, Yvon Jégou, Stephane Lanteri, Julien Leduc, Noredine Melab, et al. "Grid'5000: A large scale and highly reconfigurable experimental grid testbed". In: *International Journal of High Performance Computing Applications* 20.4 (2006), pp. 481–494 (cit. on p. 27).

[42] *Secure Shell.* `https://en.wikipedia.org/wiki/Secure_Shell` (cit. on p. 27).

[43] *Bare Metal environment.* `http://searchservervirtualization.techtarget.com/definition/bare-metal-environment` (cit. on p. 27).

[44] *OAR2.* `http://oar.imag.fr` (cit. on p. 27).

[45] *Kadeploy 3.* `https://gforge.inria.fr/projects/kadeploy3/` (cit. on p. 27).

[46] *oarsh.* `http://manpages.ubuntu.com/manpages/wily/man1/oarsh.1.html` (cit. on p. 27).

[47] Rong Chen, Jiaxin Shi, Yanzhe Chen, and Haibo Chen. "Powerlyra: Differentiated graph computation and partitioning on skewed graphs". In: *Proceedings of the Tenth European Conference on Computer Systems.* ACM. 2015, p. 1 (cit. on pp. 30, 32, 38, 52).

[48] *Source code.* `https://github.com/Mykhailenko/scala-graphx-tw-g5k` (cit. on pp. 30, 48).

[49] Nilesh Jain, Guangdeng Liao, and Theodore L Willke. "Graphbuilder: scalable graph ETL framework". In: *First International Workshop on Graph Data Management Experiences and Systems.* ACM. 2013, p. 4 (cit. on pp. 30, 32, 34, 35, 37).

[50] George Karypis and Vipin Kumar. "METIS–unstructured graph partitioning and sparse matrix ordering system, version 2.0". In: (1995) (cit. on p. 31).

[51] Alessio Guerrieri and Alberto Montresor. "DFEP: Distributed funding-based edge partitioning". In: *European Conference on Parallel Processing.* Springer. 2015, pp. 346–358 (cit. on pp. 32, 37, 43).

[52]   Fatemeh Rahimian, Amir H. Payberah, Sarunas Girdzijauskas, and Seif
        Haridi. "Distributed Vertex-Cut Partitioning". In: *4th International Confer-
        ence on Distributed Applications and Interoperable Systems (DAIS)*. Vol. LNCS-
        8460. Berlin, Germany, 2014, pp. 186–200 (cit. on pp. 31, 32, 40, 41, 60–63,
        66, 92, 99, 101).

[53]   Rong Chen, Jia-Xin Shi, Hai-Bo Chen, and Bin-Yu Zang. "Bipartite-oriented
        distributed graph partitioning for big learning". In: *Journal of Computer
        Science and Technology* 30.1 (2015), pp. 20–29 (cit. on p. 32).

[54]   Aaron Clauset, Cosma Rohilla Shalizi, and Mark EJ Newman. "Power-law
        distributions in empirical data". In: *SIAM review* 51.4 (2009), pp. 661–703
        (cit. on p. 38).

[55]   *Hybrid-Cut and HybridCutPlus partitioners.* `https://github.com/larryxiao/`
        `spark/` (cit. on pp. 38, 39, 43).

[56]   Fatemeh Rahimian, Amir H Payberah, Sarunas Girdzijauskas, Mark Jela-
        sity, and Seif Haridi. "Ja-be-ja: A distributed algorithm for balanced graph
        partitioning". In: (2013) (cit. on p. 40).

[57]   Hlib Mykhailenko, Giovanni Neglia, and Fabrice Huet. "Which Metrics for
        Vertex-Cut Partitioning?" In: *Proceedings of the 11th International Confer-
        ence for Internet Technology and Secured Transactions*. 2016 (cit. on p. 41).

[58]   Paul Erdös and Alfréd Rényi. "On random graphs, I". In: *Publicationes
        Mathematicae (Debrecen)* 6 (1959), pp. 290–297 (cit. on p. 42).

[59]   *Stanford Large Network Dataset Collection.* `https://snap.stanford.edu/`
        `data/` (cit. on pp. 43, 50, 72, 86).

[60]   Gareth James, Daniela Witten, Trevor Hastie, and Robert Tibshirani. *An
        introduction to statistical learning.* Vol. 6. Springer, 2013 (cit. on pp. 49, 51).

[61]   Hirotugu Akaike. "Akaike's Information Criterion". In: *International Ency-
        clopedia of Statistical Science.* Springer, 2011, pp. 25–25 (cit. on p. 49).

[62]   *Spark standalone cluster.* `http://spark.apache.org/docs/latest/spark-`
        `standalone.html` (cit. on p. 50).

[63] Robert Hood, Haoqiang Jin, Piyush Mehrotra, Johnny Chang, Jahed Djomehri, Sharad Gavali, Dennis Jespersen, Kenichi Taylor, and Rupak Biswas. "Performance impact of resource contention in multicore systems". In: *Parallel & Distributed Processing (IPDPS), IEEE International Symposium on.* 2010 (cit. on p. 51).

[64] Scott Kirkpatrick, C Daniel Gelatt, Mario P Vecchi, et al. "Optimization by simulated annealing". In: *science* 220.4598 (1983), pp. 671–680 (cit. on p. 59).

[65] Alexander Terenin, Daniel Simpson, and David Draper. "Asynchronous Gibbs Sampling". In: *arXiv preprint arXiv:1509.08999* (2015) (cit. on pp. 60, 61, 79–81, 89, 92, 99, 101).

[66] Hlib Mykhailenko, Giovanni Neglia, and Fabrice Huet. "Simulated Annealing for Edge Partitioning". In: *DCPerf 2017: Big Data and Cloud Performance Workshop at INFOCOM 2017.* 2017 (cit. on p. 60).

[67] Pierre Brémaud. *Markov chains: Gibbs fields, Monte Carlo simulation, and queues.* Vol. 31. Springer Science & Business Media, 2013 (cit. on pp. 62, 66, 67).

[68] *Source code of JA-BE-JA-VC and SA.* `https://bitbucket.org/hlibmykhailenko/jabejavc/` (cit. on p. 74).

[69] Xixuan Feng, Arun Kumar, Benjamin Recht, and Christopher Ré. "Towards a unified architecture for in-RDBMS analytics". In: *Proceedings of the 2012 ACM SIGMOD International Conference on Management of Data.* ACM. 2012, pp. 325–336 (cit. on pp. 94, 102).

Acronyms

BAL Balance.

BSP Bulk Synchronous Parallel.

CC Communication cost.

CRVC CanonicalRandomVertexCut.

DAG Directed acyclic graph.

LRM Linear regression model.

LRU Least Recently Used.

RAM Random Access Memory.

RDD Resilient Distributed Dataset.

RF Replication factor.

RMSE Root mean square error.

RVC RandomVertexCut.

STD Standard deviation of partition size.

VC Vertex-cut.